1986

Review of fatigue tests and design criteria on welded details, Final Report, July 1986, 180p.(NCHRP Report 286) Publication 86-21

Peter B. Keating

John W. Fisher

REVIEW OF

FATIGUE TESTS AND DESIGN CRITERIA

ON WELDED DETAILS

NCHRP PROJECT 12-15(5)

Prepared For

Transportation Research Board

National Cooperative Highway Research Program

National Academy of Sciences

Peter B. Keating

John W. Fisher

Fritz Engineering Laboratory

Lehigh University

Bethlehem, Pennsylvania 18015

July, 1986

Fritz Engineering Laboratory Report 488.1(86)

ACKNOWLEDGMENT

This work was sponsored by the American Association of State Highway and Transportation Officials, in cooperation with the Federal Highway Administration and was conducted in the National Cooperative Highway Research Program which is administered by the Transportation Research Board of the National Research Council.

Table of Contents

Acknowledgments

The research reported herein was performed under NCHRP Project 12-15(5) by the Fritz Engineering Laboratory, Department of Civil Engineering, Lehigh University, Bethlehem, Pennsylvania. John W. Fisher, Professor of Civil Engineering, was the principal investigator. Peter B. Keating, Research Assistant, is the co-author of the report.

Special thanks are extended to Sarah Halley, former student at Lehigh University, for her help in developing and compiling the fatigue test database. To Chitoshi Miki, Professor of Civil Engineering, Tokyo Institute of Technology, for his help with the Japanese fatigue data and for his review of the final draft of the report. Also, to Robert Kendi and Monica Newman, Lehigh University Computing Center, for their continued help with the database development and manuscript processing. And to Catherine Robertson for her time spent reviewing the final manuscript.

Summary

Since the AASHTO Specification fatigue resistance provisions were developed from test data reported in NCHRP Reports 102 and 147, several major fatigue studies have been conducted. By reviewing the results of these studies on full-scale, welded steel test specimens, the original database was broadened to include a wider range of detail types and sizes. Each data group was compared to the existing AASHTO fatigue design provisions in order to determine the adequacy of the resistance curves and to check for detail types whose fatigue strengths deviate from these curves. Most of the additional data correlate well with the original database. Since the current (1986) AASHTO fatigue design curves were based on a limited number of detail types, the expanded database allows for a more comprehensive assessment of the fatigue strength provisions.

From this review, a revised set of fatigue design curves is proposed that better estimates the fatigue resistance of welded steel bridge details. Though they are similar to the current AASHTO curves, the new curves are more uniform and parallel; each curve is set at a constant slope of -3.0. The available data have been compared with the appropriate curve in order to assess the validity of the proposed fatigue design curves.

Although the database has been significantly enlarged by the inclusion of new test data, several areas have been identified that require further in-depth study. This includes a more thorough examination of size effects so that test

data can be accurately correlated with field conditions. Also, additional test data is needed in the high cycle regime. This would help to better establish the constant amplitude fatigue limits and provide a better understanding of whether or not bridge structures will experience cracking at some of these details.

1. Introduction and Research Approach

1.1 Background

The current AASHTO Specifications [1] contain provisions for the fatigue design of steel bridge details. These provisions are based on a set of fatigue resistance curves which define the strength of different classes of details. The curves were developed from an extensive research program sponsored by the National Cooperative Highway Research Program (NCHRP) under the direction of the Transportation Research Board. The program, conducted over a period of six years from 1966 to 1972, involved the fatigue testing of 800 full sized welded steel bridge details. The statistically designed experimental program was conducted under controlled conditions so that analysis of the test data would reveal the parameters that were significant in describing fatigue behavior. The result was the quantification of the fatigue strength of welded bridge details and the development of comprehensive design and specification provisions.

Since the adoption of the AASHTO fatigue specifications in 1974, several major fatigue studies have been carried out on similar beam type specimens. Tests were conducted in East Germany, Japan, Switzerland, Office of Research and Experiments of the International Union of Railways - ORE (West Germany, Poland, England, and Holland), as well as here in the United States. The additional studies evaluated the applicability of the findings of the NCHRP test program to fabrication conditions elsewhere in the world and were used to develop similar fatigue codes. The additional

tests augmented the NCHRP findings and often defined the fatigue strength of details that were not tested under the NCHRP program. For example, much of the Japanese data stem from research performed to develop fatigue specifications for the design of long-span bridges for the Honshu-Shikoku Bridge Authority. Many of the simulated details are typical of those found in welded box members.

In addition, during the last several years, several countries have adopted their own set of comprehensive fatigue specification provisions. Though many of these specifications base the majority of their fatigue resistance provisions on the original NCHRP fatigue data, they have tended to deviate slightly from the AASHTO criteria. Both the International Organization of Standardization (ISO) and the European Convention for Constructional Steelwork (ECCS) have developed fatigue curves that differ slightly from the AASHTO requirements. Equally spaced S-N curves with constant slopes of -3.0 have been used to define the fatigue strength of details ranging from base metal to coverplated beam members. Many of these curves are about the same as the companion AASHTO curves.

1.2 Objectives and Scope

With the addition of the new fatigue data and the development of fatigue codes in other countries, it is beneficial to review and re-evaluate the existing AASHTO fatigue specifications using these additional resources. The principal objective of this project is to compile and review all available fatigue data. This allows for a re-evaluation of the existing fatigue specifications so that

they more accurately reflect the current state of knowledge. In addition, it provides an opportunity to provide criteria consistent with other applications in other countries. Specifically, the project was initiated with the following objectives:

- To develop a database for welded steel bridge details that includes details from all available sources. This includes the original NCHRP data used to develop the current AASHTO fatigue provisions as well as data from test programs that have been conducted since the implementation of the specifications in 1974.

- To analyze the new data on an individual basis with respect to the existing AASHTO fatigue provisions to see if changes are required in the code due to the new test results. In this way the adequacy of the current specifications can be reviewed for possible inconsistencies or for detail types whose fatigue resistance may be presently misrepresented. The possibility of this exists since, in the original test program, the number and type of details were limited, though the findings have been extended for almost all types of bridge details.

- To unify or standardize the AASHTO fatigue design curves with the increased database so that the curves more accurately reflect the present knowledge of the fatigue behavior of welded steel bridge details.

- To provide new fatigue design specifications for use in national design codes that more accurately define the fatigue resistance of welded steel bridge details.

The database has been limited to test data that can be used to define the fatigue resistance of welded steel details. This study does not attempt to analyze the fatigue strength of other types of structural details such as riveted and bolted components. Nor does it attempt to evaluate the adequacy of weld improvement techniques. While these processes tend to increase the fatigue resistance of certain details, the objective of this project is to define the lower bound fatigue resistance for as-welded details, or the minimum level of fatigue strength that would be obtained provided that standard fabrication and inspection procedures were employed.

Since the main objective of this fatigue data review is to build on the findings in NCHRP Reports 102 and 147, the database has been primarily limited to test data obtained from fatigue testing large-scale test specimens. Small-scale specimens are used in the review where no alternative exists, though reliance on this data has been minimized. As was extensively addressed in the NCHRP reports, small-scale specimens always provide higher cycle lives than large-scale beam type specimens. This behavior can be attributed to many factors, one of which is the decreased residual stress fields in small-scale specimens. Without sufficient base metal or geometric conditions to constrain the cooling weld metal, residual tensile stresses will not develop to the magnitude found in full-scale weld details. Other factors

are the distribution of defects and their frequency of occurrence, and favorable secondary stresses due to misalignment of the specimens during testing, as well as the variability of joint design. The small-scale fatigue test data does not contribute to defining the lower bound design resistance for welded steel bridge details.

1.3 Research Approach

A major portion of the project was the development of a computerized database containing fatigue test results of varying detail types [2]. Included in the database is data from the original NCHRP test program (to 1972), subsequent NCHRP test programs, Japanese and European (ORE) test data, as well as other sources. The database was developed with the intent to make it as comprehensive as possible. Therefore, for each data set (defined as one fatigue failure) not only were the detail type, stress range, and cycles to failure provided, but also critical dimensions of the test specimens were given. This allowed for studies involving the influence of size effects in the specimens. Each detail type was given a unique code number, unrelated to the category designation it would receive under the AASHTO fatigue specifications. Therefore, the lower bound fatigue strengths of the details were not predetermined or biased by the current fatigue provisions. Several computer programs were written to utilize the test data. These programs include sorting routines, plotting functions, and regression analysis. The development of this database allowed for the systematic analysis of the large amount of fatigue data compiled from various sources.

Each new source of test data was first compared with the appropriate existing AASHTO fatigue curves. This was done to determine if the results from the new tests were consistent with the findings of the original NCHRP studies or if the fatigue resistance of a particular detail had possibly been misrepresented by the current specifications. A regression analysis was performed using all the data for a given detail type to see if any significant differences arose. Once the new data was properly categorized, all data, both old and new, for each detail type were compared with the appropriate fatigue resistance curve.

Although use was made of statistical methods (primarily linear regression analysis), the results were often difficult to evaluate. This can be partly attributed to the fact that the relationship between the stress range and the number of cycles to failure is log-log in nature. Also, if the database is limited in number or is not distributed along the S-N curve, the results can easily become biased. Often, data were clustered over a small increment of stress range, and any number of regression lines could have described the relationship between stress range and life. Therefore, the primary method used for comparison and analysis was the direct comparison of the fatigue test data with various fatigue resistance curves. Since the comparison was being made against a predetermined set of design curves (defining the 95 percent confidence limit or lower bound resistance for fatigue strength), it was only necessary to show a distribution of failure points plotting above a particular curve in order to insure adequacy.

2. Findings

The findings of the fatigue test data review, conducted under NCHRP Project 12-15(5), are summarized in this chapter. A detailed examination of each new source of data, as well as a comparison of all existing fatigue data to existing provisions and a revised set of fatigue resistance curves is given in Chapter Three.

2.1 Fatigue Test Data Review

The results from each new source of fatigue test data were compared with the current AASHTO Fatigue Design Curves. Over 1500 additional test data points were added to the existing database of approximately 800 fatigue test results. The original database contained a limited number of welded steel detail types. This resulted from the need for adequate replication of the data at identical stress conditions so that the influence of stress parameters could be examined. The new test programs generally accepted the original findings; stress range and detail type are the two important parameters that determine fatigue strength. Therefore, the programs were able to perform fatigue tests on a wider variety of detail types and geometries, many of which had not been previously studied.

New detail types were added to the original database for all current AASHTO curve categories with the exception of Category A. This included longitudinal groove welds in both flat plate specimens and full size box members. Internal diaphragms for box type members were also examined. Test data that allowed for the evaluation of size effects on low strength

details were obtained. This included both thick coverplated beam flanges and thick web attachments. Also, flange attachments with varying geometries and weld conditions were included.

No major deviations were found to exist in the new test data when normal fabrication processes were practiced and standard fatigue testing procedures were followed. Nearly all the data for the majority of the detail types plotted above the lower bound resistance curve as defined by the current specifications. The results from detail types similar to the original NCHRP specimens correlated well with the original findings. Most new detail types were found to have at least the minimum fatigue resistance as set forth by the current fatigue design code. In general, the current AASHTO fatigue design curves have adequately represented the lower bound fatigue resistance for common detail types used in bridge design and construction.

2.2 Current and Proposed Fatigue Design Curves

A comparison was made between the current AASHTO fatigue design curves and those currently under consideration for adoption by the European Convention for Constructional Steelwork (ECCS) and the International Organization for Standardization (ISO). The ECCS curves represent a major effort to re-evaluate the fatigue design specifications. The analysis was based on the original NCHRP test data, limited data obtained from a specially designed test program, as well as other sources. The ECCS database was not as comprehensive as the database that resulted from the current review.

The proposed ECCS fatigue curves consist of fifteen equally spaced curves on a log-log scale. The slopes of all curves are set to a constant slope of -3.0 up to $5 \cdot 10^6$ cycles. Six of these curves closely resemble the six current AASHTO curves.

The results of this review indicate that adjustments should be made to the current AASHTO fatigue curves. The adjustments result in proposed curves that have a slope of -3.0 and are therefore compatible with the sloping portion of several of the ECCS curves. Only seven of the ECCS curves are suggested for the new set. The test data review does not support the need for fifteen fatigue resistance curves to define the strength of welded steel details. Six of the proposed curves are similar to the original AASHTO Categories A thru E′ curves in that the $2 \cdot 10^6$ intercept values are the same. Their slopes have been slightly adjusted to -3.0. The added seventh curve was necessary to define more accurately the fatigue resistance of longitudinal groove welds. The constant amplitude fatigue limits have remained unchanged with the exception of Category E. High cycle fatigue test results of coverplated beams indicated 4.5 ksi (31 MPa) provided a better estimate of the constant amplitude fatigue limit than the current 5.0 ksi (34.5 MPa) value.

2.3 Inadequacies of Current Fatigue Provisions

The fatigue test data review indicated that several detail types have not been properly accounted for in the current AASHTO fatigue provisions. This conclusion results from the analysis of test data on details not previously included in the database. Two types of longitudinal groove welds in built-up members were found to have a fatigue resistance less than the Category B curve. The decreased strength is attributed to size effects, initial flaws, and the geometry of the detail. A new Category B′, provides a better estimate of the fatigue resistance of this type of detail. The review also indicated that web attachments with plate thicknesses greater than 1.0 in. (25mm) resulted in a decreased fatigue resistance which corresponds to the Category E′ detail.

3. Data Review and Assessment

3.1 Development of Current AASHTO Specifications

Prior to the National Cooperative Highway Research Program Project 12-7 studies, only approximate fatigue design relationships were developed. This was due primarily to the limitations of the test data available at the time. Often, many variables were introduced into an experiment with a limited number of specimens. This made it impossible to establish clearly the statistical significance that stress variables, types of details, type of steel, and quality of fabrication had on fatigue life. During the previous studies, failure to properly control and measure the variables influencing the fatigue strength was the major reason for the apparent conflicts and contradictory claims on the stress variables and material characteristics. What was required was a comprehensive test program that could be conducted under controlled conditions so that analysis of the resulting data could reveal the significant parameters important in describing the fatigue behavior of welded bridge details. The NCHRP Project provided such a test program.

NCHRP Project 12-7 (NCHRP Reports 102 and 147) was developed to provide a statistically designed experimental program under controlled conditions [3, 4]. It involved the fatigue testing of some 530 test beams and girders with two or more details each. Large size specimens were used to overcome some of the limitations of smaller, simulated specimens (such as residual stress fields and shear lag). The specimens were fabricated with various details that are commonly used in the design of bridges, including

coverplates, web and flange attachments, and stiffeners. Three different types of steels were used to study the influence of yield stress on fatigue life. All specimens were tested under constant cycle loading.

3.1.1 Test Program

The principal design variables for the study were those associated with three major categories: type of detail, stress condition, and type of steel. Minimum stress, maximum stress, and the stress range were selected as the controlled stress variables. This permitted variation in one variable while the others were maintained at a constant level. The three types of steels used were: A36, A441, and A514. This provided a range of nominal yield stress that varied from 36 to 100 ksi (248 to 690 MPa).

In order for the results to be applicable to the design of bridges, test specimens that incorporated common structural details were fabricated. The tested detail types varied widely, from rolled beams to welded girders with coverplates. The basic specimen was either a rolled wide flange or a welded plate girder of one of the three steel types. These members were tested either as is (plain condition), or had attachments welded to them prior to testing. Even with the attachments on the beams or girders, failure data could still be obtained for the plain condition by repairing the failed section and retesting. The attachment details included coverplates, web stiffeners, and flange and web attachments. For the coverplates, four different types were used: wide coverplates with and without end welds, and coverplates narrower than the flange width, with and without end welds. Coverplate

thickness and multiple coverplates were also examined with the narrow coverplate. The web stiffeners were either welded to the tension flange or cut short to leave either a 1/2 in. (13 mm) or 4 in. (100 mm) web gap. The flange attachments were of varying length and were either welded flat or on edge. Also, different configurations for flange transitions were studied. The different detail types used in the test program are illustrated in Figs. 1 and 2.

3.1.2 Major Findings

The tests demonstrated that all fatigue cracks commenced at some initial discontinuity in the weldment or at the weld periphery, and grew perpendicular to the applied stresses. In the welded plate girders without attachments, most of the fatigue cracks were observed to originate in the web-to-flange welds at internal discontinuities such as porosity, incomplete fusion, or trapped slag. These discontinuities are always present, independent of the welding process and techniques used during fabrication.

With all of the different variables studied in the NCHRP Project 12-7, only two significantly influenced the fatigue strength of welded details: stress range and detail type. These findings were observed to be applicable to every beam and detail examined in the project. A major reason behind this simplification was the fact that welded steel structures contain localized residual stresses from the welding process and are of such magnitude that many other parameters can be eliminated from consideration. All welding processes result in high residual stresses, which are at or near the yield point

in the weldment and adjacent base metal. Thus, in the initial stages of fatigue crack growth in an as-welded structure, most of the fatigue life occurs in regions of high tensile residual stress. Under cyclic loading, the material at or near the initial discontinuities will be subjected to a fully effective tensile cyclic stress, even in cases of stress reversal. As a result, the stress ratio does not play a significant role when describing the fatigue strength of welded details since the maximum stress at a point of fatigue crack initiation and growth is, almost always, at the yield point. The residual stresses were found to be in the order of the yield stress irrespective of the steel type. Most of the fatigue life is exhausted by the time the fatigue crack propagates out of the high tensile residual zone or when the zone is relieved by the crack itself. It is apparent that residual stresses play an important role in both the formation of cracks from discontinuities that reside in the tensile and the arrest of cracks as they grow into a compression residual stress zone of a member subjected to compression alone.

With the stress range being the only important stress parameter in determining fatigue life, a stress range - cycle life relationship could be developed. Regression analysis showed that this relation was log-log in nature, with a constant slope. The S-N curves are defined in log form by

$$\log N = \log A - B \cdot \log S_r \qquad (1)$$

and in their exponential form by

$$N = A \cdot S_r^{-B} \qquad (2)$$

where log A is the log-N-axis intercept of the log S-N curve and B is the slope of the curve. The allowable stress range values were derived from the 95 percent confidence limits for 95 percent survival based on the regression analysis of the test data.

Six different categories were used to classify the fatigue strength of the details used in the test program. Rolled beams were used for Category A, longitudinal welds and flange splices for Category B, stiffeners and short 2-in. (50 mm) attachments for Category C, 4-in. (100 mm) attachments for Category D, coverplated beams for Category E, and thick coverplates and long attachments for Category E′. These relationships were used to provide the limits or bounds for all possible details that are normally encountered in the design of bridges and similar structures.

The current AASHTO Fatigue Design Curves [5] can be seen in Fig. 3. The tabularized form of these curves, which are actually used in the specifications, is shown in Table 1. As shown by the plot, all curves have similar slopes and have a value of approximately -3.0. The linear regression analysis for each category yielded a unique value for the slope, which was also used to set the slope of the lower confidence limit used for the design curve. The results from the regression analysis used in establishing the current design curves are shown in Table 2. This includes the calculated slope and mean intercept values for each category, as well as the standard deviation and lower bound intercept value. The plot of the curves in Fig. 3 also shows a constant amplitude fatigue limit. For stress range cycles below

this limit, no fatigue crack propagation would be expected. As seen in Fig. 3, the value of the constant amplitude fatigue limit decreases will detail severity. Test data verifying the fatigue limit in the high cycle regime (i.e., greater than 10^7 cycles) are only available for Category E and E′ details.

Concern where failure of a single element could cause collapse of a structure, resulted in a more conservative fatigue design requirement in order to minimize the possibility of fatigue crack growth in fracture critical members. The AASHTO provisions for non-redundant members were developed by shifting one range of loading cycles for the allowable stress range values in each category, as shown in Table 3. This has resulted in a variable reduction of the allowable stress range because the logarithmic increments for life are not equal. The reductions range from 20 to 40 percent.

3.2 Review of New Fatigue Test Data

In order to conduct a rational reanalysis of the AASHTO fatigue provisions, new fatigue data generated since 1972 were evaluated. The NCHRP test program, though the most comprehensive to date, still dealt with a limited number of detail types and sizes in each category. This can be attributed to the fact that a major effort of the program was to establish the significance of stress parameters influencing fatigue strength. To accomplish this, adequate replication of the data at identical stress conditions was required. Therefore, detail sizes and dimensions had to remain constant for all tests so as not to bias the results. Had it been clearly established prior to the start of the program that the stress range was the only controlling stress parameter, other detail types and sizes could have been tested resulting in a more comprehensive test program. By including new data, the existing NCHRP database can be broadened to include detail types and configurations that were not previously considered, thus overcoming some of the shortcomings of the original NCHRP data. In addition, the new data provide an independent check on the findings of the NCHRP data.

Certain problems immediately became apparent when the new data were combined with the existing NCHRP fatigue data. These problems arose mainly because each test program was developed independently and was based on a different set of test specifications and procedures. Also, the objectives of each program differed. Many of the tests were carried out on specimens that were not full scale. This meant that each specimen and resulting failures had to be checked for their validity in representing actual bridge

details. As the specimen size is decreased, the amount of constraint, which is needed to fully develop the residual welding stresses, is decreased. This will almost always result in a higher fatigue life. This was further verified by Japanese studies on small specimens machined out of longitudinal welds from larger specimens. The results gave significantly higher fatigue strengths that were unrealistic for actual field conditions. Also, the definition of failure differed between programs. For the NCHRP studies, an increase in the midspan deflection of 0.020 in. (0.5 mm) was found to be equivalent to a crack size that was considered to be failure of the section. For ORE, failure was defined simply as the inability of the specimen to sustain the applied load.

All of the new data considered in this report were initially analyzed and compared with the current AASHTO fatigue curves. Figures 4 thru 8 show plots of the original NCHRP data used to develop the Category A thru E curves. The Category E′ was defined from test data obtained in a subsequent NCHRP report, as discussed in the forthcoming section. The plots illustrate the type of distribution of scatter that occurred in that program and the resulting lower bound curves. Plain rolled beam failures were used to define the Category A curve shown in Fig. 4. Also shown in the figure are test data obtained prior to the original NCHRP program. These have been included due to the fact that both sets of data were used in developing the Category A curve and also since no additional data for the fatigue resistance of plain rolled beams were acquired during the present study. Category B was developed from longitudinal weld and flange splice

data shown in Fig. 5. A514 steel splices with straight tapered transitions were found to fall below the selected design curve as illustrated in Fig. 5. This resulted in the requirement that curved radius transitions be used with A514/A517 steel groove weld transitions in width. Transverse stiffeners and short attachments defined Category C, while intermediate length attachments were used to develop the Category D curve. Finally, Category E was defined by coverplated beams and long attachments. Tests on wide coverplates without end welds led to provisions that prevented their use (see AASHTO 1.7.12, 1977).

3.3 New Test Data

3.3.1 NCHRP Data

Subsequent to NCHRP Reports 102 and 147, several National Cooperative Highway Research Programs were conducted in the area of fatigue strength of welded bridge details. These NCHRP studies are reported in: Report 181; "Subcritical Crack Growth and Fracture of Bridge Steels," Report 188; "Fatigue of Welded Steel Bridge Members Under Variable-Amplitude Loading," Report 206; "Detection and Repair of Fatigue Damage in Welded Highway Bridges," Report 227; "Fatigue Behavior of Full-Scale Welded Bridge Attachments," and Report 267; "Steel Bridge Members Under Variable-Amplitude Long Life Loading." Each of these reports dealt with a different aspect of the fatigue problem and are discussed below.

3.3.1.1 NCHRP Report 181

NCHRP Report 181 [6] studied the fatigue crack growth behavior, corrosion fatigue propagation, stress-corrosion cracking, and fracture behavior of five grades of bridge steels, with loadings which simulated highway bridge traffic. The objective of the study was to develop information that would lead to the prevention of unstable crack growth in welded steel bridge members. The types of test specimens used, as well as the main objectives of the program, resulted in little or no information which could be included in the database for the fatigue strength of welded bridge details.

3.3.1.2 NCHRP Report 206

NCHRP Report 206 [7] deals primarily with studies involving the improvement of the fatigue resistance of details susceptible to fatigue damage where crack growth occurs at weld toes. Three improvement methods were examined: grinding, peening, and gas tungsten arc remelting. These treatments were applied to as-welded details prior to testing and to details that had experienced crack growth. Since these improvement methods tended to increase the fatigue resistance, thus biasing the results, these data were not included in the database. However, as part of the project, untreated coverplated beams were tested. The coverplate details had a beam flange thickness of 1.0 or 1.25 inches (25 or 32 mm), which was greater than those previously tested. This resulted in an expansion of available test data for coverplates and helped contribute to a new category, Category E′.

The test specimens were full-size coverplated beams with rolled W36x230 or

W36x260 sections of either A36 or A588 type steel. The 12 in. (305 mm) wide coverplates were welded to the rolled beam flanges with or without a transverse end weld. The beams were loaded under constant amplitude stress ranges varying from 4 to 8 ksi (28 to 55 MPa).

The data shown in Fig. 9 are plotted with the existing Category E and E′ AASHTO curves. This figure illustrates that the thicker coverplated beam flanges generally have a lower fatigue strength than that defined by the Category E curve. This was found true for all the levels of stress range tested. Thus, for coverplated beams with a beam flange thickness greater than 0.8 inches (20 mm), the lower bound of their resistance is best estimated by the Category E′ curve.

A pilot study was conducted to evaluate the fatigue strength of a penetrating web plate detail. Cracks had been detected in actual bridge members where flange plates were continuous through the web plate and attached to the web with a fillet weld on one side only. The detail type used in the study was a 2 x 8 x 16 in. (50 x 203 x 406 mm) plate passed through a flame-cut opening in the web plate. A 0.5 in. (13 mm) fillet weld was used to attach the plate to one side of the girder web. No weld was placed on the other side of the web plate. As shown in Fig. 10, the fatigue resistance of this type detail is approximately one-half of that defined by Category E′. The use of this type detail is undesirable.

3.3.1.3 NCHRP Report 227

The main objective of NCHRP Report 227 [8] was to examine the fatigue strength of beams with web and flange lateral attachment plates. Fatigue problems had developed in bridges where gusset plates were welded to the webs or flanges. These types of details were not examined in the original two NCHRP project; therefore, their fatigue strengths had not been adequately defined. In addition, retrofitting procedures were employed on some of the cracked details in an attempt to increase the fatigue life. These results have not been included in the database.

Eighteen full-size beams were used in the project. Each beam was a rolled section of one of the following three sizes: W27x145, W27x114, and W36x160. The type of steel used for all beams was A36. Most of the tests were conducted at a constant stress range of either 6, 9, 12, or 15 ksi (41, 62, 83, or 103 MPa). Detail types tested were: web gusset plates, flange gusset plates, web attachments with either fillet or groove welds, web attachments inserted through the web plate, and flange plates. An illustrative summary of detail types is given in Fig. 11.

The results for the web gusset plates are shown in Fig. 12. All failure points plot at or above the Category E curve. It was found that the longitudinal fillet weld joining the web gusset plate to the web provided the fatigue crack initiation sites. Of the different web gusset plate details tested, no significant differences were found in their fatigue resistance. Also, the variation of the flexural rigidity of the lateral bracing members did not affect the fatigue strength of the details.

Figure 13 shows the results from the flange tip attachments. For the plates without any end radius, it was found that the fatigue resistance was best defined by the Category E curve. For those plates which had the transition radius, the fatigue resistance was found to increase to a Category D type detail.

Also shown in Fig. 13 are test data for flange surface attachments. The detail type was a 8 x 24 x 0.5 in. (203 x 610 x 13 mm) plate attached to the flange surface with 0.37 in. (9.5 mm) transverse fillet welds. Cracks were found to develop from the weld root and propagate throughout the entire transverse weld. The crack growth from the weld root severed the connection plate from the flange surface and did not result in the crack propagating into the flange itself. This resulted in a fatigue resistance below that of Category E. Due to the low fatigue strength exhibited by this type detail, the use of flange surface attachments with only transverse end welds that are perpendicular to the cyclic stress is prohibited by the current specifications.

The web attachment data are shown in Fig. 14. The 12 in. (305 mm) attachments with a plate thickness of 2 in. (50 mm) provide a fatigue strength defined as Category E′. When the plate thickness of the web attachment was less than 1 in. (25 mm), the fatigue resistance was in agreement with Category E. Those test points that are below the Category E′ resistance curve corresponded to plates welded into slots in the girder web with coped end holes and groove welded curved girder attachments. Although different types of fabrication methods were used for the detail, the

scatter of the data does not warrant a more detailed classification than the Category E and E′ conditions.

3.3.1.4 NCHRP Reports 188 and 267

The NCHRP reports previously discussed involved the fatigue behavior of welded details subjected to constant loading. Since bridges are subjected to variable-amplitude stress cycles occurring in a random sequence, two reports dealt with this type of loading: NCHRP Reports 188 and 267 [9, 10]. Test data from these reports include results in the high cycle region where fatigue failure is governed by the constant amplitude fatigue limit. With the inclusion of this data, estimations of the fatigue life of lower strength details at low stress ranges were possible. The following section focuses primarily on the test programs for these two reports.

From the NCHRP projects on variable loading, two important conclusions were drawn. One was that variable load test data could be related to constant amplitude data by either Miner's Cumulative Damage Rule or the Root-Mean-Square (RMS) stress range method. Therefore, the cumulative effect on fatigue life of stress cycles of varying magnitude could be represented by a single effective stress range value. This allows for the inclusion of the variable amplitude test data into the database. The second conclusion was that if any of the stress range cycles in a spectrum exceeded the constant amplitude fatigue limit, the fatigue life could be predicted by the cumulative damage laws, assuming all cycles contributed to the damage.

The results of these studies indicated that both Miner's linear damage

hypothesis and the RMS stress range method provide a means of relating random variable stress cycles to constant cycle data. The effective stress range is defined by

$$S_{re} = [\sum \alpha_i \cdot S_{ri}{}^{B}]^{1/B} \qquad (3)$$

in which S_{ri} is the midwidth of the *ith* bar, or interval, in a frequency-of-occurrence histogram defining the variable amplitude spectrum and α_i is the fraction of stress ranges within that interval. If B is taken as 2.0, S_{re} from this equation is equal to the root mean square (RMS) of the stress ranges in the spectrum. If B is taken as the reciprocal of the slope of the constant amplitude S-N curve, 3.0, the equation is equivalent to Miner's Rule. For the spectrum shapes used, the difference between the two methods was found to be approximately 11 percent, with Miner's Rule resulting in the higher estimate for fatigue life. For assessments where the total fatigue life is required, Miner's Rule will give the more conservative estimate of the life.

The main objectives of NCHRP Report 188 were to develop fatigue data on welded bridge details under variable random sequence stress spectrums and to develop an analytical method of predicting the fatigue behavior under variable-amplitude stress spectrums from constant-amplitude fatigue data. Full scale welded beam test specimens were used. Detail types studied were the longitudinal web-to-flange weld and the coverplate detail, similar to those used in Project 12-7. Four different stress spectrum shapes were used to study their influence on fatigue life.

Figure 15 shows the plot of fatigue failures for the plain welded beams with the current AASHTO Category B curve. All failures originated in the longitudinal web-to-flange fillet weld. The results are well scattered and all plot above the allowable stress range curve. This indicates that variable amplitude test data can be reasonably related to constant amplitude test results by the effective stress range. The results for the coverplated beams are given in Fig. 16. Again, the results are consistent with the constant amplitude allowable stress line, in this case Category E. Given the fact that the plotted results include three types of steels and four different stress spectrums, the scatter of the data is reasonable. All but five data points plot above the lower bound limit.

Also examined under this project were small scale specimens that were fabricated to simulate a coverplate detail. The specimens consisted of a 4 in. (100 mm) long, 9/16 in. (14 mm) thick attachment plate fillet welded to a base plate. As shown in Fig. 17, the data points are well scattered above the Category E curve, the curve normally defining the coverplate detail. Due to the size limitations, mainly the 4 in. (100 mm) length, these specimens behave more closely to an intermediate attachment and are, therefore, better described by the Category D curve. Even then, much of the data plots significantly above the curve. This illustrates the possible erroneous results when small scale specimens are used to describe the fatigue behavior of large scale bridge members.

Project 267 was conducted in order to extend the results of Project 188

into the high cycle region. The main objective of the project was to study the effect of the frequency of overloads on the fatigue strength of welded details. Detail types studied were coverplates and web attachments. The test specimens, rolled beams with welded attachments, were subjected to a random variable amplitude load spectrum with most of the stress cycles below the constant amplitude fatigue limit. Exceedance rates ranged from approximately 12 to 0.1 percent.

For the coverplated beams, it were found that the data were bounded by the Category E and E′ curves (Fig. 18). The fatigue resistance of the coverplate detail used in this study is currently classified as Category E with a flange thickness of 0.57 in. (14.5 mm). The attached coverplate thickness was 1.0 in. (25 mm). Only two failures occurred at the Category E′ line, with the remainder falling between the two lines or above Category E. The results indicate that for variable amplitude loading, the fatigue resistance is more adequately defined by the E′ curve. Similar results were found for the web attachments and are also plotted in Fig. 18. The results are reasonably scattered in the high cycle region with nearly all of the points falling above the Category E′ fatigue life curve. The plate thickness of the web attachment detail was 1.0 in. (25 mm) and is therefore at the limit between Category E and E′. The test data are consistent with the Category E′ curve.

3.3.2 Other American Test Data

Three additional test programs, not sponsored by NCHRP, were conducted subsequent to NCHRP Reports 102 and 147. The first two programs that are reviewed augmented the original NCHRP results by providing test data for detail types that were not previously tested, while the third program dealt with the fatigue strength of welded attachments on horizontally curved girders. The following summarizes these programs.

The report entitled "Determination of Tolerable Flaw Sizes in Full Scale Welded Bridge Details" was sponsored by the Federal Highway Administration [11]. The main objective of the program was to determine the magnitude of flaw sizes that could be tolerated in full scale bridge weldments. Since the welding process introduces a region of material with microscopic flaws that can become macroscopic cracks when subjected to repeated loading, the possibility of unstable crack growth due to brittle fracture exists. By fatigue testing full size beams with welded details, the adequacy of the material toughness and its relationship to fatigue resistance could be evaluated.

The test specimens were 24 full size beams, either rolled sections or welded, of three types of steel: A36, A588, and A514. Each beam was 36 in. (0.9 m) deep with either 1-1/2 x 6 in. (38 x 152 mm) or 2 x 7 in. (50 x 178 mm) flange plates for the welded members. Four different types of details were tested: coverplates, lateral attachments, transverse stiffeners, and groove welded flange transitions. The detail types are illustrated in Fig. 19. Each

beam was cyclically loaded at room temperature for at least 2 million cycles and then at a reduced temperature of -40 °F (-40 °C) or lower at periodic intervals of crack extension until fracture occurred. All beams, with the exception of the coverplated details, equaled or exceeded their expected design fatigue life before brittle fracture occurred.

The test data from the coverplated beams are shown in Fig. 20. The fatigue life for each detail was found to be near or below the lower bound resistance curve defined by Category E. Since the flange plate thickness exceeded 0.8 in. (20 mm), a size effect was indicated with the fatigue strength more accurately defined by category E′. While both welded and unwelded coverplate end terminations were examined, no significant difference in fatigue strength was observed.

Two types of lateral flange attachments were tested. One was an overlapped plate with transverse fillet welds on the inside of the tension flange and a longitudinal fillet weld along the beam flange tip. The other detail type was a groove welded plate attached to the flange tip. The groove welded attachment had a end radius of approximately 0.75 in. (19 mm) where the weld ends were ground smooth. Each specimen had an attachment length of 12 in. (305 mm). As shown in Fig. 20, the test data exceed the Category E resistance curve. There is good agreement between the test results and Category E.

The transverse stiffener test data are plotted in Fig. 21. The test data fall

above the Category C resistance curve. This is consistent with the test results of similar detail types examined in NCHRP Report 147.

The flange thickness transition detail had not previously been examined to evaluate its fatigue strength. Figure 21 shows that the test data correlate well with the Category B resistance curve.

A second test program is reported in "Fatigue Resistance of Full Scale Cover-Plated Beams" which was sponsored by the Pennsylvania Department of Transportation [12]. The objective of this program was to examine the fatigue behavior of coverplated beam details in the low stress range-high cycle region. The study involved the results of field observations and laboratory tests.

The laboratory test program involved fatigue testing thirteen coverplated beam test specimens. These specimens were identical to the beams reported in NCHRP Report 102 (see Fig. 1). The beams were tested at stress ranges between 4 ksi (28 MPa) and 8 ksi (55 MPa) in order to bound the constant amplitude fatigue limit. All coverplated beam flange thicknesses were less than 0.8 in. (20 mm).

The test data for the coverplated beams are plotted in Fig. 22. The failures generally fall within the extension of the Category E resistance curve. The minimum stress range value at which fatigue failure occurred was 4.7 ksi. (32 MPa). The maximum stress range value at which no fatigue cracking was detected at $108 \cdot 10^6$ cycles was 6 ksi. (41 MPa).

The findings of the third test program are summarized in a report entitled "Fatigue of Curved Steel Bridge Elements" [13]. Sponsored by the Federal Highway Administration, the program examined the fatigue strength of structural details welded on horizontally curved steel plate and box girder members. Since horizontally curved bridges are subjected to torsional, lateral, and longitudinal forces in excess of those found in straight girder bridges, concern had been expressed that details on these types of bridges might exhibit lower fatigue strengths than implied by the existing design specifications. The test program concluded that no modification of the AASHTO fatigue provisions was necessary, provided that the nominal stress range at details was accurately calculated with consideration given to the three-dimensional behavior of the structure.

Eight full-scale, horizontally curved girder assemblies were tested: five curved plate girder pairs and three curved box girders. The centerline span lengths ranged from 36 ft. (11.0 m) for the box girders to 40 ft. (12.2 m) for the plate girders. The centerline radius was 120 ft. (36.6 m) for all members. The detail types studied were both web and flange attachments and are illustrated in Fig. 23. They included web gusset plates, transverse web stiffeners, and both flange tip and surface attachments. Each detail was designed and located such that its predicted failure would occur at approximately $2 \cdot 10^6$ cycles. This led to a distribution of test data with a limited range of stress.

The majority of the transverse diaphragm web stiffeners that experienced

fatigue cracking did so due to secondary stresses that resulted from out-of-plane displacement of the web from the transverse forces at the intermediate diaphragms. These types of failures represent a condition that is not directly related to the design evaluation. It verified the necessity to provide positive attachment of the diaphragm connection plates to both flanges of the curved girders. Only two failures of the stiffener detail occurred in the test program that were not influenced by secondary stresses, these are shown in Fig. 24 by the single point. As the figure illustrates, their fatigue resistance exceeded the lower bound estimate for Category C. Also shown in Fig. 24 are the fatigue test results for the flange surface attachment details. These are compared with the Category E curve. These attachments were sixteen inches (406 mm) in length and continuously fillet welded on all edges. Their fatigue lives are consistent with the Category E lower bound resistance curve.

Figure 25 shows the fatigue test results for flange tip attachments. The groove welded attachments with 6 in. (152 mm) radius transitions are plotted with the Category C resistance curve. Three of the eight failures plot below the curve. The reduced fatigue strength of these three points can be contributed to large discontinuities in the groove weld near the point-of-tangency. When the transition radius is ground out, the discontinuities are brought to the surface. This results in a more severe stress condition as compared to a fully embedded discontinuity. The three points are excluded from further consideration. The other set of data points plotted in Fig. 25 is for rectangular plates with groove welds. Since there is no transition radius and the attachment length is 16 in. (406 mm), the detail is classified as

Category E. All but one of the failure points plot above the Category E curve.

Web gusset plate fatigue test data are plotted in Fig. 26. The rectangular plate (zero transition radius) detail gave results consistent with Category E resistance curve for an attachment length of 16 in. (405 mm). When a transition radius of 6 in. (152 mm) is used with fillet welds, the fatigue specifications require a lower bound fatigue strength defined by Category D. The data plot above this resistance curve, though, only two failure points resulted from the test program. The data for the web gusset plates with tapered transitions plot above the Category D resistance curve. The current fatigue specifications define the lower bound fatigue strength as Category E.

3.3.3 Japanese Data

In the late 1970's an ambitious program was launched by the Honshu-Shikoku Bridge Authority to link several major islands with the main island of Japan. The program involved the design and construction of seventeen bridges consisting of three basic types: long-span suspension, cable-stayed, and truss [14]. Due to the size of the structures, several at or near previous record holders, and the combination of railway and highway type loading, it was desirable to examine the fatigue properties of various joints and details using large scale specimens. The existing Japanese fatigue specifications had been based on smaller scale specimens due to the limitations in the capacity of available testing equipment.

The specimens tested attempted to simulate members of welded box girders and other welded joints common to bridge structures. Particular attention was paid to size effects and the role of defects in the assessment of fatigue strength. The specimens tested were larger than specimens from previous tests in an attempt to obtain full residual stresses in the welds. Because defects are inherent to all welds, tests were run on specimens with varying defect sizes in order to relate defect size to an allowable fatigue strength. All tests were conducted under constant amplitude loading.

The principle design variables for the tests were detail type and stress range. The type of steel was varied to conform with standard practices. High strength steel was used for specimens simulating longitudinal members of suspension bridges while test specimens representing members of railway bridges were fabricated out of mild steel.

The fatigue strength of longitudinal welds was studied through the use of flat plate test specimens [15, 16, 17, 18, 19, 20]. Two plates were joined by a partial penetration longitudinal weld which resulted in a varying size and shape of the blowholes or varying root gaps. This allowed for the study of fatigue crack initiation as a function of defect size in order to define a maximum allowable defect size corresponding to an allowable fatigue strength. Also, box section specimens were tested in order to study the influence of different types of longitudinal corner welds [21]. Three different weld types were tested: fillet, single-bevel-groove weld, and single-J-groove weld. The second type of detail tested was non-load carrying cruciform fillet welded

joints [21, 22]. These simulated the stress concentration condition at the joint of a diaphragm attached to a chord member. The influencing variables examined were the fillet size, fillet shape, and weld penetration. Model joints of truss structures 1/4 to 1/3 scale of truss structures were tested [23, 21, 24]. The specimens differed in the method of connection of the diagonal members, the number of diaphragms in the bottom chord, and in the fillet radii of the gusset plate. Finally, a full size box member was tested to assure the fully developed resistance due to residual stresses [25]. Figure 27 shows examples of specimen types used in these test programs.

The Japanese test specimens with details of three basic types were utilized in the database. Longitudinal groove welds in flat plates and longitudinal welded box girders correspond to Category B details in the AASHTO code while non-load carrying cruciform fillet welded joints are comparable to a Category C detail.

The longitudinally groove welded joints in flat plates were of two types: single-vee and double-vee type joints. None of the data points for the partial penetration single-vee groove welds fell below the existing AASHTO Category B curve. There is considerable spread in the data which can be seen in the plot given in Fig. 28. This is partially due to the levels of stress range utilized in the testing, from 18 to 70 ksi (124 to 483 MPa). Also, the specimens were purposely fabricated with defects (blowholes) of varying sizes. As the defect size increased, the fatigue strength decreased. This can be seen by the range of fatigue failures for a given stress range. The full penetration

double-vee weld joint test data plot significantly above the the existing Category B curve (Fig. 28). The higher strength exhibited in this type of detail as compared to the single-vee type joint can be attributed to the lack of a root gap normally found with a partial penetration type weld. There were less specimens of this type detail than the single-vee and also a smaller spread in the stress range levels tested. For both types of groove welds the regression analysis yields a slope that is flatter that the existing AASHTO curve. Each individual variable tended to provide S-N curves with a slope near -3.0.

The second major group of specimens tested were longitudinally welded box members. The longitudinal groove welds used were of two types: single-bevel-groove weld and single-J-groove weld. In addition, a limited number of tests were carried out with fillet welds in the box corners. The test results are shown in Fig. 29. Almost half of the data points for the single-bevel-groove welds fall below the curve. The cycle life is about the same over a wide level of stress range. The tests with single-J-groove welds and fillet welds are limited although all fall above Category B. It seems probable that smaller flaws are developed with these joints. A possible explanation is that these particular test data are from the truss lower chord. No location of failure was given; therefore, it is difficult to classify the failure in the database. Almost all the data lie between one and two million cycles making it difficult to find a "best fit" curve. Specimens of this type need to be examined further in order to determine if these results are unique to this test or if this type of detail should be in a lower fatigue strength category.

Non-load carrying cruciform fillet welded joints represent the third basic group of specimens, corresponding to a Category C detail. The data points plot significantly above the existing curve, as shown in Fig. 30. The best fit slope is very close to the actual AASHTO slope and the variance is approximately the same. The data are well distributed which results in a more reliable regression analysis. The higher fatigue strength of these specimens resulted from improved electrodes which provided a more favorable weld profile.

All the Japanese Category B data, with the exception of the single bevel box corner welds, plot above the AASHTO Category B curve (see Figs. 28 and 29). The data cover a wide variation of stress range levels and cycles to failure. From the plot of all the data, it appears that the AASHTO curve provides a good lower bound estimate of the fatigue resistance.

3.3.4 ORE Data

The Office of Research and Experiments of the International Union of Railways (ORE) carried out a test program entitled "Bending Tests of Structures Consisting of Two Beams Welded at Right Angles" [26] which yielded unusually low fatigue test results. They showed that the fatigue strength was considerably overestimated according to the various design specifications of most railways. In some cases, the fatigue strength was found to be only half as strong as recommended by the existing regulations.

In a follow-up study, a limited number of simple specimens were tested to

determine if the earlier results were biased by the complexity of the specimens tested or if the design procedures were indeed unsafe. The investigation, "Fatigue Phenomena in Welded Connections of Bridges and Cranes" [27], was divided into a series of experiments, ten reports in all. In general, the tests were not run to compile data for developing design curves but were used to compare the test data for various details with the existing curves. Failure for the tests was defined as the point where the specimen could no longer sustain the applied load.

Specimens representing common structural members and containing commonly used details were tested under constant amplitude loading. The main variables studied included detail type and stress range. In addition, a limited number of simple specimens were tested to determine the effects of eccentricity and variable amplitude loading on fatigue strength.

The basic specimens tested were either a longitudinally welded beam or a longitudinally groove welded box beam. The welded beams with shop-welded transverse groove welds in the flanges were first tested until failure. The two halves were then turned end-for-end and groove welded under conditions simulating site work and then retested. Both the welded beams and the box beams had attachments welded to the compression flange and the part of the web in compression. Attachments were welded to the flange of box members before and after fabrication to assess the effects of residual stresses. Box beams with internal diaphragms and transverse groove welds were tested under axial loading. Finally, transverse stiffeners welded to the webs, with or

without gaps, were examined The types of specimens used in the investigation are shown in Fig. 31.

Identical specimens were tested under both constant amplitude loading and spectrum loading to check the accuracy of the Palmgren-Miner Cumulative Damage hypothesis for prediction of fatigue life. Box beams were also loaded with some eccentricity to produce distortions in the cross section. The fatigue strength was not affected; therefore, it was concluded that eccentricity of loading could be ignored.

The study yielded a relatively small number of test data. This was primarily due to the fact that the test program did not involve continued testing of a specimen after failure had taken place at one detail, and not all details were tested to failure. If a particular specimen survived beyond its predicted lower bound fatigue life, the test was often stopped. As a result, for many details tested, a regression analysis of specific detail types yielded little useful information. In addition, some failures occurred at distinct notches or at load points, making the failures difficult to evaluate. However, the data that were obtained are useful for checking the current AASHTO design curves and for providing data not represented by the original curves. This program does consider a large variety of detail types tested under a variety of stress ranges.

Longitudinal welded beams, corresponding to a Category B detail, yielded the most data of any detail type (Fig. 32). The only points that fall below

the AASHTO curve are either runouts or are points where cracking initiated at a notch (a severe defect condition). No failures occurred at stress range levels below the constant amplitude fatigue limit used for Category B. The tests were terminated at cycle lives that exceeded the extended portion of the curve.

Another detail tested was a transverse stiffener attached to the flange which corresponds to a Category C detail. Only two data points were obtained under the variable amplitude loading test. Both points fall below the constant amplitude fatigue limit (10 ksi (69 MPa)) for such a given detail, but plot above the straight line extension of the Category C curve as expected (Fig. 33). Constant amplitude tests yielded three failure points for the transverse stiffener detail and all plot above the Category C curve as shown in Fig. 33. Flange surface attachments with a length of 6.3 in. (160 mm) plotted significantly above the Category E curve defining their fatigue strength. Welded beams containing transverse groove welds, fabricated under conditions simulating both shop and field work, were examined. All the failures in the shop welded specimens plotted above the corresponding AASHTO Category B curve (Fig. 34). There are only two data points for the field welded specimens and one point plots just below the Category B resistance curve (Fig. 34).

Box sections with longitudinal groove welds yielded very disappointing results when plotted against the corresponding Category B curve. All but one of the data points plotted below the existing curve (Fig 35) which was similar to the Japanese test results (see Fig. 29).

Box sections with internal diaphragms at the midspan position were also examined. The corresponding fatigue category under the AASHTO provisions for this type of detail is Category C. All but one point plotted between the Category B and C curves, though there is not much spread in the data (Fig. 35).

Specimens containing compression flange attachments were also tested. For example, plates were fillet welded to compression flanges with their longitudinal axis either parallel or perpendicular to the longitudinal axis of the test beam. The corresponding AASHTO curve depends on the longitudinal dimension of the plate, but all failures obtained in the ORE study fall into a Category E detail (Fig. 36). Two data points plot above the curve while two points fall below the curve correspond to longitudinally welded plates.

3.3.5 English Fatigue Data

The following summarizes a test program which involved a fatigue study of improved fillet welds [28]. By shot peening the fillet welds of attachments, it was found that the fatigue strength could be increased. The weld improvement was more effective on transverse welds than on welds around the ends of longitudinal attachments. Also, the effectiveness of the shot peening was found to decrease as the stress ratio increased. The as-welded test results were extracted from the report for use in the database.

Two types of small scale test specimens were used for the test program: a

longitudinal fillet welded attachment and a transverse fillet welded attachment, the latter often called a non-load carrying cruciform detail. Each was welded to a flat 1/2 in. (13 mm) thick plate and then tested under constant cycle loading. Different stress ratios were used for the transverse attachments: 0, -1, and 0.5. The specimens are illustrated in Fig. 37.

The transverse and longitudinal attachment results are plotted in Figs. 38 and 39 respectively. The transverse attachments plot close to the Category C fatigue strength curves with approximately one-quarter of the points falling below the curve. No cracks were detected in specimens tested near the constant amplitude fatigue limit. The number of longitudinal attachment results is more limited. The longitudinal attachment specimens were all tested at a stress ratio of 0. With an attachment length of approximately 6 in. (152 mm), this type of detail results in test data between the Category E and the Category D resistance curves. All tests plot above the Category D curve. The higher fatigue strength might be contributed to the small scale specimens. If the attachments were welded to flange or web plates of beams, the increased constraint would result in higher residual stress, thereby lowering the fatigue resistance.

A second fatigue test program, conducted by the Transport and Road Research Laboratory [29], involved the study of intermittent fillet welds. Though intermittent fillet welds have been used in the fabrication of steel bridge members, test data for this type of connection is sparse. Prior to this program, no reliable test data existed at endurance levels above $2 \cdot 10^6$ load cycles.

The 33 test specimens used in the test program were welded wide flange beams. The 5/16 x 8 in. (8 x 200 mm) flanges were attached to a 5/16 x 7 in. (8 x 180 mm) web plate with 1/4 in. (6 mm) longitudinal fillet welds. Varying weld gap patterns were used in the constant moment region (Fig. 37). The different weld hit-miss ratios ranged from 1:1 to 1:25. All tests were conducted under constant cycle loading.

The results from the fatigue tests indicated that the cracking initiated at the toe of an end section of intermittent weld. No significant variation in the fatigue behavior of the different weld gap patterns was found. As shown in Fig. 40, the test data is consistent with the fatigue resistance defined by Category C. Specimens were fatigue tested without cracking at stress range levels above the constant amplitude fatigue limit. No tests were conducted below the limit. The current AASHTO fatigue provisions classify this type detail as Category E, which is obviously conservative. The use of intermittent welds will introduce many weld ends. These can have a wide range of weld termination conditions, resulting in undercutting and other weld defects. The use of this type of weld should not be encouraged, as would be the case if a higher resistance category were assigned to it.

3.3.6 ICOM Fatigue Data

Several tests were conducted by the Swiss Federal Institute of Technology (ICOM) that dealt with the fatigue life of structural details that result in high stress concentrations [30, 31, 32]. The tests were used to study and monitor fatigue crack propagation so that analytical procedures could be

developed and verified. Also studied were fatigue strength improvement techniques on structural details fabricated with high strength steels. As with other reports on improvement procedures, only the as-welded test results have been included in the database.

The tests of welded attachments generally result in a relatively low fatigue strength due to the high stress concentration occurring at the welded ends of the attachment plate. Both full-size beam specimens and small flat plate test specimens were used. For the full-size specimens three types of attachments were tested: rectangular gusset plates welded to the flange tip, flange tip gusset plates with ground weld toes, and rectangular web gusset plates. The ground weld toes had radii that ranged between 0.4 to 2.8 in. (10 to 70 mm). All tests were conducted under constant amplitude loading with the nominal stress range between 8 and 20 ksi (55 and 138 MPa). For the smaller specimens, the attachments were welded to flat plates with 3/16 in. (4 mm) fillet welds. The attachment plates, 4 in. (100 mm) in length, were either welded flat (simulating a coverplate type detail) or welded on edge in the transverse direction. These were tested at stress ranges varying from 12 to 35 ksi (83 to 241 MPa). The detail types are illustrated in Fig. 41. Also tested were web stiffeners welded to the flange and flange surface attachments.

Plain welded beam test results are shown in Fig. 42. The data plot consistent with the Category B resistance curve. The web stiffener data plot at the Category B curve, though the three failure points are grouped

together. Also shown in Fig. 42 are the results for the 8.0 in. (200 mm) long fillet welded rectangular web attachments. The data points all fall above the Category E curve. This is consistent with other test results on web attachment lengths greater than 6 in. (150 mm).

Figure 43 shows flange tip attachments, both rectangular plates and plates with ground radius transitions. The 8 in. (200 mm) length of the rectangular plate classifies the detail as Category E. As Fig. 43 illustrates, both the groove welded and fillet welded details are consistent with this design curve. Though the groove welded rectangular plates had dressed or ground weld ends, their resulting fatigue resistance was not significantly higher than the as-welded fillet welded plates. The results of the flange tip attachments with radius transitions all resulted in fatigue strengths exceeding the minimum specified by the current specifications, although all tests were performed at a stress range of approximately 20 ksi (138 MPa). The fillet welded details with a radius transition of less than 2.0 in. (50 mm) and the groove welded details with 2.8 in. (70 mm) radius both resulted in comparable fatigue strengths with the 2.8 in. (70 mm) radius providing a slightly higher resistance, though the data are limited and not well distributed.

Flange surface attachments were also tested and are shown in Fig. 44. Both the 2 in. (50 mm) and 4 in. (100 mm) length details gave results consistent with the Categories C and D curves, respectively. The 8 in. (200 mm) long details resulted in fatigue strengths greater than that defined by the Category E curve, plotting at or above the Category D curve.

The small plate specimens with 4 in. (100 mm) long attachments plotted above the Category D curve, as shown in Fig. 45. The majority of the test data plots above the Category C resistance curve. The plate attachments welded to the beam flange are given in Fig. 45 and plot near or above the Category C curve.

3.3.7 East German Fatigue Data

A series of fatigue tests was conducted in conjunction with the development of the fatigue specifications for steel structures in East Germany [33]. The primary objective of the program was to study the load capacity of different welded structural components so that they could be classified according to their fatigue resistance. Also studied was the effect of stress ratio on fatigue strength; both cyclic tension and reversal tests were carried out. It was concluded that the stress range concept could be used in the new edition of the specifications of steel structures in East Germany.

The test specimens for this program were welded beams with different types of attachments. They included flange tip attachments with 8.0 in. (200 mm) long rectangular plates and longer plates (12.5 to 17.7 in. (317 to 460 mm)) with end radii of approximately 2.5 (63 mm) and 6.0 in. (150 mm)(see Fig. 46). Plates were also welded to the flange surface. They were either welded flat or welded on edge in the transverse direction. Coverplate details were also tested. The different detail types are shown in Fig. 46. The specimens were run under constant cycle loading at two different stress ratios: -1.0 and 0.5.

The results of the test program are plotted in Figs. 47 thru 49. Figure 47 shows the test data for the flange tip attachments. The results are consistent with the findings of the original NCHRP studies. The rectangular plates, with a length of approximately 8 in. (200 mm), provide a fatigue resistance corresponding to Category E. When an end radius was used, the fatigue resistance increased, although the data is scattered between the Category D and C curves and extend beyond Category C as well.

Figure 48 summarizes the results for attachments welded to the flange surface. When the plate was welded on-edge in the transverse direction and the attachment length was 2.0 in. (50mm), the data plotted well above the Category C resistance curve. Beams with attachments welded flat with a length of approximately 6 in. (150 mm) in the longitudinal direction provided a fatigue strength best defined by Category E. These test results are consistent with the original NCHRP findings.

The coverplated beam data are plotted in Fig. 49. The test results provide a reasonable scatter distribution above the Category E curve. This is consistent for coverplates attached to beam flanges with a thickness of approximately 0.5 in. (13 mm).

3.3.8 West German Fatigue Data

A research program was conducted which examined the fatigue strength of welded high strength steels in the as-welded and TIG-dressed condition [34]. Pilot tests with small specimens showed a significant increase in fatigue

strength when TIG- or Plasma-dressing was used to improve fatigue resistance. One objective of the study was to evaluate the applicability of the test results on small-scale specimens to full-size welded beams.

Constant amplitude fatigue tests were performed on both rolled and welded high strength steel beams with 65 and 100 ksi (448 and 690 MPa) yield stresses. All tests were run at a stress ratio of 0.1. The detail types examined were: web stiffeners welded to flanges, staggered splices, and flange butt welds. Both TIG-dressed and as-welded conditions were examined on each type of detail. The detail types are shown in Fig. 50.

This test program consistently yielded results that were significantly below the predicted strength of each detail type tested. The main reason for the reduced fatigue strength was reported to be due to welding deficiencies, namely hydrogen induced cold cracking and weld undercutting. Figure 51 shows the test results for the Category B type details: the plain welded beams and the flange transverse groove weld. For both detail types most of the test data fall below the resistance curve for Category C. The stiffener detail test data are plotted in Fig 52. Again all the data fall significantly below the curve that defines the fatigue strength. Approximately one-half of this data would plot below the Category E curve. With all the data falling below the minimum level of fatigue strength due to substandard welding procedures, these data were excluded from further consideration in this report.

3.3.9 Canadian Fatigue Data

Two separate studies by Kulak et al. have been included in this survey of fatigue test data. One dealt with full-scale web attachments [35] while the other examined the effects of backing bars on the fatigue strength of transverse groove welds [36].

The web detail study examined two types of web attachments: plates intersecting the web plate and lateral bracing attachments (gusset plates). Six rolled beams were fabricated, each with two different web attachments. For one detail, a 3/4 x 12 in. (19 x 300 mm) long plate passed through a flame cut opening in the web. The other consisted of two 3/4 x 6 x 12 in. (19 x 150 x 300 mm) plates welded to each side of the web plate. For both details, 1/4 in. (6 mm) continuous fillet welds were used to attach the plates to each side of the web. Two fillet welded gusset plate details (lateral bracing attachments) were examined on a total of nine rolled beams. Three of the beams had 24 in. (610 mm) long gusset plates with tapered ends. On one detail the end welds were ground smooth. The remaining six beams were fabricated with a ground circular transition gusset plate, 29 in. (736 mm) long with a 4 in. (100 mm) radius. For both details the plates were coped to accommodate a vertical stiffener. The detail types are shown in Fig. 53.

Figure 54 gives the results for the 7 in. (180 mm) long web plate attachments. Since their lengths were greater than 4 in. (100 mm), and their thicknesses less than one inch (25 mm), they would correspond to a Category E type detail. The test data are in good agreement with this resistance

curve. No significant difference in fatigue strength was observed between the through web detail or the discontinuous plate detail. The beam webs were 1/4 in. (6 mm) thick and this resulted in cracks forming at the fillet weld toes rather than at the weld root.

The web gusset plate results are plotted in Fig. 55. The transition radius (4 in. (100 mm)) details plotted near or beyond the Category D curve, and are consistent for a total attachment length of 29 inches (736 mm). The tapered end condition did not improve the fatigue strength of the detail. All but one data point for the gusset plates with tapered ends plotted between the Category D and E curves. This is about the same variability observed at coverplate ends.

A limited study was conducted in order to examine the effect of backing bars on the fatigue strength of transversely loaded groove welds. Only one simple plate specimen configuration was tested; its dimensions are shown in Fig. 53. The results from this test are given in Fig. 56, plotted against the Category B and C curves. All failures initiated on the flush-ground side of the groove weld and were likely caused by secondary bending stresses. As indicated by the scatter of the data, the Category C curve provides a lower bound to the test data for this particular detail type.

3.3.10 Weathering Steel

Two separate studies investigated the fatigue characteristics of weathering steel; one by Albrecht [37] and the other by Yamada [38]. Both test programs used plate specimens fabricated with automatic submerged arc welds which resulted in very good profiles. The specimens were tested under constant amplitude load conditions. Each program examined unweathered and weathered specimens. The weathered specimens were subjected to varying degrees of atmospheric exposure prior to testing. The tests did not simulate actual field conditions since the weathering process was not continued during the actual fatigue testing.

The Albrecht study involved the fatigue testing of 176 specimens that either simulated a transverse stiffener detail or an attachment plate. The stiffener type specimens were 1.0 in. (25 mm) and 0.4 in. (10 mm) thick plates, smaller than similar cruciform specimens used in other studies. The test results all exceeded the Category C resistance curve. The attachment specimens consisted of a 4 in. (100 mm) long plate welded around the entire perimeter to a base plate, similar to the NCHRP report 188 test results shown in Fig. 17. This would normally correspond to a Category D type detail. An schematic of this specimen may be seen in Fig. 57. The specimens were fatigue tested as-fabricated (unweathered), after two years of exposure, and after they were weathered for four years.

The results from this study are plotted in Fig. 58 and compared with the Category D resistance curve. All data plot significantly above this curve just as observed with the small scale simulated tests shown in Fig. 17.

The Yamada study used two different types of plate specimens: non-load carrying cruciform joints and a gusset plate type specimen. The detail types are shown in the lower portion of Fig. 57. Both weathering steel and standard structural steel were used for the specimens. The cruciform stiffener specimens consisted of two transverse attachments welded to a 1/2 x 3 in. (13 x 75 mm) base plate. The gusset specimens were fabricated with two longitudinal attachment plates, each 4 in. (100 mm) long, welded on edge to the base plate. The specimens were fatigue tested as fabricated, after they were weathered for two years, and after four years of exposure. In addition, stiffener type details were cut out of the web of an actually weathered steel bridge that had been in service for approximately 5.5 years.

Figure 59 shows the results of the fatigue failures for the cruciform joints. All failures plot beyond the Category C curve. The gusset plate specimen results are compared with the Category D resistance curve in Fig. 60. Again the test data fall significantly above the resistance curve.

3.4 Proposed Fatigue Design Curves

The current AASHTO fatigue design curves (except Category E′) were developed from the test results and data analysis provided in NCHRP Reports 102 and 147. Although a large number of test results were generated from these programs, the number and variety of detail types tested were limited. The design curves were developed from linear regression analyses of the data using the 95 percent confidence limits defining the lower bounds of the fatigue resistance. This resulted in a set of curves which varied slightly in slope since the actual computed slopes were used. These curves have since been used to define the fatigue strength for other types of welded bridge details based on geometric similarities and test results that correspond to the originally tested detail types.

As the database for a given detail has increased it has generally been observed that the slope of the S-N curve tends to stabilize to a slope of -3.0. This can be seen from the NCHRP studies on coverplated beams summarized in Fig. 8. The regression analysis of the test data provides a slope that is -3.02. This large well distributed set of data is an exception. Generally, the specific data sets that were reviewed were found to be limited in number, or the data were not well distributed along the S-N curve. No other test program, other than the original NCHRP studies, resulted in a data set that was sufficiently distributed for a regression analysis. Often data were clustered over a small increment of stress range, and any number of regression lines could be used to describe the relationship between stress range and life. This becomes most evident for the higher strength Categories A

and B. For these higher strength details the data are bounded by the constant amplitude fatigue limit and the yield stress of the steel. This often results in a relatively limited range of stress and a grouping of the data points.

Another factor that influences the regression analysis for a particular data group is the variability that exists between test programs. For a given test series, the distribution of the initial flaws, residual stress fields, weld profile, and specimen size are controlled and are therefore similar. These factors play a major roll when different sets of data are grouped together. Of particular importance is the defect size. This was noted in the Japanese studies (Ref. 15) where each series of tests yielded a slope near -3.0. When these tests were combined, major deviations existed between series and this resulted in a wide variation of the test results and also caused the slope provided by the regression analysis to change.

For the majority of welded details used in welded steel structures, the number of cycles for crack initiation is small and the fatigue life can be attributed to crack propagation alone. Numerous crack growth studies have demonstrated that the crack growth rate is reasonably related to the third power of the stress intensity range [39]. This relationship has been used in most analytical studies where fracture mechanics of crack growths have been examined. This has also led to good agreement between the experimental tests on welded details and the theoretical prediction of fatigue life. The crack growth relationship has been used to evaluate service failures and was also used to develop the design resistance curve for Category E′.

As reported in NCHRP Reports 188 and 267, variable loading studies have shown that the use of an exponent of -3.0 and Miner's Rule provide a reasonable estimate of variable stress cycle cumulative fatigue damage. Variable loading is what a bridge structure experiences from normal traffic, not the constant cycle loading used in most of the tests that the fatigue design curves have been developed from. The variable load test results plotted in Figs. 15 thru 18 show that a slope of -3.0 provides good agreement with the resistance curves. This is particularly true in the long life regions applicable to most bridge structures. All tests indicate that the straight-line extension at a slope of -3.0 is an appropriate lower bound estimate.

Recognition of the relationship between crack growth and the experimental results on welded details has led to the adoption of a slope of -3.0 for other design S-N curves. This was first adopted when the NCHRP test data was used to develop the S-N relationships used in the draft Swiss Fatigue Provisions in 1974 [40]. Since that time, a slope of negative three has been adopted in the British standard [41] and more recently in the recommendations adopted by the European Convention Constructional Steelwork (ECCS) fatigue specifications [42]. These criteria are also being considered by the International Organization for Standardization (ISO).

The proposed "European Fatigue Strength Curves" (ECCS) are an attempt to provide uniformity to the fatigue design curves. The curves are based on most of the same fatigue data considered in this study. This includes the

ORE program, the initial NCHRP Reports, as well as data from other sources. The ECCS curves define a set of equidistant log-log S-N curves that can be used to classify fatigue data regardless of origin or type. That is, test data for a particular detail can be compared with these curves and a specific curve chosen to define its fatigue strength. In this way uniformity is maintained since there is no need to develop a new curve for each new detail.

The proposed ECCS fatigue curves are shown in Fig. 61. They consist of fifteen equally spaced curves on a log-log scale. The vertical spacing corresponds to an approximate 10 percent variation in fatigue strength. The slopes of all curves are equal to -3.0 in the life range up to $5 \cdot 10^6$ cycles. At $5 \cdot 10^6$ cycles two options are provided. One option changes the slope to -5.0 until $50 \cdot 10^6$ cycles where a cut off is provided. The intercept at $50 \cdot 10^6$ cycles establishes a fatigue limit regardless of the type of loading. All cycles below this limit can be ignored when evaluating fatigue damage. The second option is provided by the dashed lines which correspond to a straight line extension of the -3.0 slope S-N curves. The reference fatigue strength or detail category identification is the stress range value at $2 \cdot 10^6$ in MPa.

The proposed ECCS fatigue curves in their entirety have several shortcomings. The test data review provided in Figs. 4 to 60 indicates that the accuracy of a set of fifteen different classes of fatigue resistance is questionable. It does not seem reasonable to define the resistance of welded steel details with the accuracy that this number implies. The adoption of a constant cycle fatigue limit at $5 \cdot 10^6$ cycles for all details is not compatible

with the actual fatigue test data, as can be seen in the test data plots. The test data indicate that the constant cycle fatigue limit occurs at increasing cycles as the severity of the detail increases. For a high fatigue strength detail (i.e. Category A) this limit is near $2 \cdot 10^6$ cycles. For a severe fatigue strength detail this limit is reached near $20 \cdot 10^6$ cycles. Finally, the use of a -5.0 slope for fatigue resistance below the constant cycle fatigue limit is not in agreement with the random variable fatigue results shown in Figs. 15 through 18. Test results support the use of -3.0 for all stress cycles.

When the ECCS fatigue design curves are compared to the existing AASHTO curves it becomes evident that the differences are not great, as can be seen in Fig. 62. The six AASHTO curves (A thru E′) are the heavier lines and correspond closely to six of the ECCS curves. A tabular comparison of the two sets of curves is given in Table 4. The slope of several AASHTO curves are slightly different since they were based on the results of a regression analysis, whereas the ECCS curves all have a slope of -3.0. In general, the fatigue resistance is slightly less at higher cycle life when the fatigue strength is defined by the ECCS curves. The most significant difference is the constant amplitude fatigue limits. For Categories A thru C, the ECCS limits are lower, while for Categories D to E′, the AASHTO limits are lower.

The results of this review suggest that adjustments should be made to the current AASHTO fatigue design curves. The slope of these curves should be established at -3.0 and thus be compatible with the sloping portions of the

corresponding ECCS/ISO curve and bring uniformity to the world's fatigue design provisions. This adjustment is shown in Fig. 63. A cross bar has been placed above the category letter in order to distinguish between the proposed and current categories and curves. The cross bar notation will be used throughout the remainder of the report. In addition, since the review of the fatigue data demonstrated that Category B overestimated the fatigue strength of certain longitudinal groove welds, a curve has been added which corresponds to a new category, $\overline{B}'$.

The proposed curves were developed using the stress range intercept values at $2 \cdot 10^6$ cycles. The constant amplitude fatigue limits for each curve, with the exception of Category $\overline{E}$, correspond to their current values as the review of the data did not indicate a need to change these values. High cycle fatigue test results of coverplated beams indicated 4.5 ksi (31 MPa) provided a better estimate of the fatigue limit than the current 5.0 ksi (34.5 MPa) value. For Category $\overline{B}'$, a constant amplitude fatigue limit of 12.0 ksi (83 MPa) has been used. The stress range intercept values for $1 \cdot 10^5$, $5 \cdot 10^5$, and $2 \cdot 10^6$ cycles as well as the constant amplitude fatigue limits for each proposed curve are given in Table 5.

The major difference between the existing and proposed curves is their slope. With the exception of Category A, the $2 \cdot 10^6$ intercept values for the two sets of curves are identical. The majority of the existing curves have a slope which is slightly greater than -3.0. Because of this slope difference the proposed curves result in a slightly higher fatigue resistance in the low cycle

regime. The current AASHTO design provisions [5] were based on Miner's Rule and the assumption that the slope of the fatigue resistance curve was -3.0. Hence, the damage estimate was compatible with the damage that would result from the relationships shown in Fig. 63. This same assumption was used in Ref. 12 when evaluating the growth of cracks in steel bridge structures.

3.5 Comparison of Test Data with Proposed Fatigue Resistance Curves

The proposed set of fatigue design curves (Fig. 63) are compared with all available test data in this section. The data are reviewed in order of detail category, beginning with Category $\overline{A}$. Where the fatigue resistance is a function of the detail geometry, as is the case with web and flange attachments, the data is plotted as a group with the corresponding curves.

Initial analysis of the database for a particular detail type indicated that a rigorous regression analysis was of limited, practical use. As discussed in the previous section of this report, many variables influence a regression analysis. This is particularly true when results from different test programs are combined and analyzed. Complete regression analyses were performed on all detail groups and the results may be found in Ref. 2.

By comparing the test data with the proposed curves their adequacy can be analyzed. The data for a particular detail type should be distributed above the lower bound provided by these fatigue resistance curves. Since these curves represent the 95% lower confidence limits, most of the test data should plot above the curve. Furthermore, test data for a particular detail should not deviate significantly from the applicable curve. Table 6 gives the number of data points plotted for each detail type in the figures referred to in comparison of all the test data with the proposed fatigue resistance curves. Since the data from each test program have been individually compared to the current AASHTO fatigue curves and only minor changes have been made, no significant variation should occur.

3.5.1 Base Metal

For the Category $\overline{A}$, no additional test data have been acquired since the results were reported in NCHRP reports 102 and 147. The database is provided by plain rolled beams without any welded connections or attachments. The fatigue design condition seldom governs as the stress range is usually limited by a detail with lower fatigue strength. The test data are plotted in Fig. 64 and compared with the $\overline{A}$. All failure points plot above the resistance curve.

3.5.2 Longitudinal Welds

The data from continuous longitudinal welds are given in Fig. 65. These only include data from web-to-flange longitudinal fillet welds and from large flat plate specimens with single and double bevel groove welds. The review has resulted in a sizable increase in the number of test data for these types of details. Altogether, 350 test values are shown in Fig. 65. The data are well distributed above the Category $\overline{B}$ curve with few points falling below. The constant amplitude test points shown below the constant amplitude fatigue limit are failures from the original NCHRP test program. Several flange splice detail specimens yielded fatigue crack failures outside the splice transition zone and were therefore classified as longitudinal weld detail failures. The cracks originated at poor weld repair locations and were independent of the steel yield stress. The remaining failures plotting below the constant amplitude fatigue limit are test results from variable amplitude studies.

3.5.3 Transverse Flange Splices

The flange splice data are compared with both the Category $\overline{B}$ and $\overline{B}'$ curves in Fig. 66. The types of details included in the data are: flange splices with both curved and tapered transitions, and flange groove welds in both box girders and welded beams. While the majority of the failure points plot above $\overline{B}$, a number of points fall below. These are primarily the straight tapered flange splices in A514/A517 high strength steel. The current specifications require a 2.0 ft. (0.61 m) transition radius when A514/A517 steel is spliced. An alternative would be to classify straight tapered transitions in A514/A517 steel as Category $\overline{B}'$. The test results for flange transverse groove welds in box and plate girders also provide a fatigue resistance that is consistent with the $\overline{B}$ category. All constant cycle tests at stress ranges below the constant amplitude fatigue limit showed no evidence of cracking at the time the test was discontinued. No variable cycle test data are available.

3.5.4 Box Girder Longitudinal Welds

As the data review revealed, the fatigue resistance of full size partial penetration longitudinal groove welds was overestimated by the $\overline{B}$ category. The available test data are compared with the Category $\overline{B}'$ curve in Fig. 67. All but one test plots above the curve. The proposed curve provides a more accurate lower bound fatigue strength for this detail. The decreased resistance is due to size effects, both in the initial flaws and in the geometry of the detail. Larger initial defects were found to develop in the large scale

sections as a result of blowholes and root gap flaws. These defects appear to be larger than the discontinuities observed in fillet welds. This same condition has been observed in longitudinal groove welds with backing bars left in place. The longitudinal fillet weld data show no reduction in fatigue strength, indicating that Category $\overline{B}$ remains adequate for this type of weld.

3.5.5 Transverse Stiffeners and Diaphragms

The transverse stiffener data are compared with the proposed Category $\overline{C}$ curve in Fig. 68. No failure points fall below the lower bound limit. Included in the plot are web stiffeners with their end cut short or welded to the flange and internal diaphragms in box girder members. Each detail type resulted in comparable fatigue resistance. The two test results plotting below the constant amplitude fatigue limit are the result of variable amplitude loading. Both tests plot beyond the straight line extension of the resistance curve. The effective stress range based on Miner's Rule provides a reliable estimate of the fatigue strength under this type of loading.

3.5.6 Web Attachments

The Current AASHTO fatigue code does not provide for thickness effects on the attachments. As indicated in Fig. 69, the plate thickness influences the fatigue resistance of the detail. Since all tested details had an attachment length greater than 4.0 in. (100 mm) or 12.0 times the thickness, the maximum fatigue strength would be correspond to Category $\overline{E}$. But with a 1.0 in. (25 mm) thickness or greater the resistance of the detail is reduced to Category $\overline{E}'$. Extensive results on 1.0 in. (25 mm) thick attachments

subjected to variable amplitude loading were also obtained and are plotted in the high cycle region. These also confirm the applicability of Category $\overline{E}'$ to this detail.

3.5.7 Web Gusset Plates

Although web gusset plates are a form of web attachment, they have been plotted separately in Fig. 70. These tested details are usually associated with lateral bracing elements and frequently have a vertical stiffener passing through the plate. The web gusset plates that have been included in the database all have a minimum attachment length of 24 in. (600 mm), therefore the detail corresponds to Category $\overline{E}$. The plot indicates that the failure data are well distributed above the curve. No difference in fatigue resistance was indicated when tapered ends were used, this being primarily due to the long attachment length. The details with a 4 in. (100 mm) radius transition provided a fatigue resistance equal to Category $\overline{D}$, similar to other fillet welded attachments with a radius transition.

3.5.8 Rectangular Flange Tip Attachments

Figure 71 shows the fatigue data for attachment plates welded to the flange tips. The plates were all rectangular in shape, without any treatment of the end condition. In all cases the attachment length was greater than 4.0 in. (100 mm), which would classify the detail fatigue strength as Category $\overline{E}$. Only three of the points fall below the curve.

3.5.9 Flange Tip Attachments with Transition Radius

When a ground transition radius is used at the ends of an attachment plate welded to the flange tip, the fatigue strength is increased (Figs. 72 and 73). All test specimens had the longitudinal attachment length greater than 4.0 in. (100 mm), which corresponds to Category $\overline{E}$ without any end treatment. All groove welded test data (Fig. 72) plotted above the Category $\overline{C}$ curve when the termination had a radius equal to or greater than 2 in. (50 mm). Many of the tests were stopped without any evidence of cracking. These test data are identified by arrows. Fillet welded transition radius details (Fig. 73) do not appear to be able to provide the fatigue resistance attainable with groove welded details, just as was observed with the web attachments.

3.5.10 Flange Surface Attachments

When the attachment plate is welded on the flange surface, the fatigue strength is also governed by the longitudinal length. The test data plotted in Fig. 74 show reasonable correlation with the current specifications. When plates are welded transverse to the flange, the attachment length is the thickness of the plate. The length in the direction of stress was less than 2.0 in. (50 mm) for all test specimens. All test data provided a fatigue resistance that equals or exceeds Category $\overline{C}$. For intermediate attachment lengths between 2.0 and 4.0 in. (50 and 100 mm) the fatigue resistance is defined by the Category $\overline{D}$. The test data for 2.0 in. (50 mm) attachments plots at the Category $\overline{C}$ curve. The 4.0 in. (100 mm) attachment test specimens plot between Category $\overline{C}$ and $\overline{D}$. The long attachment details, with lengths greater than 4.0 in., gave results consistent with the Category $\overline{E}$.

3.5.11 Coverplated Beams

The fatigue data for coverplated beam details are summarized in Figs. 75 to 77. For coverplated beams with a narrow plate (width of the coverplate less than the width of the flange) and with or without transverse end welds, the fatigue strength is adequately defined by the Category $\overline{E}$ curve as shown in Fig. 75. All fatigue test data in this plot correspond to a beam flange thickness less than 0.8 in. (20 mm). The treatment of the end weld condition had no influence on the fatigue strength. This was found true for details with or without a transverse end weld. It can be seen that several of the variable amplitude tests fell below the resistance curve when Miner's Rule was used to determine the effective stress range.

Figure 76 shows the test data for wide coverplated beams in which the coverplate overlaps the beam flange. As indicated in the plot, the end weld condition influences the fatigue life. The details with a transverse end weld gave a fatigue resistance corresponding to Category $\overline{E}$, as did beams with a narrow coverplate. When no transverse end weld was used, the strength was decreased to $\overline{E}'$. This decrease in strength results because crack growth initiates at the flange tip. This results in a more severe crack geometry and a reduction in fatigue strength.

When the beam flange thickness is increased above 0.8 in. (20 mm), the fatigue strength is further reduced to Category $\overline{E}'$ as shown in Fig. 77. All data are for narrow coverplate specimens. It is not presently known if thick beam flanges with wide coverplates will result in a further reduction in fatigue resistance.

3.5.12 Simulated Specimens

Figures 78 to 80 summarize test data from smaller flat plate specimens that simulated design details. While these smaller type specimens were fabricated and tested to simulate full scale details, the majority of the test data plot significantly above the lower bound fatigue resistance curve defining the strength of the large scale detail. Figure 78 gives the non-load carrying cruciform joint data. With the exception of the English data, the remaining data all plot well above the Category $\overline{C}$ curve. In Fig. 79 short longitudinal attachments (plates welded on edge) plot well above the Category $\overline{D}$. Most specimens had an attachment length of 4.0 in. (100 mm), so their classification would be Category $\overline{D}$. The specimens with the attachment welded flat and the attachment length of approximately 4.0 in. (100 mm) are given in Fig. 80. These test data are also scattered significantly above the Category $\overline{D}$ curve although the distribution is more consistent and the lower bound test results plot near the Category $\overline{C}$ curve. The test data indicate that small scale specimens overestimate the fatigue resistance of full scale welded details.

4. Recommendations and Applications

The findings of this study should be of value to structural engineers involved in the design of welded steel bridge components, researchers working in the subject area, and members of specification writing bodies. The suggested revisions to the AASHTO *Standard Specifications for Highway Bridges* included here warrant consideration. These suggested revisions can also be applied to other specifications, such as those of the American Institute of Steel Construction and the American Railway Engineering Association. The findings of this report resulted from a comprehensive review and analysis of all pertinent fatigue test data on welded steel bridge details. The adjustments to the current design specifications need immediate consideration in order to reflect these findings.

The results of this study have shown that minor adjustments should be made to the current AASHTO fatigue design curves. The adoption of the set of curves shown in Fig. 63 would better reflect the results from the expanded fatigue database and would be consistent with fatigue resistance curves used in other countries and being considered for adoption by the ISO.

1) The adjustments made to the current AASHTO fatigue design curves were derived from a larger, more comprehensive database. The proposed curves are a result of an analysis that examined a wider variety of detail types and more extensive test data. They provide a better estimate of the fatigue resistance of welded bridge details.

2) The use of a -3.0 slope for the resistance curves better reflects the increase in the fatigue test database. Regression analysis has shown that as the sample size for a given detail increases, the slope of the S-N curve tends to converge to a slope of -3.0.

3) The review of longitudinal groove welds has shown that the fatigue strength of this type of detail is overestimated by the Category B design curve. It was found that a more accurate estimate would be provided with a new resistance curve identified as Category $\overline{B}'$. In addition, the limitations placed on the use of straight tapered transitions for flange splices in A514/A517 high strength steels could be incorporated into the the Category $\overline{B}'$ curve.

4) Table 5 shows the stress range values that result from the proposed S-N curves for cycle lives defined in the AASHTO Specifications. The maximum deviation between the proposed and current design values is 10 percent.

5) In order to provide a more rational and consistent criteria for non-redundant members, a uniform reduction of 20 percent has been applied to the allowable stress range values at 100,000, 500,000, and 2,000,000 design cycles. The 20 percent reduction provides uniformly the minimum reduction that was used in the earily versions of the AASHTO specifications. It should be noted that the revised allowable stress range values are analogous to designing the structure for a 25 percent higher load. The design values for more than 2,000,000 cycles were retained from the current specifications as

these correspond to the fatigue limit or a modest reduction for the higher fatigue strength details. For the lower fatigue strength details, more substantial reductions were introduced to discourage the use of low fatigue resistant details. The allowable stress range values for non-redundant load path members are shown in Table 7.

6) The family of equations that define the proposed curves only differ in the value of their intercept. Table 8 provides the intercept coefficients for each of the proposed curves.

7) Corrections and additions to the AASHTO connection descriptions and conditions are given in Table 9 (a revision to Table 10.3.1B, AASHTO 1983). The illustrative examples of detail types that correspond to Table 9 are shown in Fig. 81 (a revision to Fig. 10.3.1C, AASHTO 1983). The current AASHTO descriptions are given in Table 10 for comparative purposes. The connection descriptions have been revised to reflect the findings of this study. The major changes are described hereafter:

- Category $\overline{B}'$ for continuous partial penetration groove welds or continuous full penetration groove welds with backing bars not removed in built-up members.

- Category $\overline{E}'$ for coverplates wider than the flange without welds across the ends in redundant load path members.

- A clarification of Category $\overline{B}$ for full penetration groove welded flange splices with 2 ft. (0.61 m) radius transitions in width for all steel types.

- Category $\overline{B}'$ for full penetration groove welded splices of A514/A517 base metal with tapered transitions.

- Category $\overline{C}$ for full or partial penetration groove welded attachments with detail lengths less than 2 in. (50 mm).

- Category $\overline{E}'$ for both groove and fillet welded attachments with lengths greater than 12 times the plate thickness or greater than 4 in. (100 mm) when the attachment plate thickness is 1.0 in. (25 mm) or greater.

- Expansion of description for groove and fillet welded attachments with radius transitions.

- Provision for transversely loaded fillet welds for cases where weld and plate sizes reduce the fatigue resistance of the connection below that of Category $\overline{C}$ due to lack of fusion at the weld root [43].

- Separate classification of longitudinally and transversely loaded groove or fillet welded attachments.

- Prohibition of transversely loaded partial penetration groove welds.

- Clarification of the prohibition of gusset plates attached to girder flange surfaces with only transverse fillet welds.

5. Conclusions

The conclusions in this chapter are based on an analysis and evaluation of existing fatigue test results on welded steel bridge details. The test data were compiled from a number of independent test programs that were conducted during the last twenty years. The conclusions are based on a review of all available test data analyzed as a whole without relying on the results from any one particular test program.

5.1 Test Data Acquired Since 1972

1) The review of the test data that have been produced since NCHRP Reports 102 and 147 were published has significantly increased the database for welded steel details. The current AASHTO fatigue resistance curves were based on approximately 800 fatigue test failure results. The review, as outlined in this report, has added 1500 additional test results to the database.

2) New types of details that were not previously considered in the original provisions have been added to the database. This includes longitudinal groove welds in both flat plate specimens and in box members. Internal diaphragms for box type members were also included. Large scale coverplate and web attachment details that provided information on size effects. Also, a wider range of flange attachment details with varying geometries and weld condition results have been added to the database. A number of large simulated test specimens were examined, such as gusset attachments and non-load carrying cruciform joints.

3) The comparison of the test data with the current AASHTO fatigue provisions did not result in any major deviations between the design fatigue strength and test results. Almost all data for each detail type plotted above the appropriate curve defining its lower bound fatigue resistance.

4) The findings that were reported in the original NCHRP reports have been supported by the subsequent test programs. No indications were given in these new reports that the NCHRP results were in error.

5.2 Inadequacies of Current Fatigue Provisions

1) Partial penetration longitudinal groove welds such as those used in box-type or built-up members were found to exhibit a fatigue strength that was overestimated by the Category B resistance curve. The original longitudinal weld detail strength was based on test results with fillet welds providing the web-to-flange connections. The test data indicate that partial penetration groove welds can result in a more severe initial defect condition, thereby decreasing their fatigue strength below Category B.

2) Web attachments with the plate thickness greater than 1.0 in. (25 mm) resulted in a fatigue strength that was less than that provided by the Category E resistance curve. It was found that Category E′ gave a more reasonable lower bound estimate of the fatigue resistance of this detail.

3) Additional fatigue tests of coverplated beams in the high cycle region have indicated that the constant amplitude fatigue limit for Category $\overline{E}$ is more accurately defined by a stress range value of 4.5 ksi (31 MPa) rather than the current value of 5.0 ksi (34.5 MPa).

5.3 Proposed Fatigue Design Curves

The adjustments to the AASHTO fatigue design curves presented in this report provide a better fit to the test data, and are compatible with crack propagation concepts and cumulative damage theories. The following statements summarize the basis for these changes:

1) The test data review was generally in good agreement with the current AASHTO curves. Large samples of test data for a given detail tended towards a better fit when the slope was a constant value of -3.0.

2) The proposed curves coincide with the current resistance curves at the $2 \cdot 10^6$ intercept values. The exception is Category $\overline{A}$, which showed a slight change. The tabularized form of the curves showed only minor deviations at all life increments.

3) The proposed curves would provide more compatibility between the AASHTO fatigue provisions and the fatigue resistances adopted or under consideration in many other parts of the world (i.e. the ECCS and ISO provisions).

4) A seventh resistance curve, Category $\overline{B}'$ is required to provide a better estimate of the fatigue strength of partial penetration longitudinal groove welds and longitudinal welds with backing bars. The fatigue test data for these types of welds have provided a fatigue strength significantly lower than that defined by Category B.

5) The proposed curves are easily described in mathematical terms. They can be defined by one equation with only a varying intercept value. The use of an equation in design and damage assessment procedures should lead to more accurate estimates. The estimated life for each category is tabulated at four discrete intervals. The equations would provide a continuous relationship between stress range and cycle life and would therefore avoid inaccurate extrapolation.

6) Comparisons of the test data with the proposed curves indicated that they adequately defined the fatigue resistance of welded steel details commonly used in the design and fabrication of bridge structures.

6. Recommendations for Further Research

The fatigue test data reviewed in this report significantly increases the knowledge base on the fatigue strength of welded steel connections and details. Detail types were examined that had not been previously considered in the studies reported in NCHRP Reports 102 and 147. Nevertheless, this study has indicated that the database is still incomplete.

1) Studies are needed to provide rational design criteria for welds in shear. The Category F resistance values are based on test data on small samples and a variety of fillet weld geometries. These included longitudinal and transverse fillet welds, plug and slot welds, and combinations of these weldments. The resistance curve in use today has a slope of -5.0. Furthermore, the high cycle, low stress range conditions are not well defined. Most test specimens were fabricated with 1/2 in. (12mm) plate so that the weld root condition is not as critical as provided by thicker plates that result in larger lack of fusion areas.

2) Additional work is needed in the extreme life region of most categories of joints in order to establish the constant cycle fatigue limits. Only coverplated beams defined by Category E and E′ have been tested to 10^7 and 10^8 cycles. Substantial differences exist between the values assumed by the ECCS/ISO proposed resistance values and the values suggested in this report.

3) Further study of size effects in the coverplate detail is needed. The reduction of fatigue strength from Category $\overline{E}$ to $\overline{E}'$ is currently based on

the flange thickness. The existing database does not allow for an adequate parametric study to determine the influence of the coverplate thickness or weld size used in attaching the coverplate to the flange. In general, this detail type is the most severe and, therefore, the most critical for bridges in service.

References

[1] AASHTO.
Standard Specifications for Highway Bridges, Thirteenth Edition.
American Association of State Highway and Transportation Officials, 1983.

[2] Keating,P.B., Halley,S.A., and Fisher,J.W.
Fatigue Test Database for Welded Steel Bridge Details.
Fritz Engineering Laboratory Report 488.2(86), Lehigh University, May, 1986.

[3] Fisher,J.W., Frank,K.H., Hirt,M.A., and McNamee,B.M.
Effects of Weldments on the Fatigue Strength of Steel Beams.
NCHRP Report 102, National Cooperative Highway Research Program, 1970.

[4] Fisher,J.W., Albrecht,P.A., Yen,B.T., Klingerman,D.J., and McNamee,B.M.
Fatigue Strength of Steel Beams with Welded Stiffeners and Attachments.
NCHRP Report 147, National Cooperative Highway Research Program, 1974.

[5] Fisher,J.W.
Bridge Fatigue Guide - Design and Details.
American Institute of Steel Design, Chicago, 1977.

[6] Barsom,J.M. and Novak,S.R.
Subcritical Crack Growth and Fracture of Bridge Steels.
NCHRP Report 181, National Cooperative Highway Research Program, 1977.

[7] Fisher,J.W., Hausammann,H., Sullivan,M.D., and Pense,A.W.
Detection and Repair of Fatigue Damage in Welded Highway Bridges.
NCHRP Report 206, National Cooperative Highway Research Program, 1979.

[8] Fisher,J.W., Barthelemy,B.M., Mertz,D.R., and Edinger,J.A.
Fatigue Behavior of Full-Scale Welded Bridge Attachments.
NCHRP Report 227, National Cooperative Highway Research Program, 1980.

[9] Schilling,C.G., Klippstein,K.H., Barsom,J.M., and Blake,G.T.
Fatigue of Welded Steel Bridge Members under Variable-Amplitude Loading.
NCHRP Report 188, National Cooperative Highway Research Program, 1978.

[10] Fisher,J.W., Mertz,D.R., and Zhong,A.
Steel Bridge Members under Variable Amplitude Long Life Fatigue Loading.
NCHRP Report 267, National Cooperative Highway Research Program, 1983.

[11] Roberts,R., Fisher,J.W., Irwin,G.R., Boyer,K.D., Hausammann,H., Krishna,G.V., Morf,V., and Slockbower,R.F.
Determination of Tolerable Flaw Sizes in Full Scale Welded Bridge Details.
FHWA 12d-77-170, Federal Highway Administration, December, 1977.

[12] Slockbower,R.F. and Fisher,J.W.
Fatigue Resistance of Full Scale Cover-Plated Beams.
Fritz Engineering Laboratory Report 386-9(78), Lehigh University, June, 1978.

[13] Daniels,J.H., Fisher,J.W., and Yen,B.T.
Fatigue of Curved Steel Bridge Elements.
FHWA RD-79-138, Federal Highway Administration, April, 1980.

[14] ENR.
Island-Hopping Road, Rail Links Will Unify Japan.
Engineering News Record :42-44, 1984.

[15] Miki,C., Nishino,F., Harabayashi,Y., and Ohga,H.
Fatigue Strength of Longitudinal Welded Joints Containing Blowholes.
Proceedings of JSCE (325):155-165, September, 1982.

[16] Miki,C., Tajima,J., Asahi,K., and Takenouchi, H.
Fatigue of Large-Size Longitudinal Butt Welds with Partial Penetration.
Proceedings of JSCE (322):143-156, June, 1982.

[17] Miki,C., Nishimura,T., Tajima,J., and Okukawa.,A.
Fatigue Strength of Steel Members Having Longitudinal Single-Bevel-Groove Welds.
Trans. of Japan Welding Society 11(1):43-56, April, 1980.

[18] Miki,C., Nishino,F., Sasaki,T., and Mori,T.
Influence of Root Irregularity of Fatigue Strength of Partially-Penetrated Longitudinal Welds.
Proceedings of JSCE (337):223-226, September, 1983.

[19] Miki,C. Nishino,F., Tajima,J., and Kishimoto,Y.
Initiation and Propagation of Fatigue Cracks in Partially-Penetrated Longitudinal Welds.
Proceedings of JSCE (312):129-140, August, 1981.

[20] Nishimura,T. and Miki,C.
Fatigue Strength of Longitudinal Welded Members of 80 kg/mm^2 Steel.
Technical Report 22, Tokyo Institute of Technology, January, 1978.

[21] Tajima,J., Asama,T., Miki,C., and Takenouchi,H.
Fatigue of Nodal Joints and Box-Section Members in a Bridge Truss.
Proceedings, IABSE Colloquium - Lausanne, Fatigue of Steel and Concrete Structures :353-359, 1982.

[22] Shimokawa,H., Takena,K., Ito,F., and Miki,C.
Effects of Stress Ratio on the Fatigue Strength of Cruciform Fillet Welded Joints.
Proceedings of JSCE (344):121-128, April, 1984.

[23] Tajima,J., Shimokawa,H., Takena,K., Miki,C. and Ito,F.
Fatigue Tests of Truss Made of 600 MPa and 800 MPa Class Steels.
IIW Doc. XIII-1045-82 , May, 1982.
29 pp.

[24] Tajima,J., Okukawa,A., Sugizaki,M., and Takenouchi,H.
Fatigue Tests of Panel Point Structures of Truss made of 80 kg/mm^2 High Strength Steel.
IIW Doc. XIII-831-77 , July, 1977.
37 pp.

[25] Shimokawa,H., Takena,K., Fukazawa,M., and Miki,C.
A Fatigue Test on the Full-size Truss Chord.
Proceedings of JSCE (344):57-64, April, 1984.

[26] *ORE Report D 86 - Bending Tests of Structure Consisting of Two Beams Welded at Right Angles*
Office of Research and Experiments of the International Union of Railways, 1971.

[27] *ORE Report D 130 - Fatigue Phenomena in Welded Connections of Bridges and Cranes*
Office of Research and Experiments of the International Union of Railways, 1974-1979.
Reports D130/RP 1/E thru D130/RP 10/E.

[28] Maddox,S.J.
Improving the Fatigue Lives of Fillet Welds by Shot Peening.
Proceedings, IABSE Colloquium - Lausanne, Fatigue of Steel and Concrete Structure :377-384, 1982.

[29] TRRL.
Fatigue Behaviour of Intermittent Fillet Welds.
Technical Report LF860, Transport and Road Research Laboratory, 1979.

[30] Hirt,M.A. and Crisinel,M.
La résistance à la fatigue des poutres en ame pleine composées - soudées: Effect des plaquettes et groussels soudés à l'aile.
ICOM 017, Swiss Federal Institute, Lausanne, Switzerland, December, 1975.

[31] Smith,I.F.C., Bremen,U., and Hirt,M.A.
Fatigue Thresholds and Improvement of Welded Connections.
ICOM 125, Swiss Federal Institute, Lausanne, Switzerland, March, 1984.

[32] Yamada,K. and Hirt,M.A.
Fatigue Life Estimation Using Fracture Mechanics.
Proceeding, IABSE Colloquium - Lausanne, Fatigue of Steel and Concrete Structures :361-368, 1982.

[33] Berger,P.
Fatigue Testing of Welded Beams.
Proceedings, IABSE Colloquium - Lausanne, Fatigue of Steel and Concrete Structures :323-330, 1982.

[34] Minner,H.H. and Seeger,T.
Improvement of Fatigue Life of Welded Beams by TIG-Dressing.
Proceedings, IABSE Colloquium - Lausanne, Fatigue of Steel and Concrete Structures :385-392, 1982.

[35] Comeau,M.P. and Kulak,G.L.
Fatigue Strength of Welded Steel Elements.
Technical Report 79, University of Alberta, Canada, October, 1979.

[36] Baker,K.A. and Kulak,G.L.
Fatigue Strength of a Groove Weld on Steel Backing.
Canadian Journal of Civil Engineering 11(4):692-700, 1984.

[37] Albrecht,P. and Naeemi,A.H.
Performance of Weathering Steel in Bridges.
NCHRP Report 272, National Cooperative Highway Research Program, 1984.

[38] Yamada,K. and Kikuchi,Y.
Fatigue Tests of Weathered Welded Joints.
Journal of the Structural Division, ASCE 110(9):2164-2177, September, 1984.

[39] Paris,P.C.
The Fracture Mechanics Approach to Fatigue.
Proceedings, 10th Sagamore Conference :107, 1965.

[40] Basler,K.
Kommentar zur Norm SIA 161 Stahlbauten.
Technical Report A5, Schweizerische Zentralstelle fur Stahlbau, Zurich, 1979.

[41] *Steel, Concrete and Composite Bridges, Part 10: Code of Practice for Fatigue*
British Standards Institute, London, 1980.
BSI BS 5400.

[42] *Recommendations for the Fatigue Design of Structures, Committee TC6 Fatigue*
First edition, European Convention for Constructional Steelwork, 1985.

[43] Frank,K.H. and Fisher,J.W.
Fatigue Strength of Fillet Welded Cruciform Joints.
Journal of the Structural Division, ASCE 105(ST9):1727-1740, September, 1979.

Redundant Load Path Structures				
	Allowable Range of Stress F_{sr}, ksi			
Category	For 100,000 Cycles	For 500,000 Cycles	For 2,000,000 Cycles	For over 2,000,000 Cycles
A	60	36	24	24
B	45	27.5	18	16
C	32	19	13	10 12
D	27	16	10	7
E	21	12.5	8	5
E′	16	9.4	5.8	2.6
F	15	12	9	8

Table: 1 Current Allowable Fatigue Stress Ranges for Redundant Load Path Structures (AASHTO, Table 10.3.1A)

Category	Slope	Intercept (mean)	Standard Deviation	Intercept (lower)
A	3.178	11.121	0.221	10.688
B	3.372	10.870	0.147	10.582
C	3.25	10.038	0.063	9.915
D	3.071	9.664	0.108	9.453
E	3.095	9.292	0.101	9.094
E′	3.000	---	---	8.61

Table: 2 Regression Analysis Coefficients for Current AASHTO Curves

Non-Redundant Load Path Structures				
	Allowable Range of Stress F_{sr}, ksi			
Category	For 100,000 Cycles	For 500,000 Cycles	For 2,000,000 Cycles	For over 2,000,000 Cycles
A	36	24	24	24
B	27.5	18	16	16
C	19	13	10 12	9 11
D	16	10	7	5
E	12.5	8	5	2.5
F	12	9	8	7

Table: 3 Current Allowable Fatigue Stress Ranges for Non-Redundant Load Path Structures (AASHTO, Table 10.3.1A)

Category AASHTO	Category (ECCS)	Allowable Range of Stress F_{sr}, ksi For 100,000 Cycles	For 2,000,000 Cycles	For over 2,000,000 Cycles
A	(160)	60 (62)	24 (23)	24 (17)
B	(125)	45 (48)	18 (18)	16 (13)
C	(90)	32 (35)	13 (13)	10 (9.7)
D	(71)	27 (28)	10 (10)	7 (7.4)
E	(56)	21 (22)	8 (8)	5 (5.8)
E′	(40)	16 (16)	5.8 (5.8)	2.6 (4.4)

Table: 4 Comparison of Current AASHTO and Proposed ECCS Allowable Fatigue Stress Ranges

Redundant Load Path Members				
	Allowable Range of Stress F_{sr}, ksi			
Category	For 100,000 Cycles	For 500,000 Cycles	For 2,000,000 Cycles	For over 2,000,000 Cycles
$\overline{A}$	63	37	24	24
$\overline{B}$	49	29	18	16
$\overline{B}'$	39	23	14.5	12
$\overline{C}$	35.5	21	13	10 12
$\overline{D}$	28	16	10	7
$\overline{E}$	22	13	8	4.5
$\overline{E}'$	16	9.2	5.8	2.6
F	15	12	9	8

Table: 5 Proposed Allowable Fatigue Stress Ranges For Redundant Load Path Members

Figure Number	Detail Type	Category	Number of Test Data
64	Plain Rolled Beams	$\overline{A}$	49
65	Longitudinal Welds		
	Welded Beams	$\overline{B}$	182
	Flat Plate Specimens	$\overline{B}$	169
66	Flange Splices	$\overline{B}$	81
	A514/A517 Straight Transition	$\overline{B}'$	16
67	Box Girder Longitudinal Welds	$\overline{B}'$	48
68	Transverse Stiffeners	$\overline{C}$	118
69	Web Attachments		
	Plate thickness less than 1.0 in.	$\overline{E}$	31
	Plate thickness 1.0 in or greater	$\overline{E}'$	37
70	Web Gusset Plates		
	Rectangular Plate	$\overline{E}$	39
	Transition Radius	$\overline{D}$	12
	Tapered Plate End	$\overline{E}$	12
71	Flange Tip Attachments, Rectangular Plate	$\overline{E}$	67

Table: 6 Number of Test Data Plotted in Figs. 64 thru 80

Figure Number	Detail Type	Category	Number of Test Data
72	Flange Tip Attachments with Transition Radius, Groove Welded		
	Radius greater than 6.0 in.	$\overline{C}$	5
	Radius between 2.0 and 6.0 in.	$\overline{D}$	46
	Radius less than 2.0 in.	$\overline{E}$	7
73	Flange Tip Attachments with Transition Radius, Fillet Welded		
	Radius greater than 2.0 in.	$\overline{D}$	3
	Radius less than 2.0 in.	$\overline{E}$	6
74	Flange Surface Attachments		
	Attachment length less than 2.0 in.	$\overline{C}$	29
	Attachment length between 2.0 and 4.0 in.	$\overline{D}$	66
	Attachment length greater than 4.0 in.	$\overline{E}$	84
75	Coverplated Beams, Narrow Plate	$\overline{E}$	399
76	Coverplated Beams, Wide Plate		
	Welded end	$\overline{E}$	30
	Unwelded end	$\overline{E}'$	30
77	Thick Flange Coverplated Beams	$\overline{E}'$	39
78	Cruciform Joint Specimens	$\overline{C}$	127
79	Longitudinal Attachment Specimens	$\overline{D}$	94
80	Attachment Specimens	$\overline{D}$	158

Table: 6 (continued)

Non-Redundant Load Path Members				
	Allowable Range of Stress F_{sr}, ksi			
Category	For 100,000 Cycles	For 500,000 Cycles	For 2,000,000 Cycles	For over 2,000,000 Cycles
$\overline{A}$	50	29	24	24
$\overline{B}$	39	23	16	16
$\overline{B}'$	31	18	11	11
$\overline{C}$	28	16	10 12	9 11
$\overline{D}$	22	13	8	5
$\overline{E}$	17	10	6	2.3
$\overline{E}'$	12	7	4	1.3
F	12	9	7	6

Table: 7 Proposed Allowable Fatigue Stress Ranges for Non-Redundant Load Path Members

General Equation:

$$N = A \cdot S_r^{-3.0}$$

N = estimated minimum number of cycles to failure

S_r = allowable stress range, ksi

A = constant as listed below

Category	Constant A
$\overline{A}$	$2.500 \cdot 10^{10}$
$\overline{B}$	$1.191 \cdot 10^{10}$
$\overline{B}'$	$6.109 \cdot 10^{9}$
$\overline{C}$	$4.446 \cdot 10^{9}$
$\overline{D}$	$2.183 \cdot 10^{9}$
$\overline{E}$	$1.072 \cdot 10^{9}$
$\overline{E}'$	$3.908 \cdot 10^{8}$

Table: 8 General Equation and Coefficients for Proposed Lower Bound Fatigue Design Curves

General Condition	Situation	Kind of Stress	Stress Category (See Table 10.3.1A)	Illustrative Example (See Figure 10.3.1C)
Plain Member	Base metal with rolled or cleaned surface. Flame cut edges with ANSI smoothness of 1,000 or less.	T or Rev[a]	$\bar{A}$	1,2
Built-Up Members	Base metal and weld metal in members of built-up plates or shapes (without attachments) connected by continuous full penetration groove welds (with backing bars removed) or by continuous fillet welds parallel to the direction of applied stress.	T or Rev	$\bar{B}$	3,4,5,7
	Base metal and weld metal in members of built-up plates or shapes (without attachments) connected by continuous full penetration groove welds with backing bars not removed, or by continuous partial penetration groove welds parallel to the direction of applied stress.	T or Rev	$\bar{B}'$	3,4,5,7
	Calculated flexural stress at the toe of transverse stiffener welds on girder webs or flanges.	T or Rev	$\bar{C}$	6
	Base metal at ends of partial length welded coverplates narrower than the flange having square or tapered ends, with or without welds across the ends, or wider than flange with welds across the ends			
	(a) Flange thickness $\leq$ 0.8 in.	T or Rev	$\bar{E}$	7
	(b) Flange thickness $>$ 0.8 in.	T or Rev	$\bar{E}'$	7
	Base metal at ends of partial length welded coverplates wider than the flange without welds across the ends.	T or Rev	$\bar{E}'$	7
Groove Welded Connections	Base metal and weld metal in or adjacent to full penetration groove welded splices of rolled or welded sections having similar profiles when welds are ground flush with grinding in the direction of applied stress and weld soundness established by nondestructive inspection.	T or Rev	$\bar{B}$	8,10
	Base metal and weld metal in or adjacent to full penetration groove welded splices with 2 ft. radius transitions in width, when welds are ground flush with grinding in the direction of applied stress and weld soundness established by nondestructive inspection.	T or Rev	$\bar{B}$	13

Table: 9 Corrections and Additions to Table 10.3.1B, AASHTO (1983)

	Base metal and weld metal in or adjacent to full penetration groove weld splices at transitions in width or thickness, with welds ground to provide slopes no steeper than 1 to 2 1/2, with grinding in the direction of the applied stress, and weld soundness established by nondestructive inspection			
	(a) A514/A517 base metal	T or Rev	$\bar{B}'$	11,12
	(b) Other base metals	T or Rev	$\bar{B}$	11,12
	Base metal and weld metal in or adjacent to full penetration groove weld splices, with or without transitions having slopes no greater than 1 to 2 1/2, when the reinforcement is not removed and weld soundness is established by nondestructive inspection.	T or Rev	$\bar{C}$	8,10,11,12
Groove Welded Attachments - Longitudinally Loaded[b]	Base metal adjacent to details attached by full or partial penetration groove welds when the detail length, L, in the direction of stress, is less than 2 in.	T or Rev	$\bar{C}$	6,15
	Base metal adjacent to details attached by full or partial penetration groove welds when the detail length, L, in the direction of stress, is between 2 in. and 12 times the plate thickness but less than 4 in.	T or Rev	$\bar{D}$	15
	Base metal adjacent to details attached by full or partial penetration groove welds when the detail length, L, in the direction of stress, is greater than 12 times the plate thickness or greater than 4 in.			
	(a) Detail thickness $<$ 1.0 in.	T or Rev	$\bar{E}$	15
	(b) Detail thickness $\geq$ 1.0 in.	T or Rev	$\bar{E}'$	15
	Base metal adjacent to details attached by full or partial penetration groove welds with a transition radius, R, regardless of the detail length:			
	- With the end welds ground smooth	T or Rev		16
	(a) Transition radius $\geq$ 24 in.		$\bar{B}$	
	(b) 24 in. $>$ Transition radius $\geq$ 6 in.		$\bar{C}$	
	(c) 6 in. $>$ Transition radius $\geq$ 2 in.		$\bar{D}$	
	(d) 2 in. $>$ Transition radius $\geq$ 0 in.		$\bar{E}$	
	- For all transition radii without end welds ground smooth.	T or Rev	$\bar{E}$	16

Groove welded Attachments - Transversely Loaded[b,c]	Detail base metal attached by full penetration groove welds with a transition radius, R, regardless of the detail length and with weld soundness transverse to the direction of stress established by nondestructive inspection:			
	- With equal plate thickness and reinforcement removed	T or Rev		16
	(a) Transition radius $\geq$ 24 in.		$\bar{B}$	
	(b) 24 in. > Transition radius $\geq$ 6 in.		$\bar{C}$	
	(c) 6 in. > Transition radius $\geq$ 2 in.		$\bar{D}$	
	(d) 2 in. > Transition radius $\geq$ 0 in.		$\bar{E}$	
	- With equal plate thickness and reinforcement not removed	T or Rev		16
	(a) Transition radius $\geq$ 6 in.		$\bar{C}$	
	(b) 6 in. > Transition radius $\geq$ 2 in.		$\bar{D}$	
	(c) 2 in. > Transition radius $\geq$ 0 in.		$\bar{E}$	
	- With unequal plate thickness and reinforcement removed	T or Rev		16
	(a) Transition radius $\geq$ 2 in.		$\bar{D}$	
	(b) 2 in. > Transition radius $\geq$ 0 in.		$\bar{E}$	
	- For all transition radii with unequal plate thickness and reinforcement not removed.	T or Rev	$\bar{E}$	16
Fillet Welded Connections	Base metal at details connected with transversely loaded welds, with the welds perpendicular to the direction of stress			
	(a) Detail thickness $\leq$ 0.5 in.	T or Rev	$\bar{C}$	14
	(b) Detail thickness > 0.5 in.	T or Rev	See Note [d]	
	Base metal at intermittent fillet welds.	T or Rev	$\bar{E}$	-
	Shear stress on throat of fillet welds.	Shear	$\bar{F}$	9
Fillet Welded Attachments - Longitudinally Loaded[b,c,e]	Base metal adjacent to details attached by fillet welds with length, L, in the direction of stress, is less than 2 in. and stud-type shear connectors.	T or Rev	$\bar{C}$	15,17,18 20
	Base metal adjacent to details attached by fillet welds with length, L, in the direction of stress, between 2 in. and 12 times the plate thickness but less than 4 in.	T or Rev	$\bar{D}$	15,17

	Base metal adjacent to details attached by fillet welds with length, L, in the direction greater than 12 times the plate thickness or greater than 4 in.			
	(a) Detail thickness $<$ 1.0 in.	T or Rev	$\bar{E}$	7,9,15,17
	(b) Detail thickness $\geq$ 1.0 in.	T or Rev	$\bar{E}'$	7,9,15
	Base metal adjacent to details attached by fillet welds with a transition radius, R, regardless of the detail length:			
	- With the end welds ground smooth	T or Rev		16
	(a) Transition radius $\geq$ 2 in.		$\bar{D}$	
	(b) 2 in. $>$ Transition radius $\geq$ 0 in.		$\bar{E}$	
	- For all transition radii without the end welds ground smooth.	T or Rev	$\bar{E}$	16
Fillet Welded Attachments - Transversely Loaded with the weld in the direction of principal stress[b,e]	Detail base metal attached by fillet welds with a transition radius, R, regardless of the detail length (shear stress on the throat of fillet welds governed by Category F):			
	- With the end welds ground smooth	T or Rev		16
	(a) Transition radius $\geq$ 2 in.		$\bar{D}$	
	(b) 2 in. $>$ Transition radius $\geq$ 0 in.		$\bar{E}$	
	- For all transition radii without the end welds ground smooth.	T or Rev	$\bar{E}$	16
Mechanically Fastened Connections	Base metal at gross section of high strength bolted slip resistant connections, except axially loaded joints which induce out-of-plane bending in connecting material.	T or Rev	$\bar{B}$	21
	Base metal at net section of high strength bolted bearing-type connections.	T or Rev	$\bar{B}$	21
	Base metal at net section of riveted connections.	T or Rev	$\bar{D}$	21

[a] "T" signifies range in tensile stress only, "Rev" signifies a range of stress involving both tension and compression during a stress cycle.

[b] "Longitudinally Loaded" signifies direction of applied stress is parallel to the longitudinal axis of the weld. "Transversely Loaded" signifies direction of applied stress is perpendicular to the longitudinal axis of the weld.

[c] Transversely loaded partial penetration groove welds are prohibited.

[d] Allowable fatigue stress range on throat of fillet welds transversely loaded is a function of the effective throat and plate thickness. (See Frank and Fisher, Journal of the Structural Division, ASCE, Vol. 105, No. ST9, Sept. 1979.)

$$S_r = S_r^C \left(\frac{0.06 + 0.79\, H/t_p}{1.1\, t_p^{1/6}} \right)$$

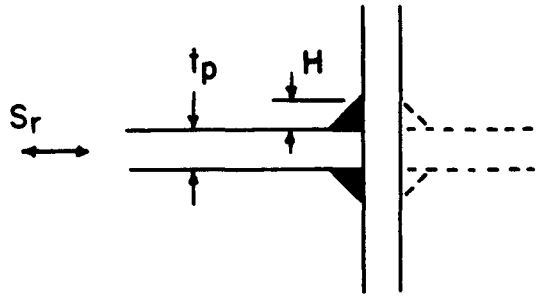

where S_r^C is equal to the allowable stress range for Category $\overline{C}$ given in Table 10.3.1A. This assumes no penetration at the weld root.

[e] Gusset plates attached to girder flange surfaces with only transverse fillet welds are prohibited.

General Condition	Situation	Kind of Stress	Stress Category (See Table 10.3.1A)	Illustrative Example (See Figure 10.3.1C)
Plain Material	Base metal with rolled or cleaned surfaces. Flame cut edges with ASA smoothness of 1,000 or less.	T or Rev[a]	A	1,2
Built-Up Members	Base metal and weld metal in members without attachments, built-up plates, or shapes connected by continuous full or partial penetration groove welds or by continuous fillet welds parallel to the direction of applied stress.	T or Rev	B	3,4,5,7
	Calculated flexural stress at toe of transverse stiffener welds on girder webs or flanges	T or Rev	C	6
	Base metal at end of partial length welded cover plates having square or tapered ends, with or without welds across the ends			
	(a) Flange thickness < 0.8 in.	T or Rev	E	7
	(b) Flange thickness > 0.8 in.	T or Rev	E'	7
Groove Welds	Base metal and weld metal at full penetration groove welded splices of rolled and welded sections having similar profiles when welds are ground flush and weld soundness established by nondestructive inspection.	T or Rev	B	8, 10, 14
	Base metal and weld metal in or adjacent to full penetration groove welded splices at transitions in width or thickness, with welds ground to provide slopes no steeper than 1 to 2 1/2, with grinding in the direction of applied stress, and weld soundness established by nondestructive inspection.	T or Rev	B	11, 12
	Base metal and weld metal in or adjacent to full penetration groove welded splices, with or without transitions having slopes no greater than 1 to 2 1/2 when reinforcement is not removed and weld soundness is established by nondestructive inspection	T or Rev	C	8, 10, 11, 12, 14
	Base metal at details attached by groove welds subject to longitudinal loading when the detail length, L, parallel to the line of stress is between 2 in. and 12 times the plate thickness but less than 4 in.	T or Rev	D	13
	Base metal at details attached by groove welds subject to longitudinal loading when the detail length, L, is greater than 12 times the plate thickness or greater than 4 inches long.	T or Rev	E	13
	Base metal at details attached by groove welds subjected to transverse and/or longitudinal loading regardless of detail length when weld soundness transverse to the direction of stress is established by nondestructive inspection.			
	(a) When provided with transition radius equal to or greater than 24 in. and weld end ground smooth	T or Rev	B	14
	(b) When provided with transition radius less than 24 in. but not less than 6 in. and weld end ground smooth	T or Rev	C	14
	(c) When provided with transition radius less than 6 in. but not less than 2 in. and weld end ground smooth	T or Rev	D	14
	(d) When provided with transition radius between 0 in. and 2 in.	T or Rev	E	14

Table: 10 Current Connection Descriptions and Conditions (Table 10.3.1B, AASHTO(1983))

General Condition	Situation	Kind of Stress	Stress Category (See Table 10.3.1A)	Illustrative Example (See Figure 10.3.1C)
Fillet[b] Welded Connections	Base metal at intermittent fillet welds	T or Rev	E	—
	Base metal adjacent to fillet welded attachments with length L, in direction of stress less than 2 in. and stud-type shear connectors	T or Rev	C	13, 15, 16, 17
	Base metal at details attached by fillet welds with detail length, L, in direction of stress between 2 in. and 12 times the plate thickness but less than 4 in.	T or Rev	D	13, 15, 16
	Base metal at attachment details with detail length, L, in direction of stress (length of fillet weld) greater than 12 times the plate thickness or greater than 4 in.	T or Rev	E	7, 9, 13, 16
	Base metal at details attached by fillet welds regardless of length in direction of stress (shear stress on the throat of fillet welds governed by stress category F)			
	(a) When provided with transition radius equal to or greater than 2 in. and weld end ground smooth	T or Rev	D	14
	(b) When provided with transition radius between 0 in. and 2 in.	T or Rev	E	14
Mechanically Fastened Connections	Base metal at gross section of high-strength bolted slip resistant connections, except axially loaded joints which induce out-of-plane bending in connected material.	T or Rev	B	18
	Base metal at net section of high-strength bolted bearing-type connections	T or Rev	B	18
	Base metal at net section of riveted connections	T or Rev	D	18
Fillet Welds	Shear stress on throat of fillet welds	Shear	F	9

[a]"T" signifies range in tensile stress only: "Rev" signifies a range of stress involving both tension and compression during a stress cycle.

[b]Gusset plates attached to girder flanges with only transverse fillet welds, not recommended.

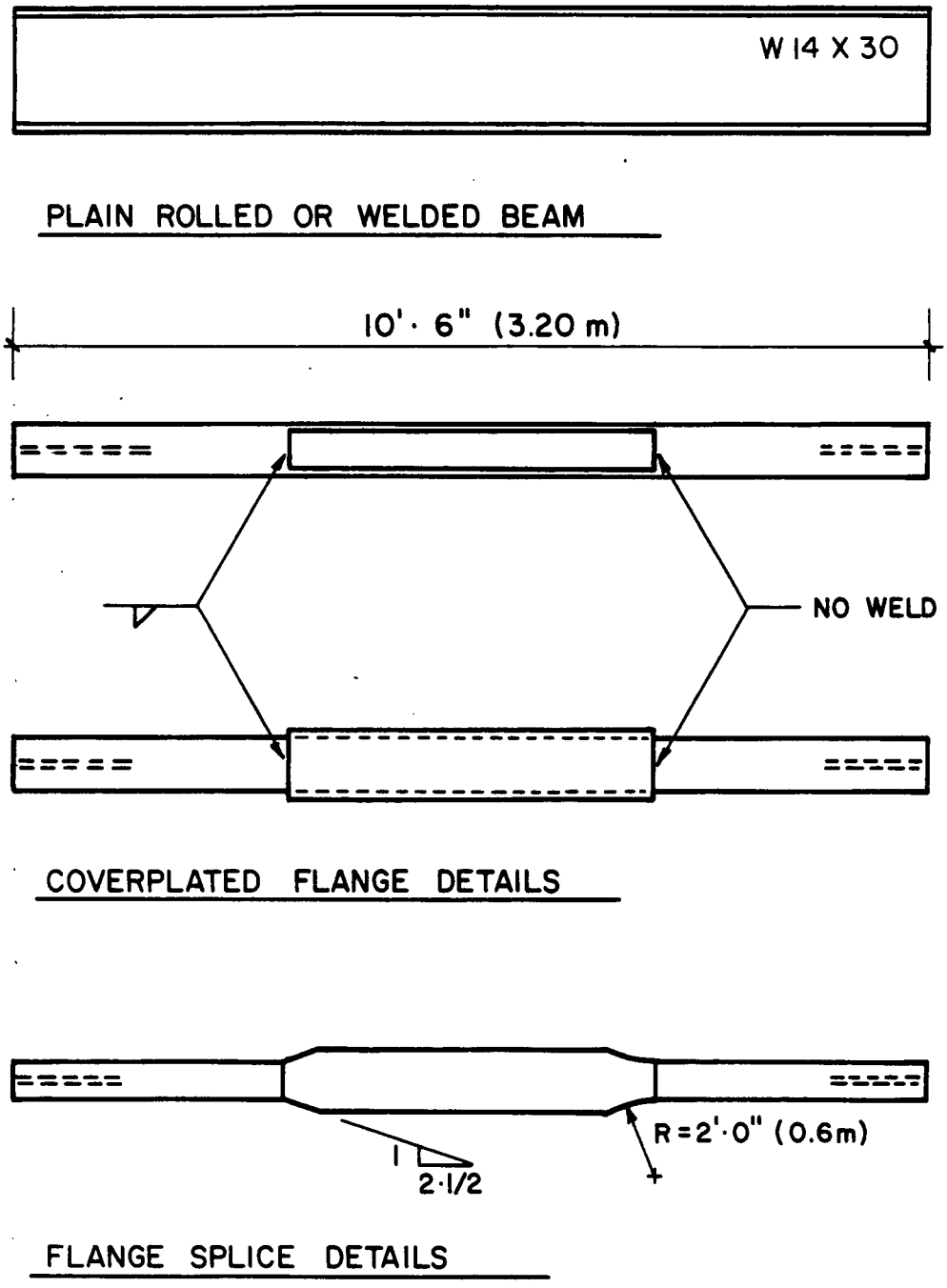

Figure: 1 Test Specimens for NCHRP Report 102

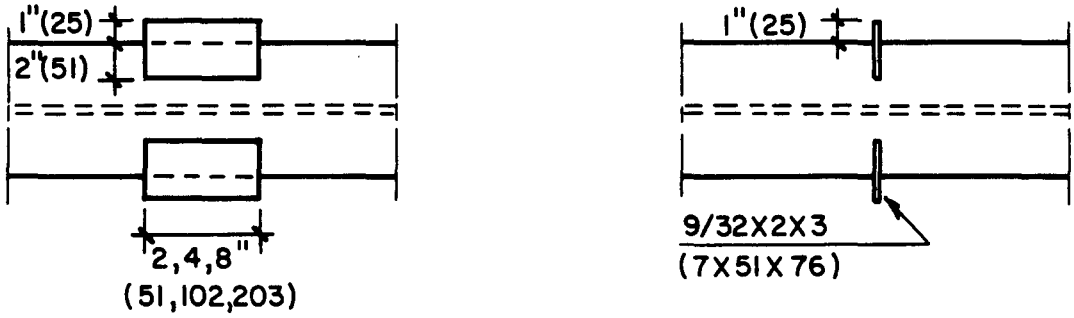

FLANGE ATTACHMENTS

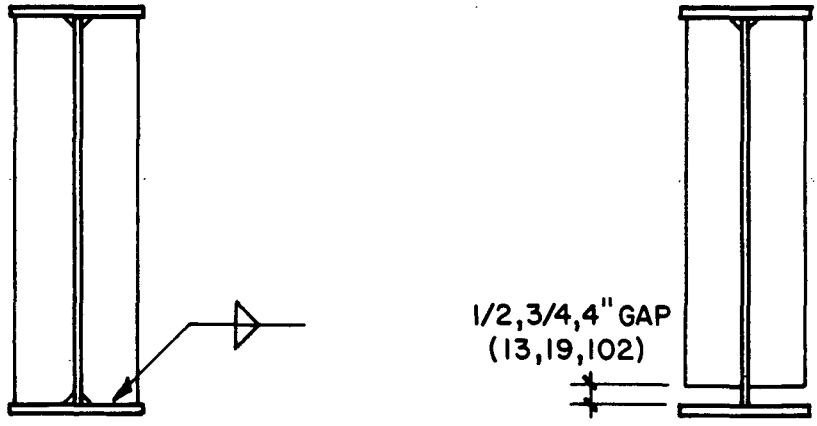

TRANSVERSE WEB STIFFENERS

Figure: 2 Test Specimens for NCHRP Report 147

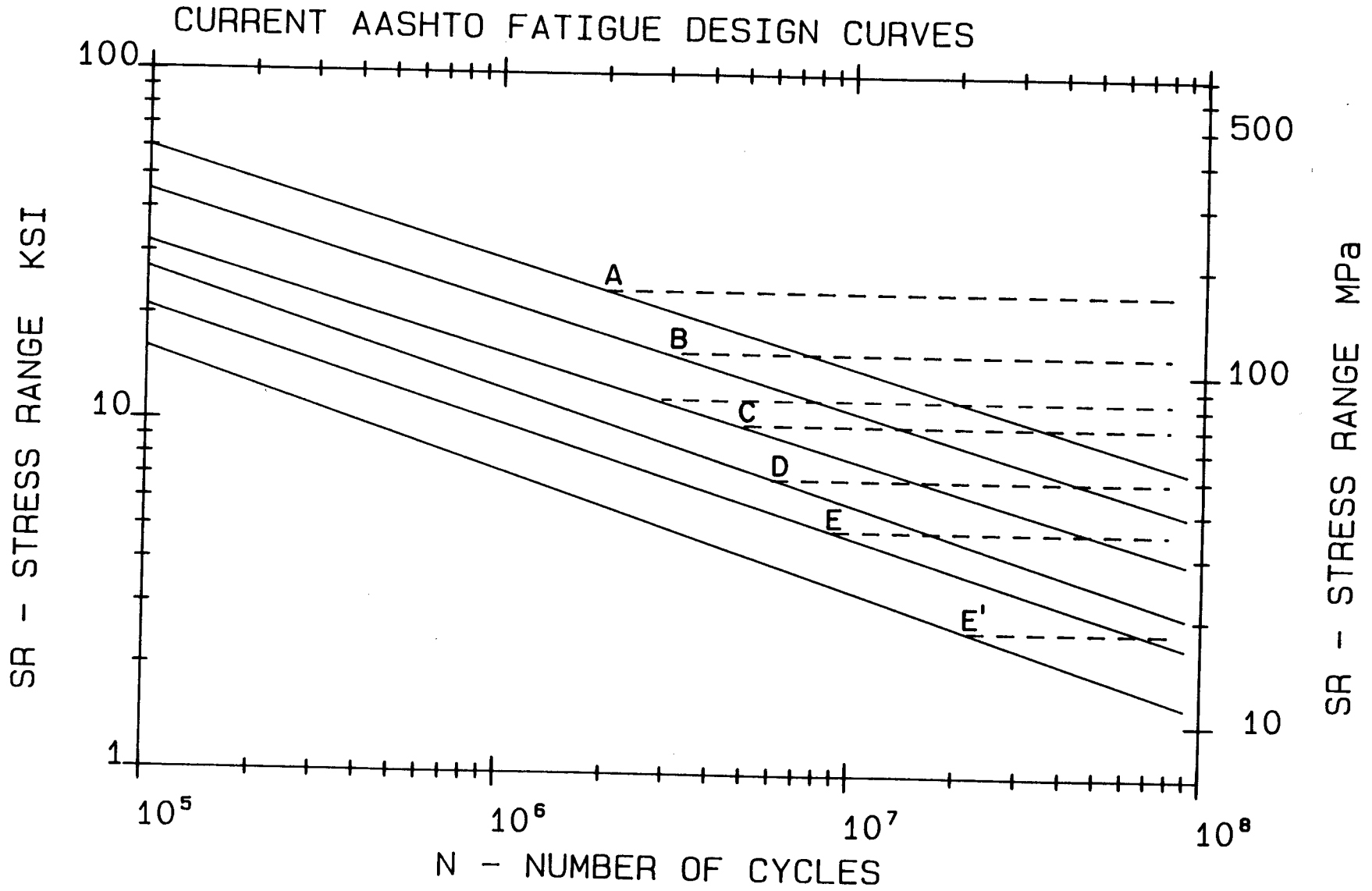

Figure: 3 Current AASHTO Fatigue Design Curves

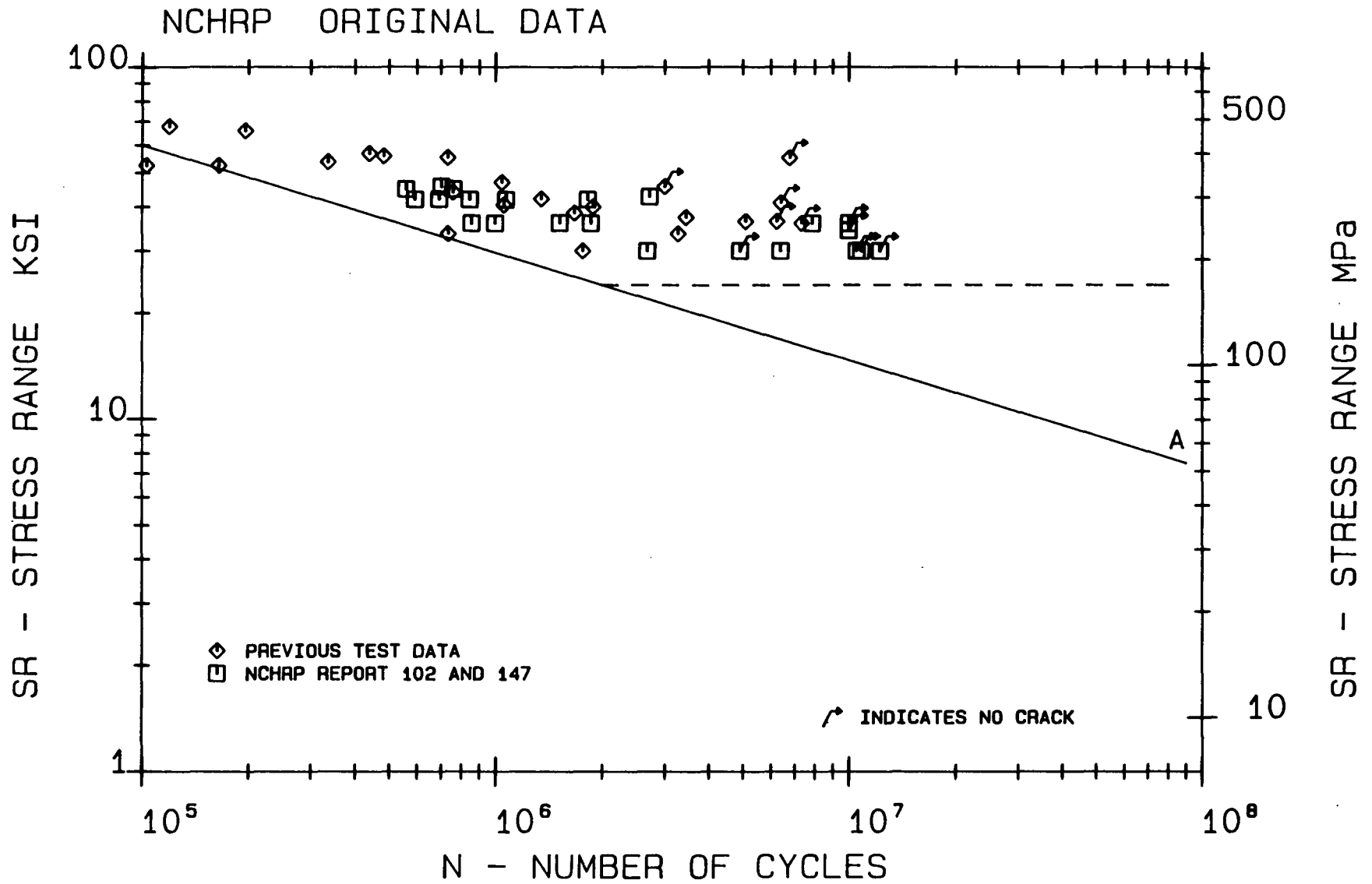

Figure: 4 Fatigue Resistance of Category A Details, Original Database

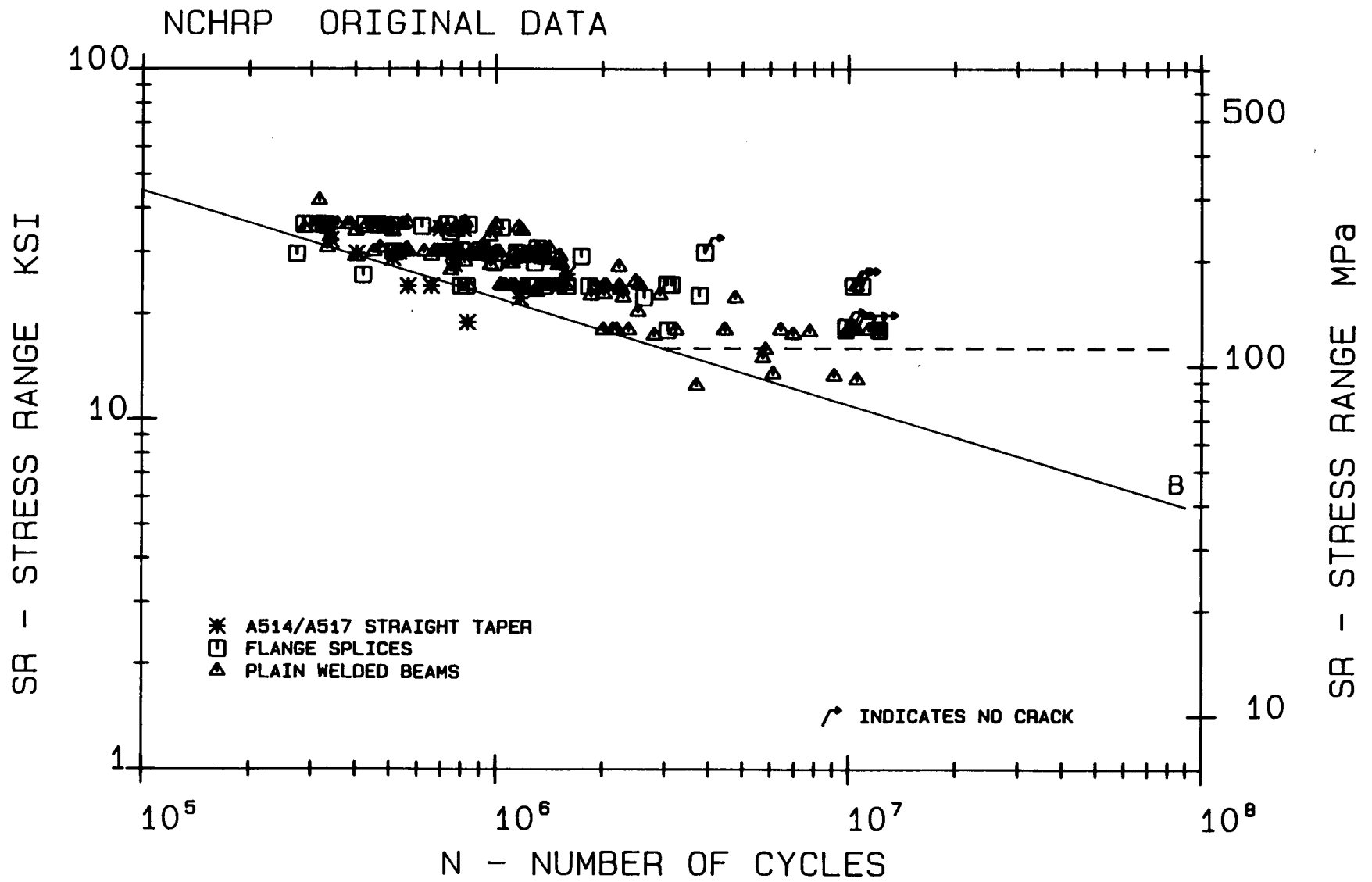

Figure: 5 Fatigue Resistance of Category B Details, Original Database

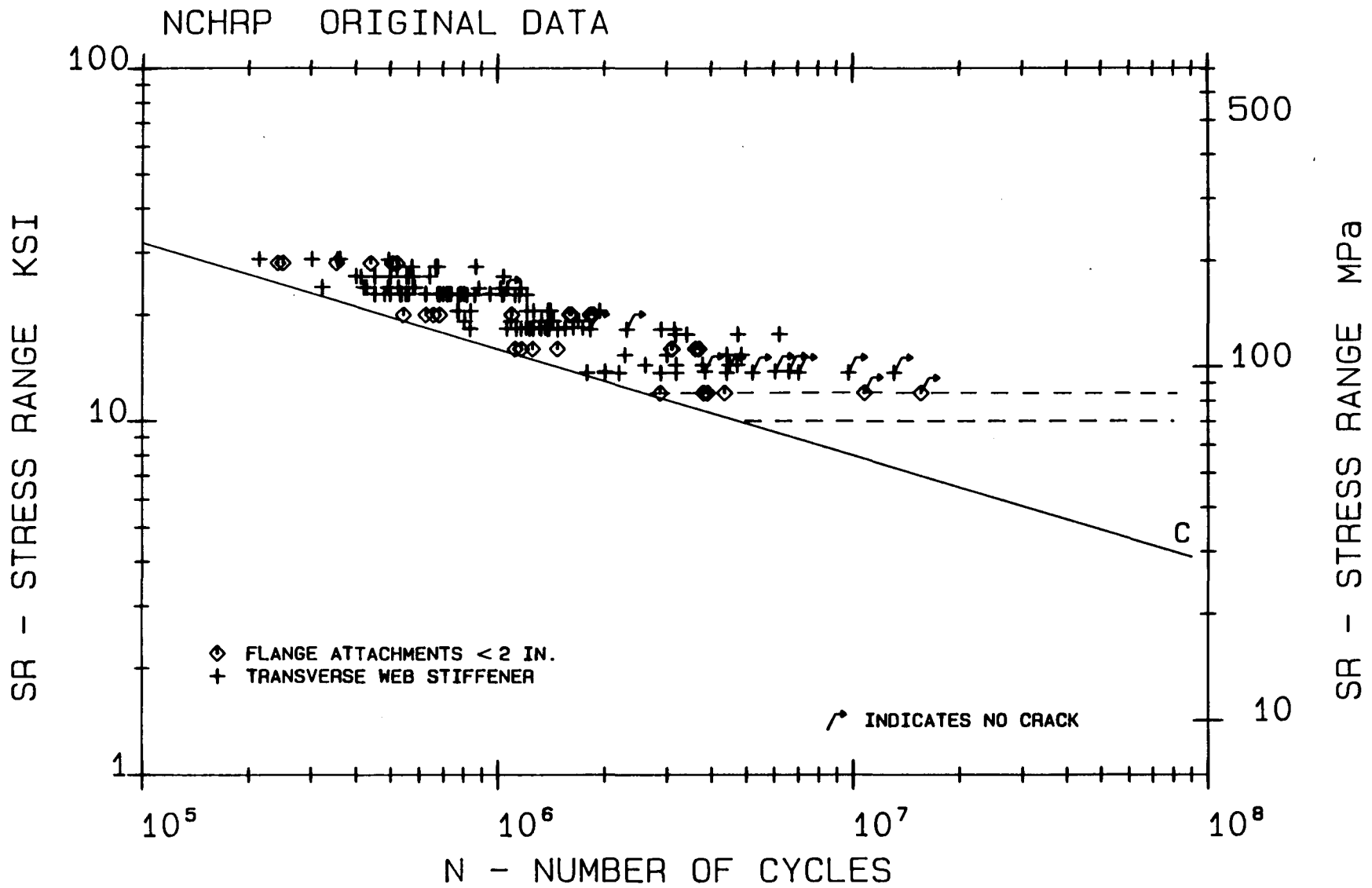

Figure: 6 Fatigue Resistance of Category C Details, Original Database

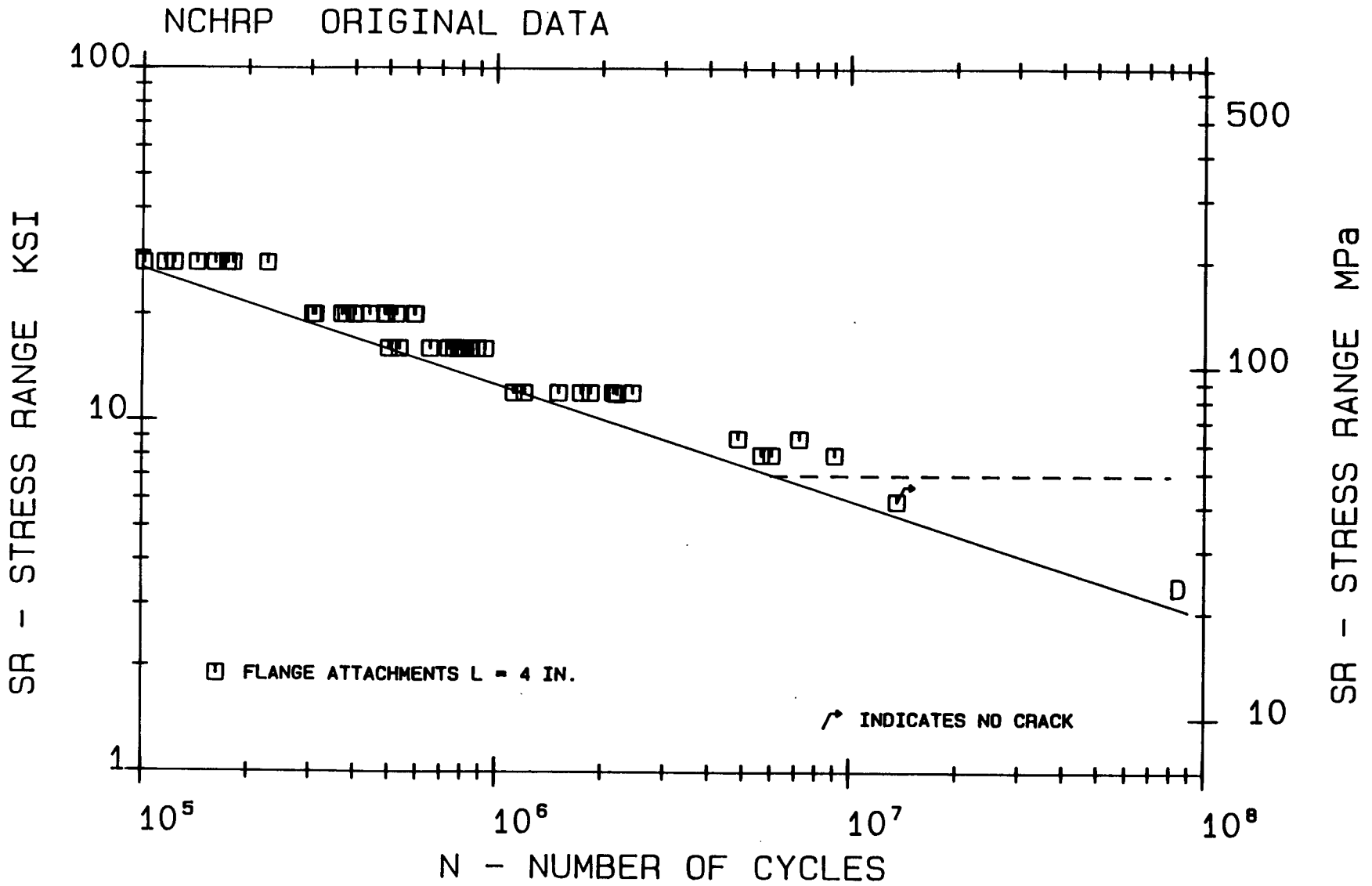

Figure: 7 Fatigue Resistance of Category D Details, Original Database

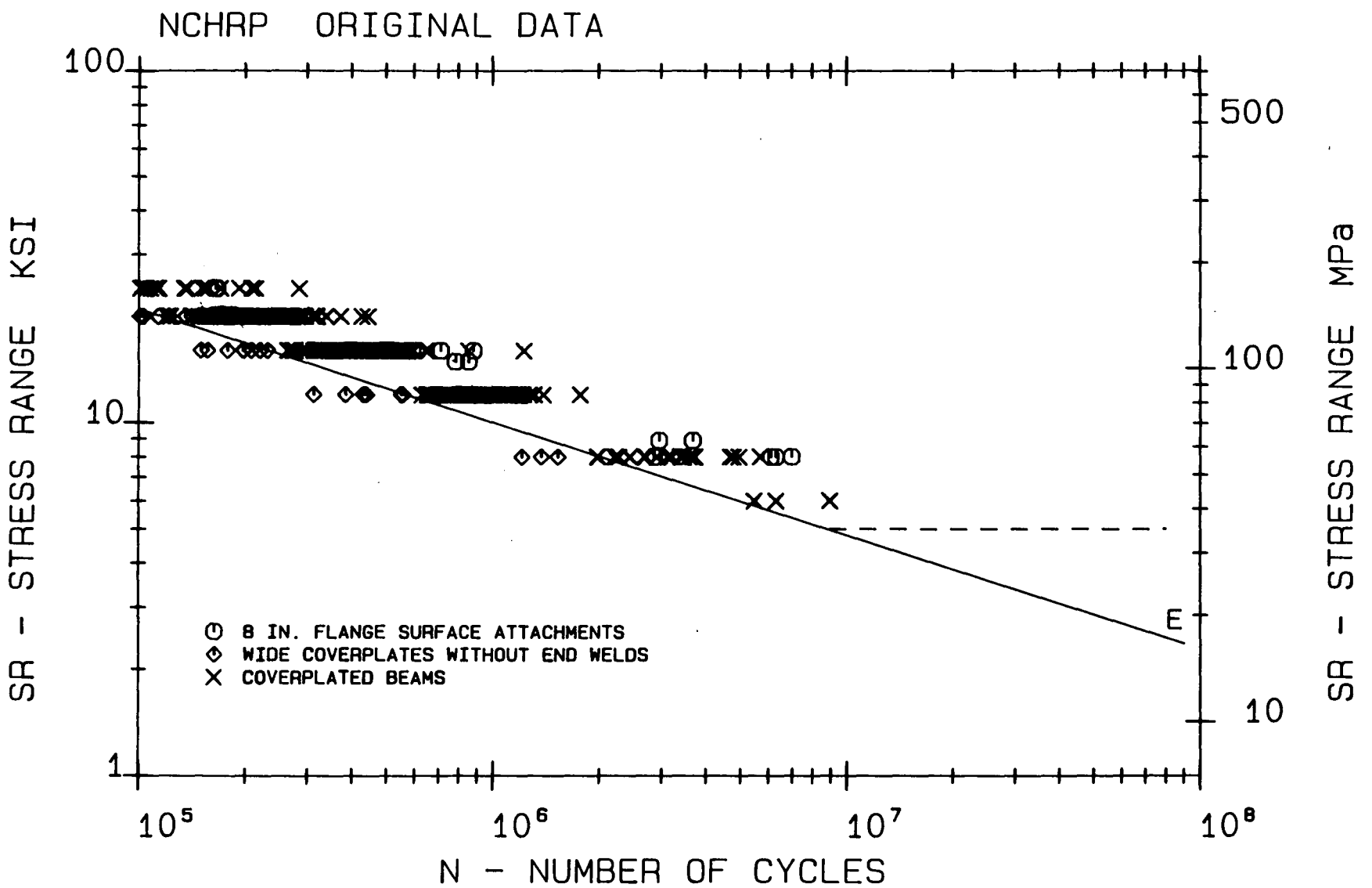

Figure: 8 Fatigue Resistance of Category E Details, Original Database

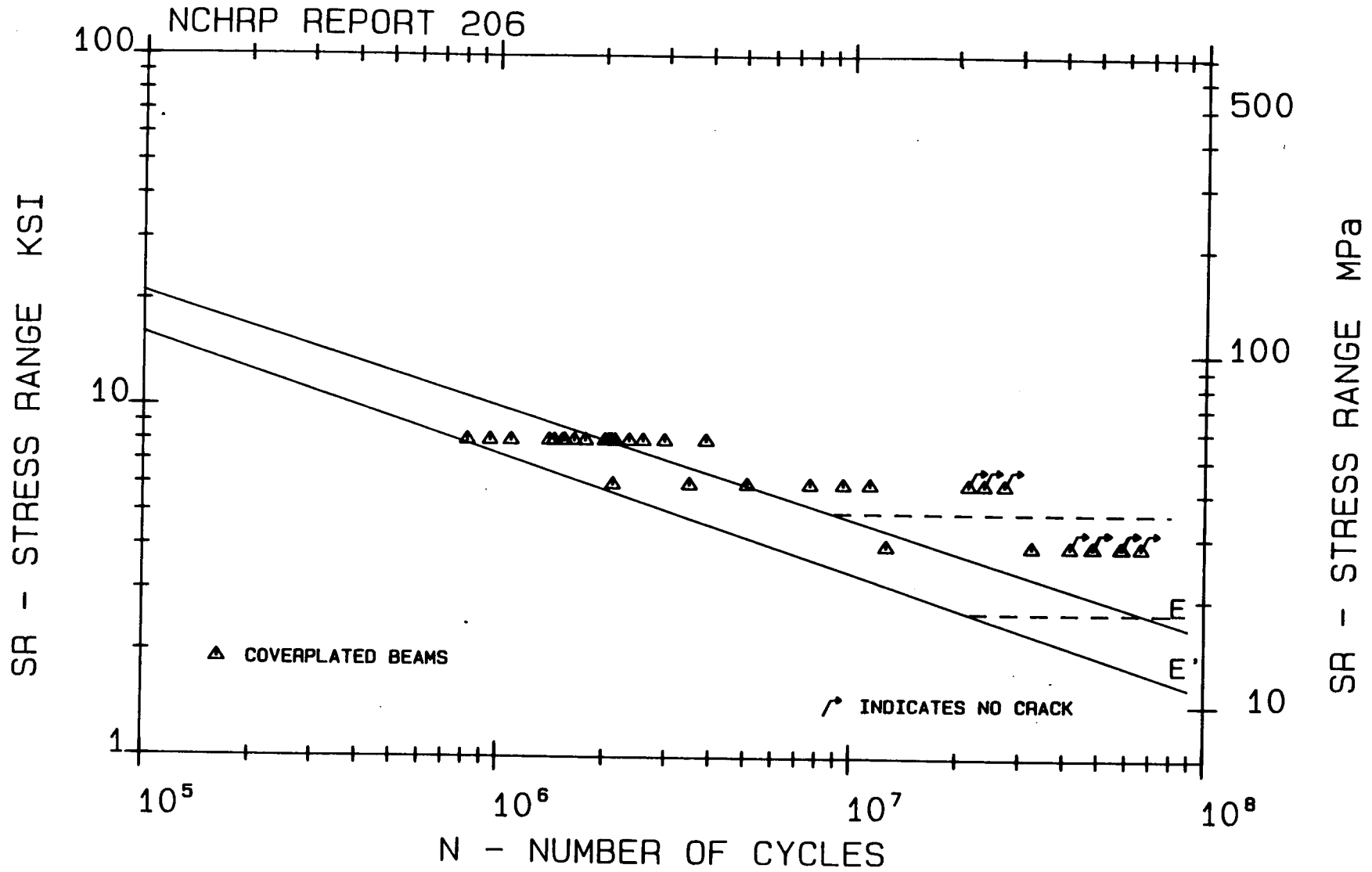

Figure: 9 Fatigue Resistance of Coverplated Beams, NCHRP Report 206

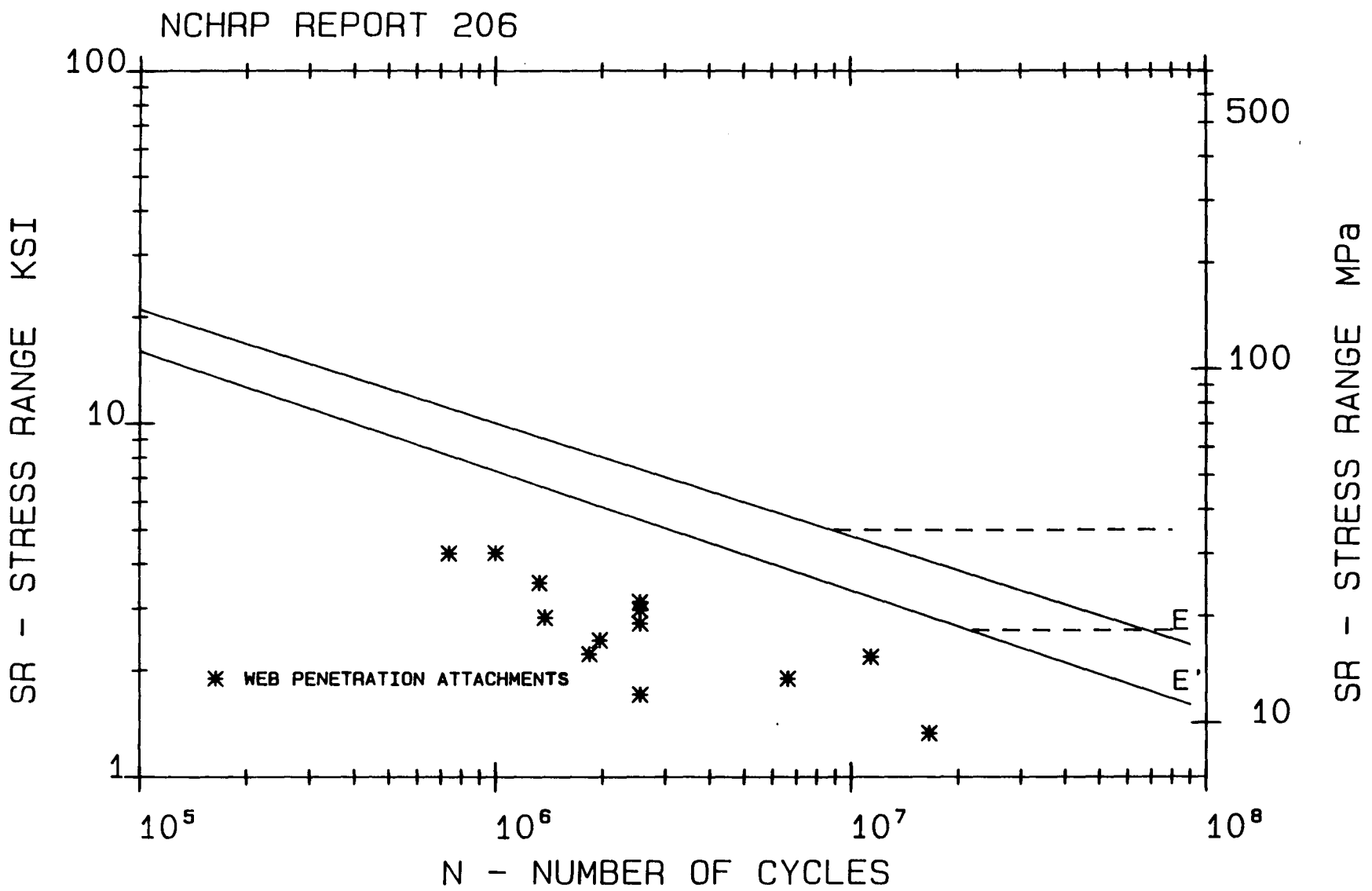

Figure: 10 Fatigue Resistance of Penetrating Web Details, NCHRP Report 206

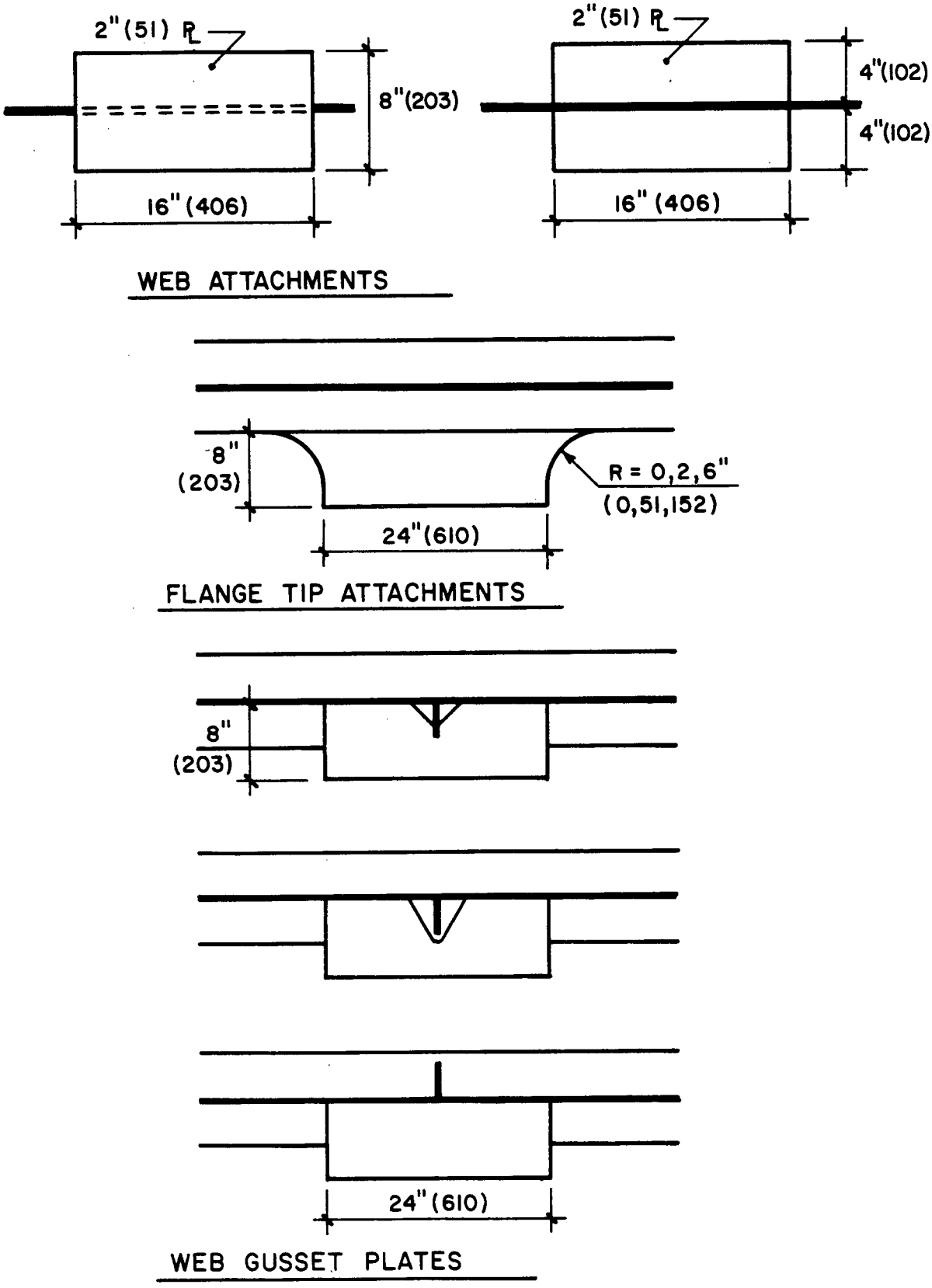

Figure: 11 Test specimens for NCHRP Report 227

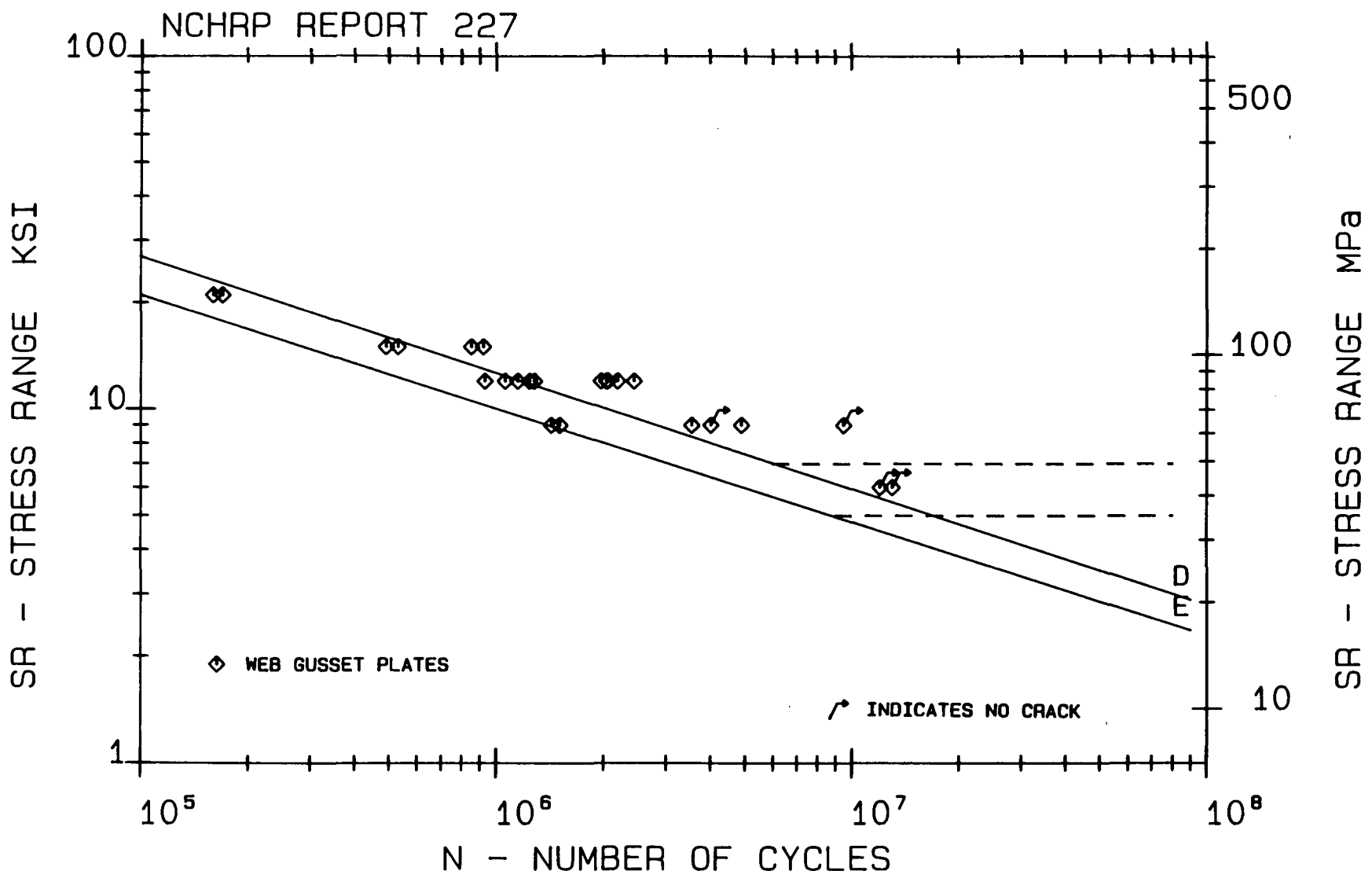

Figure: 12 Fatigue Resistance of Web Gusset Plates, NCHRP Report 227

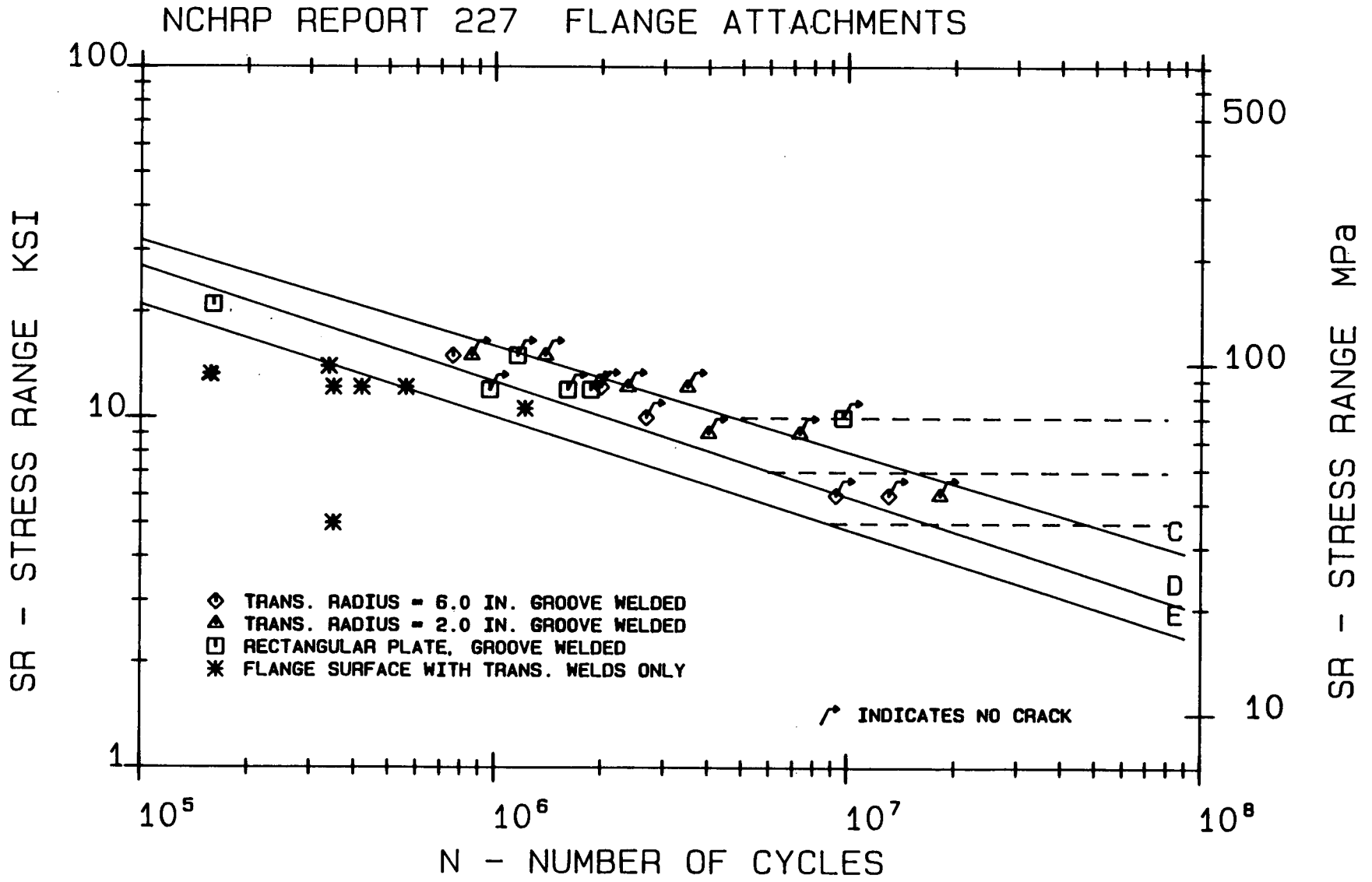

Figure: 13 Fatigue Resistance of Flange Tip Attachments, NCHRP Report 227

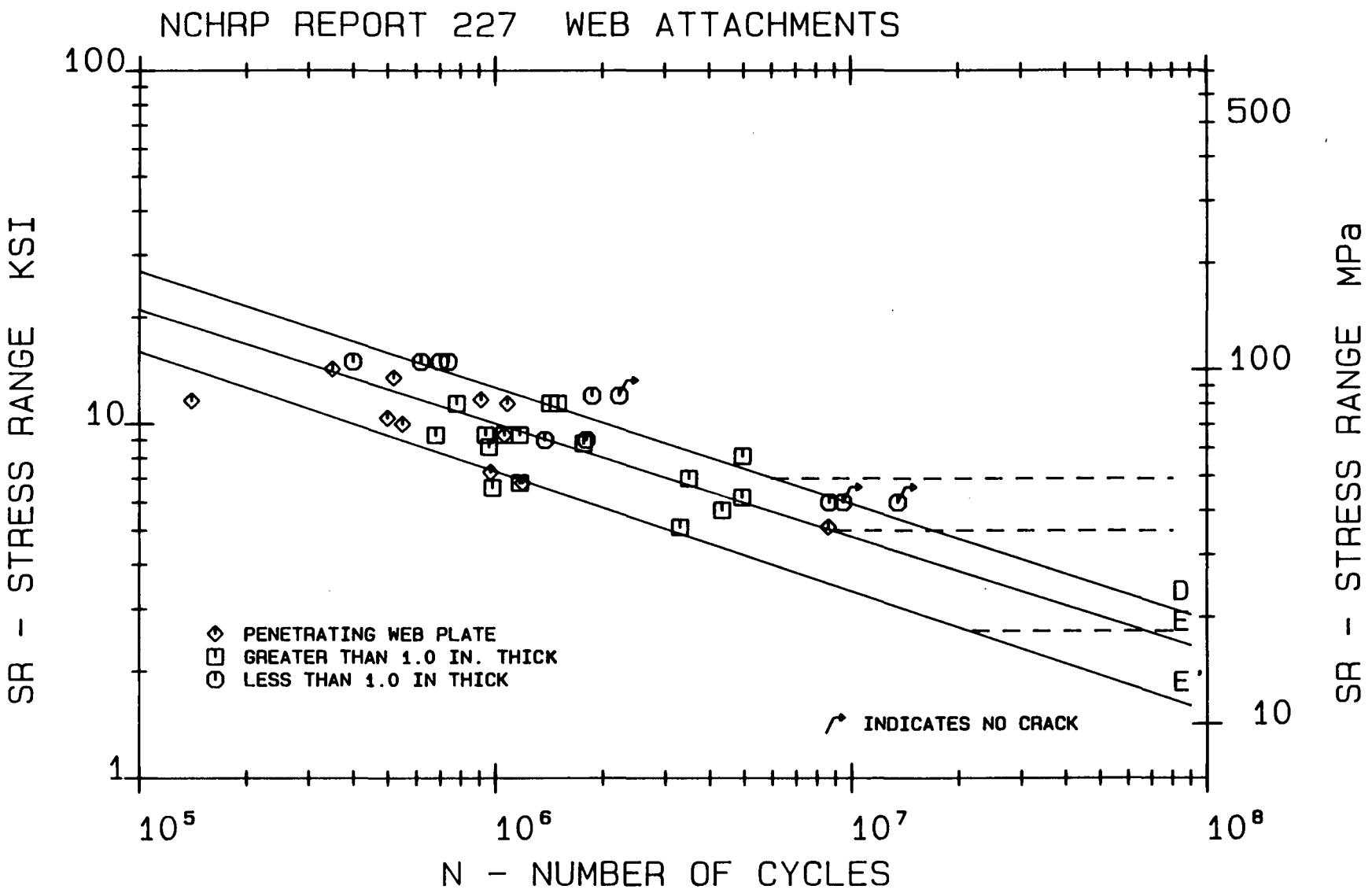

Figure: 14 Fatigue Resistance of Web Attachments, NCHRP Report 227

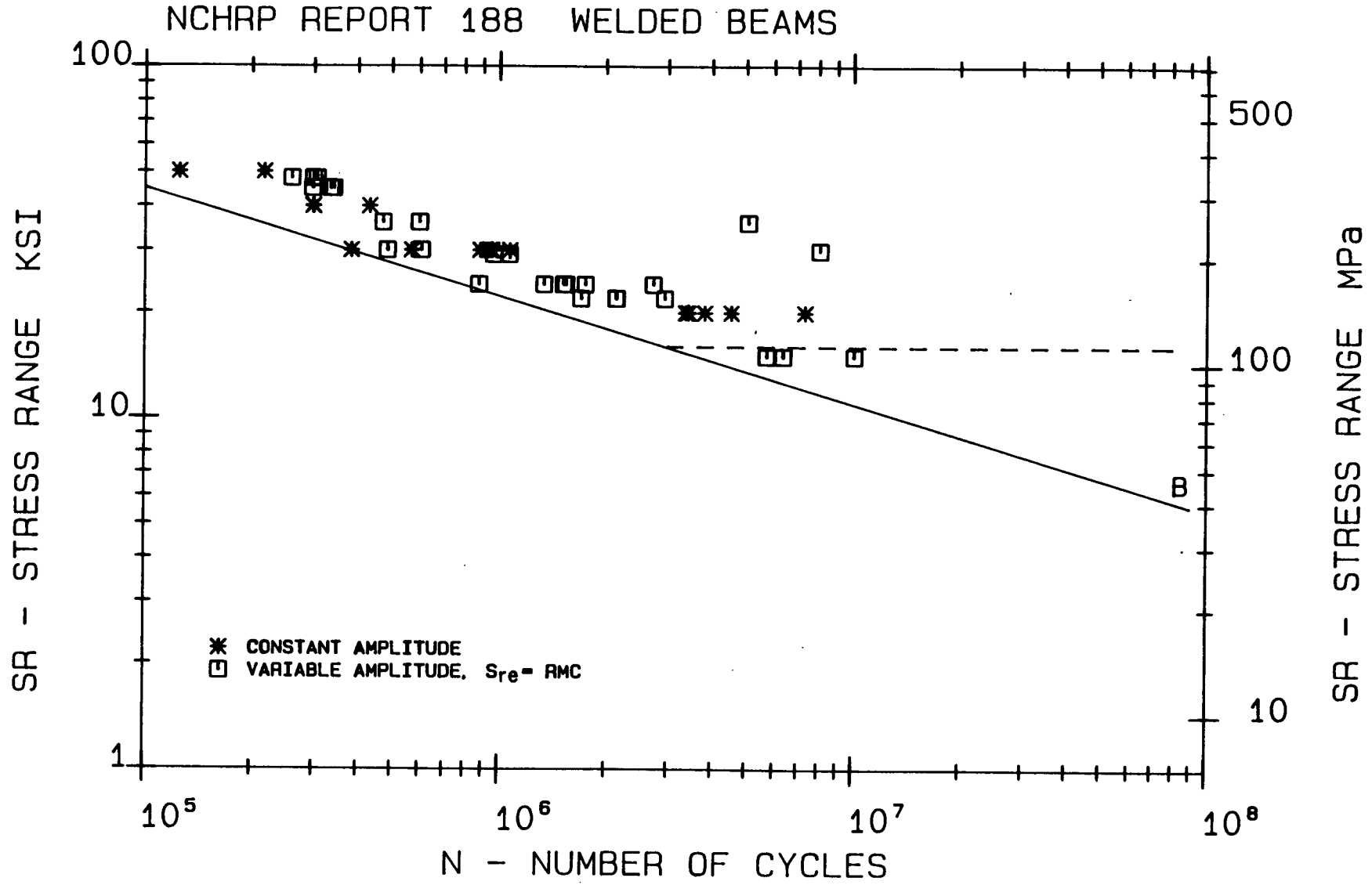

Figure: 15 Fatigue Resistance of Welded Beams under Variable Loading, NCHRP Report 188

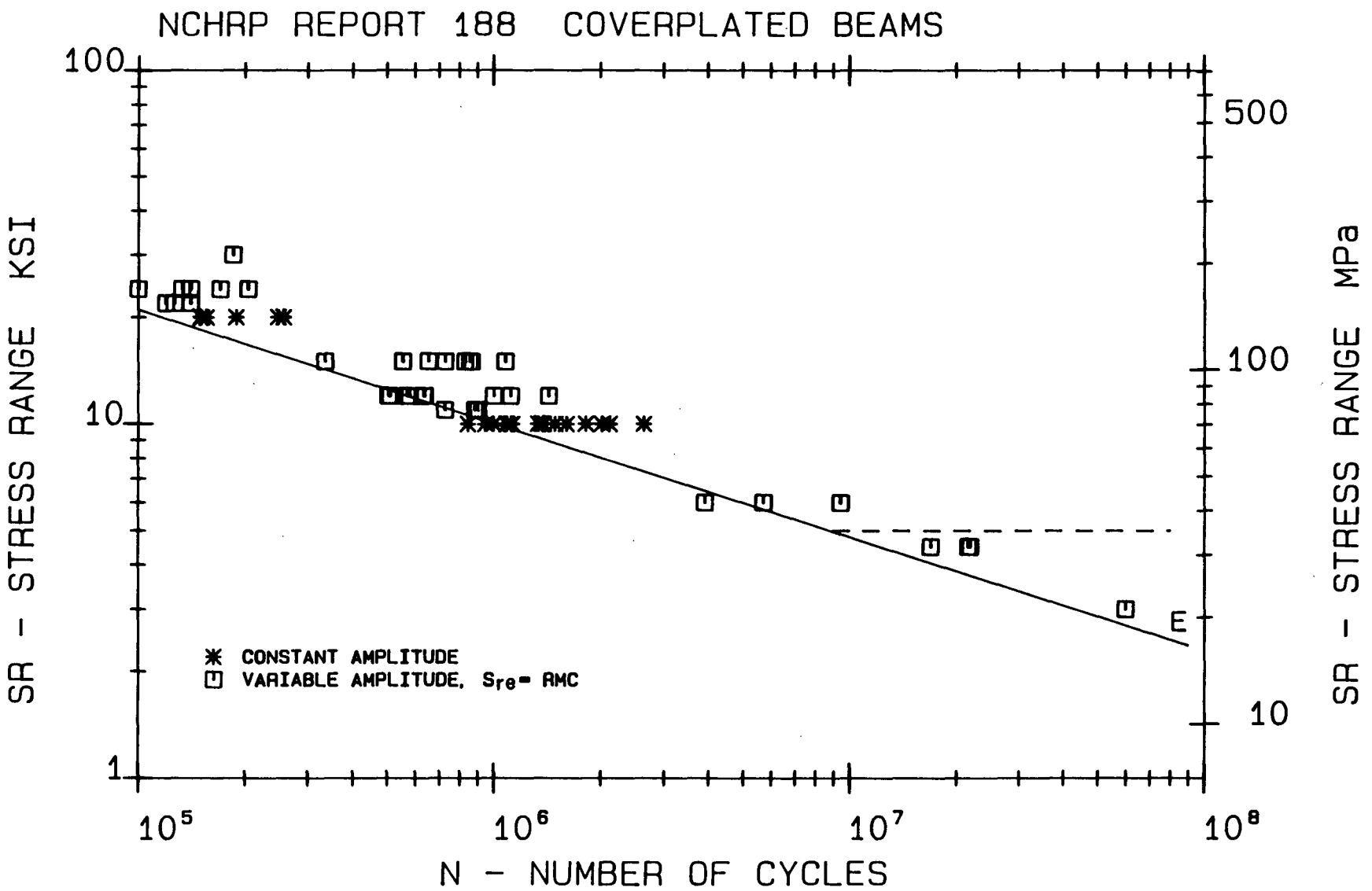

Figure: 16 Fatigue Resistance of Coverplated Beams under Variable Loading, NCHRP Report 188

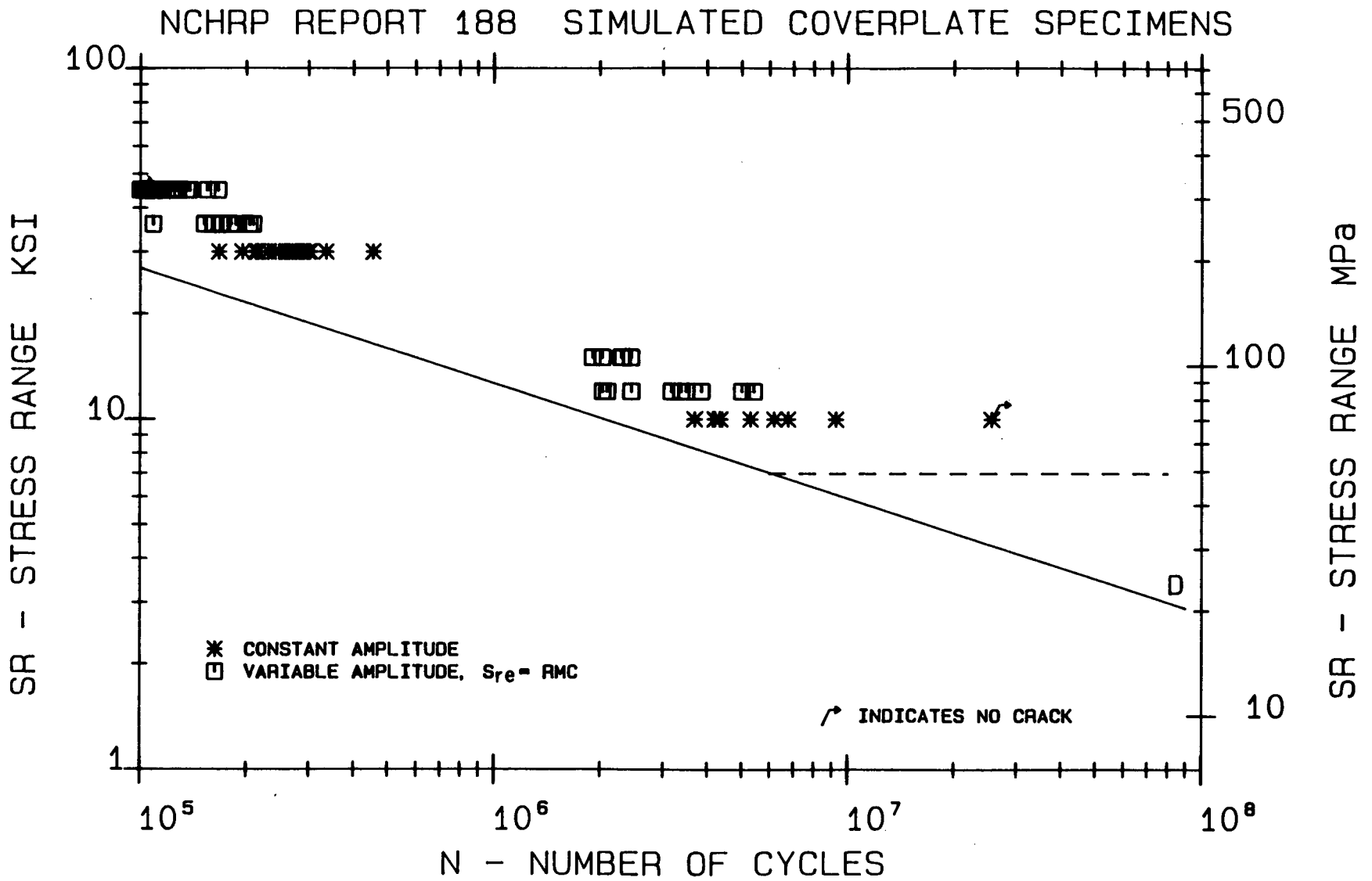

Figure: 17 Fatigue Resistance of Simulated Coverplate Specimens under Variable Loading, NCHRP Report 188

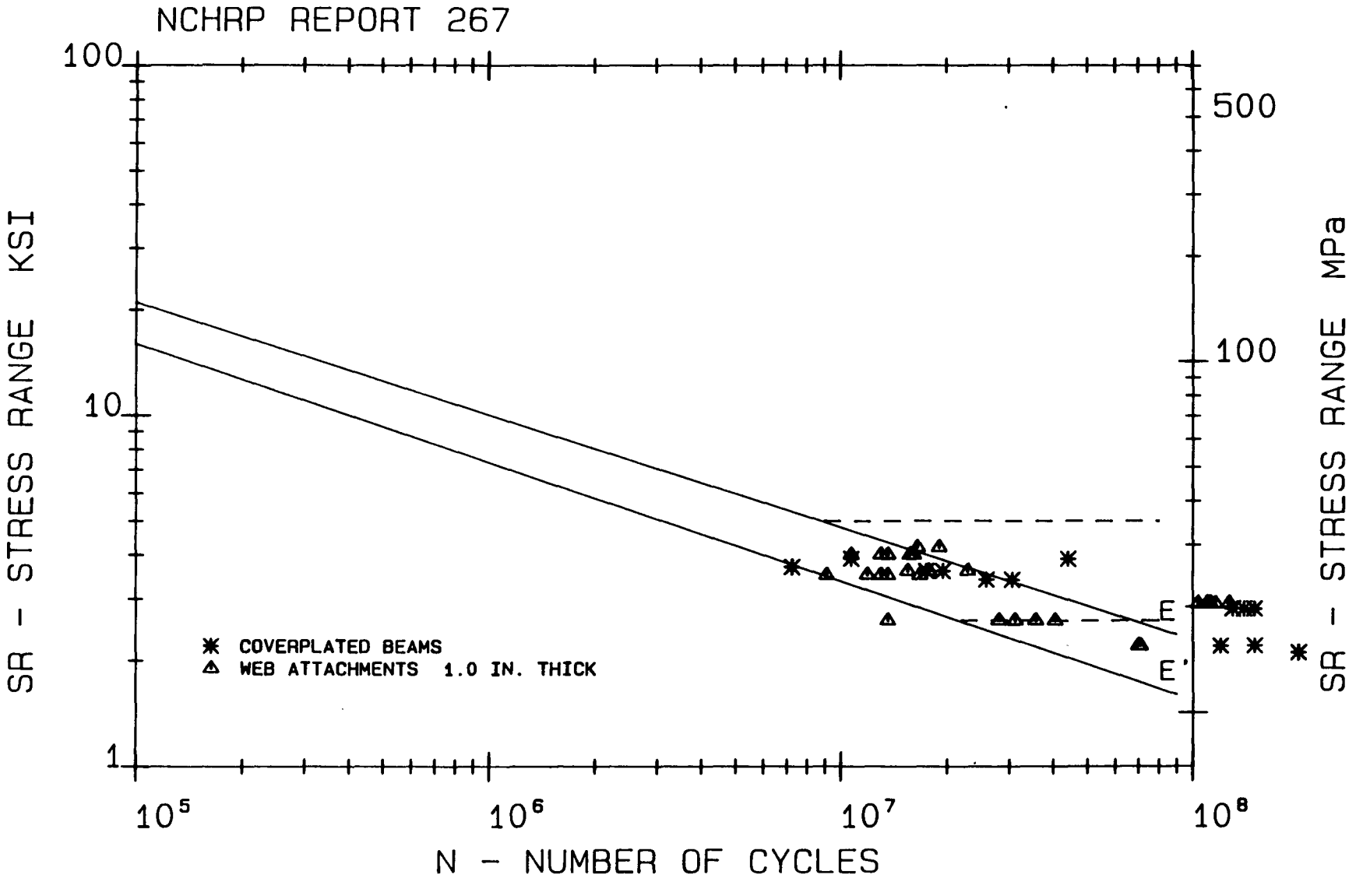

Figure: 18 Fatigue Resistance of Coverplated Beams and Web Attachments under Variable Loading, NCHRP Report 267

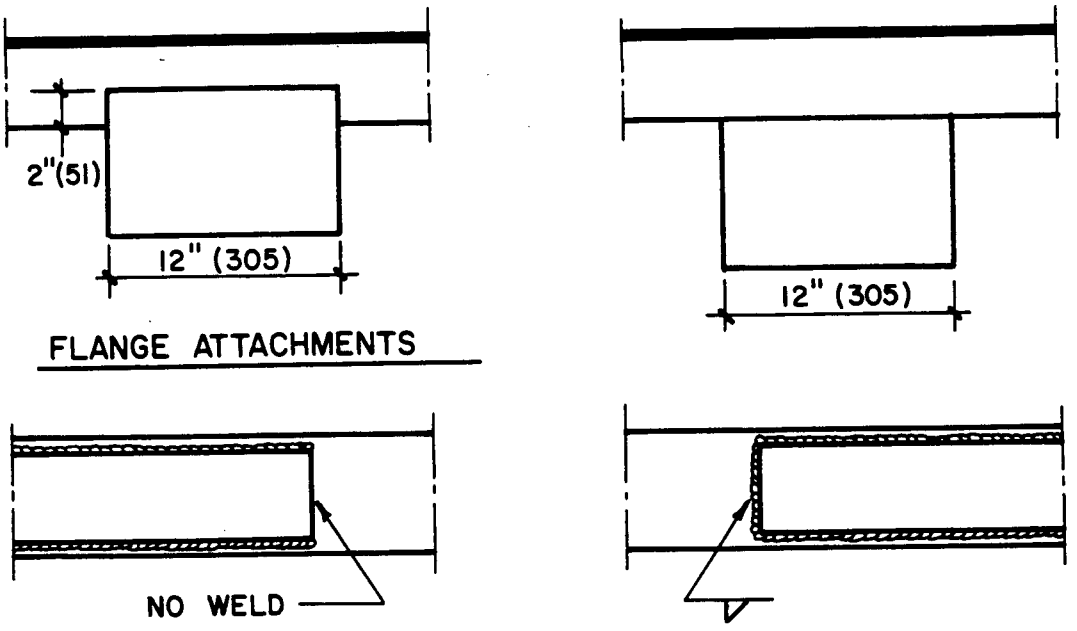

Figure: 19 Test Specimens for FHWA 12D-77-170

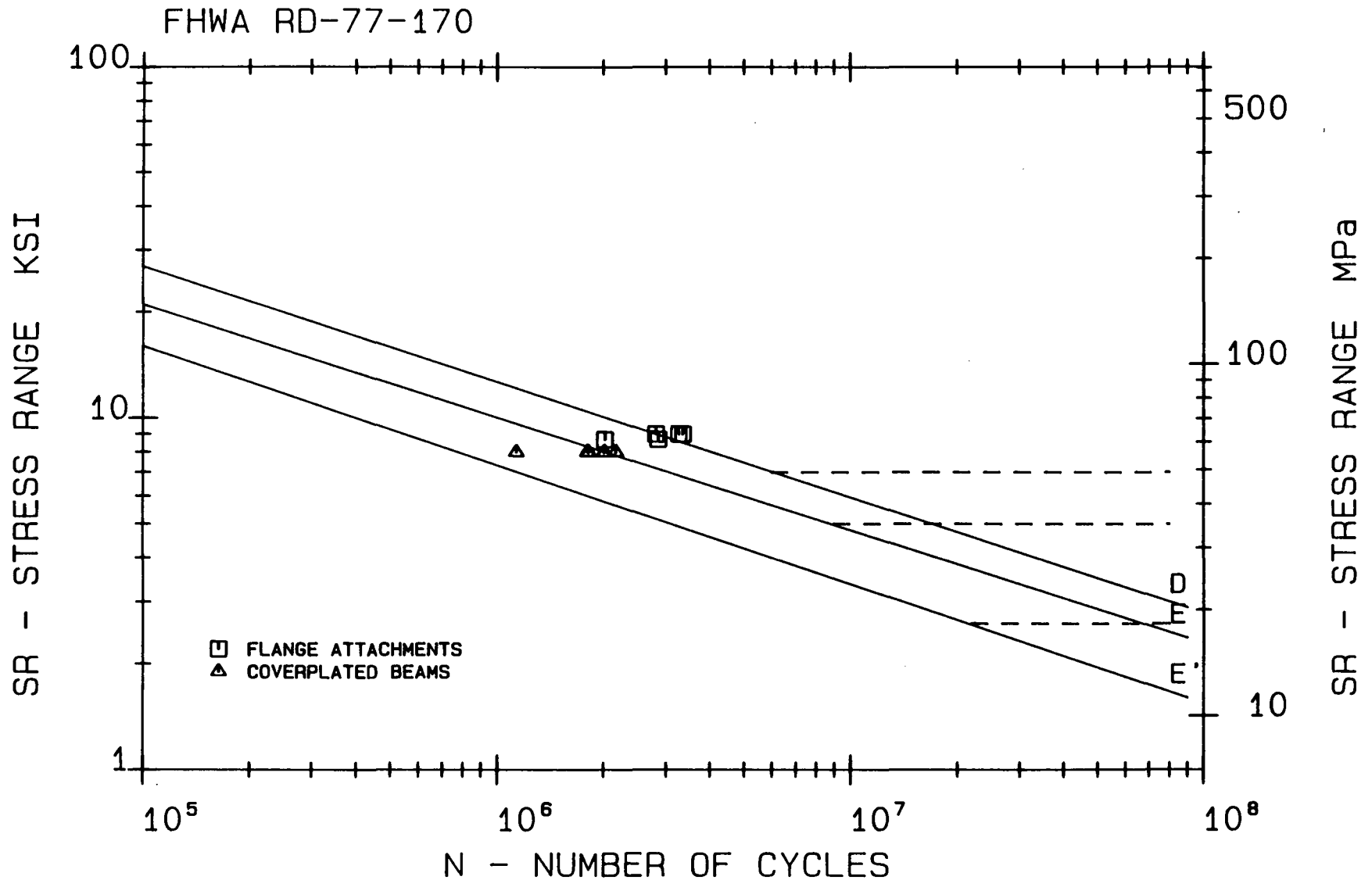

Figure: 20 Fatigue Resistance of Coverplated Beams and Flange Tip Attachments, FHWA 12D-77-170

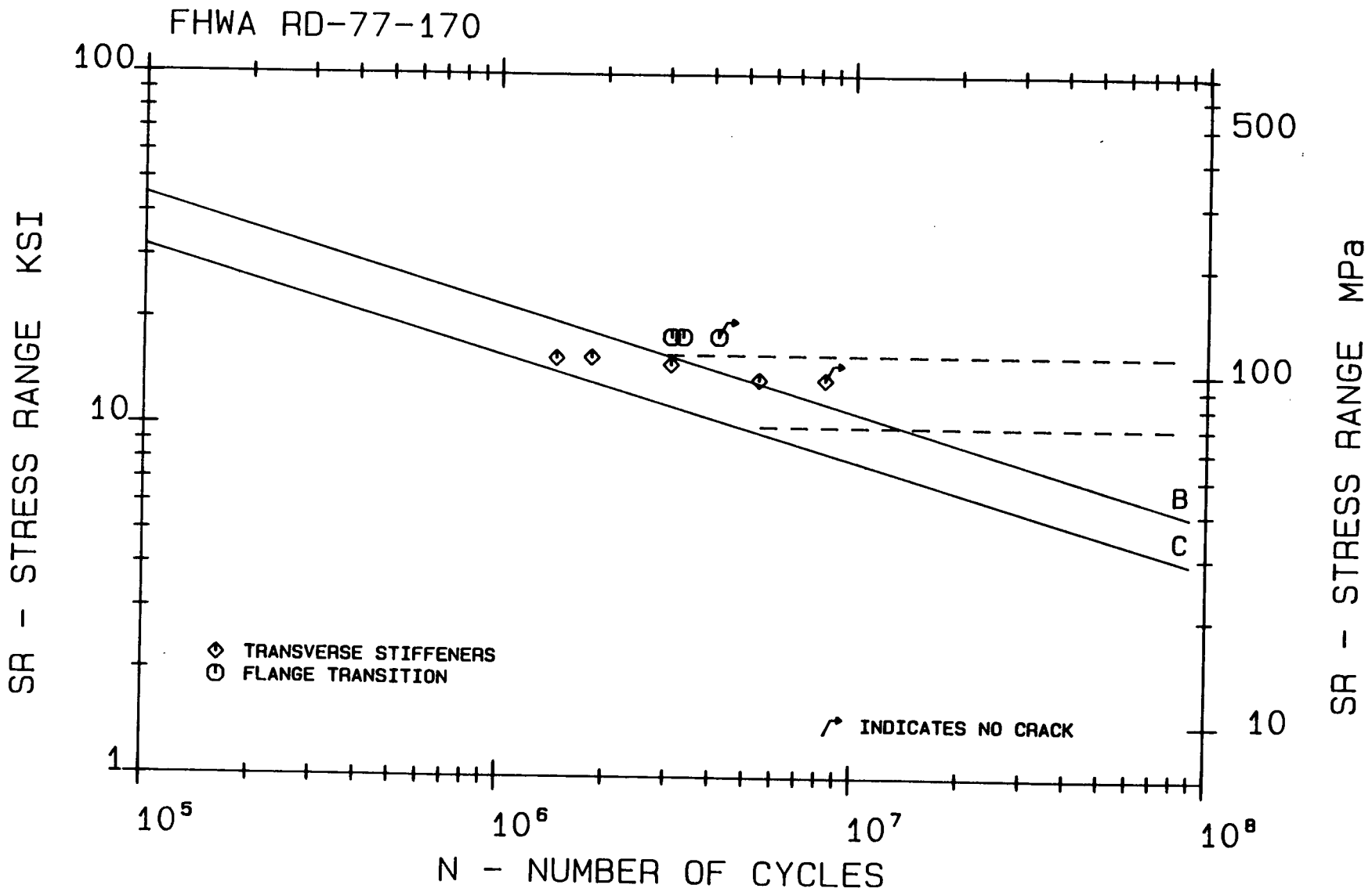

Figure: 21 Fatigue Resistance of Flange Transitions and Transverse Stiffeners, FHWA 12D-77-170

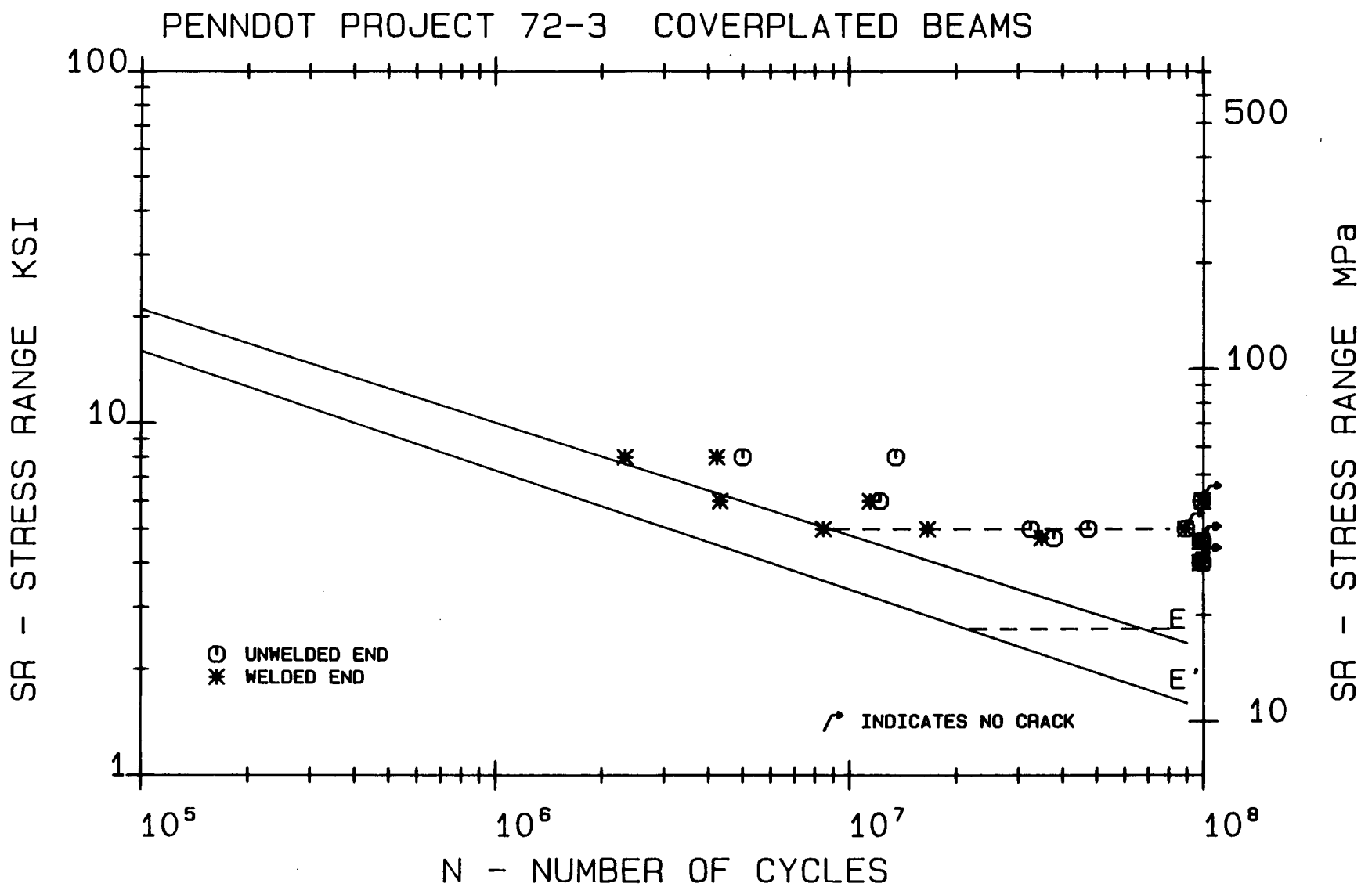

Figure: 22 Fatigue Resistance of Coverplated Beams, PennDot Project 72-3

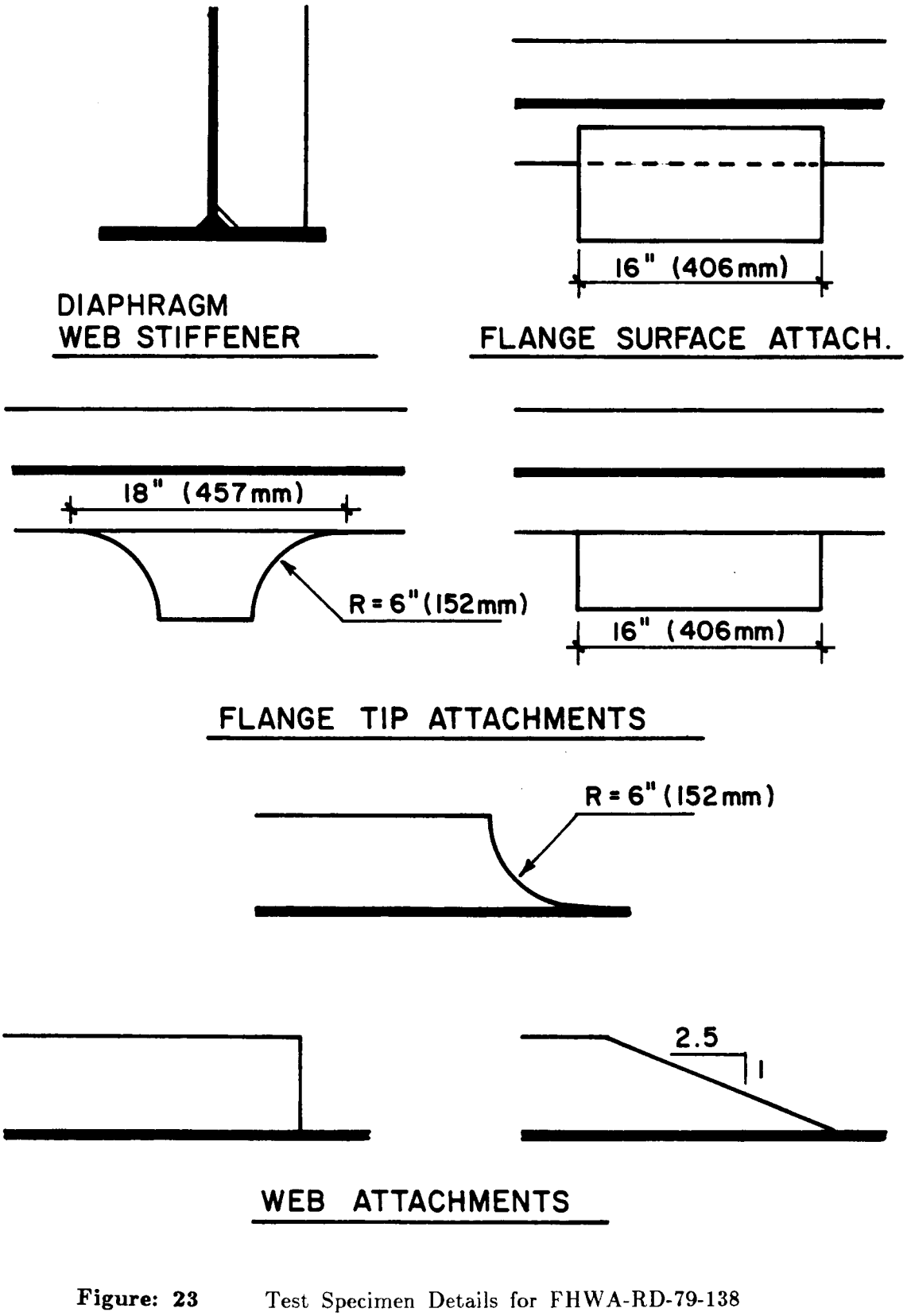

Figure: 23 Test Specimen Details for FHWA-RD-79-138

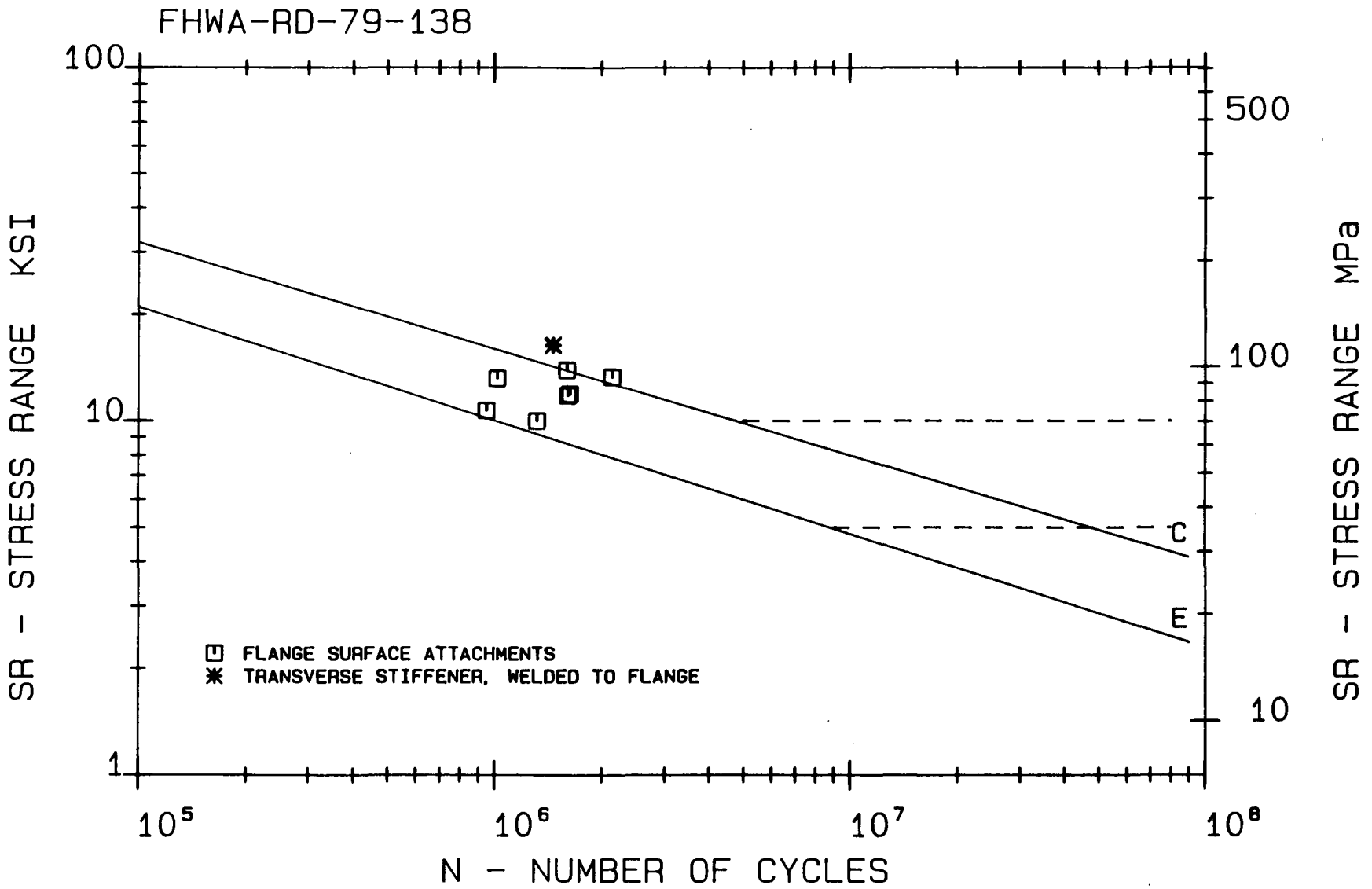

Figure: 24 Fatigue Resistance of Transverse Stiffeners and Flange Surface Attachments, FHWA-RD-79-138

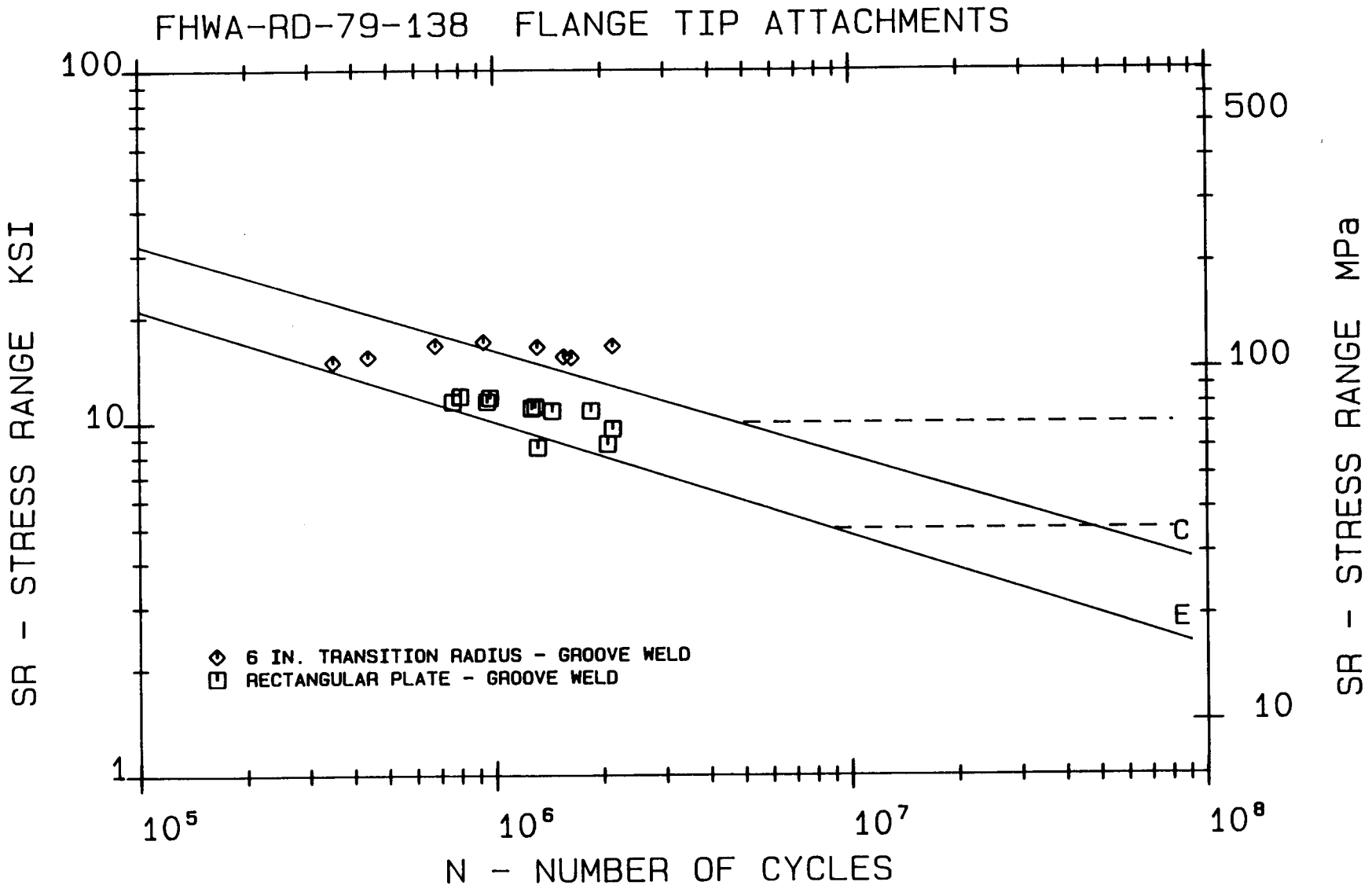

Figure: 25 Fatigue Resistance of Flange Tip Attachments, FHWA-RD-79-138

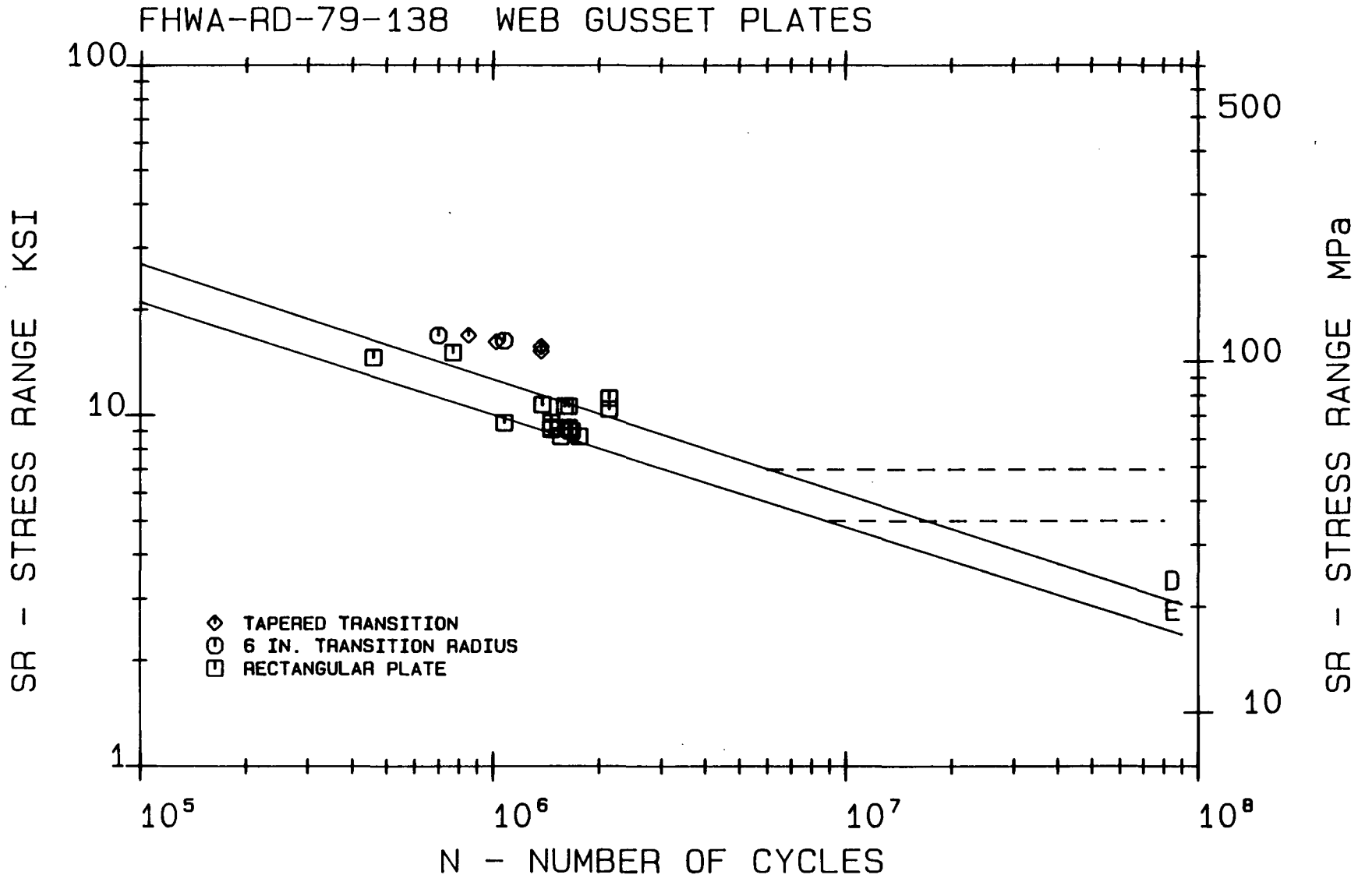

Figure: 26 Fatigue Resistance of Web Gusset Plates, FHWA-RD-79-138

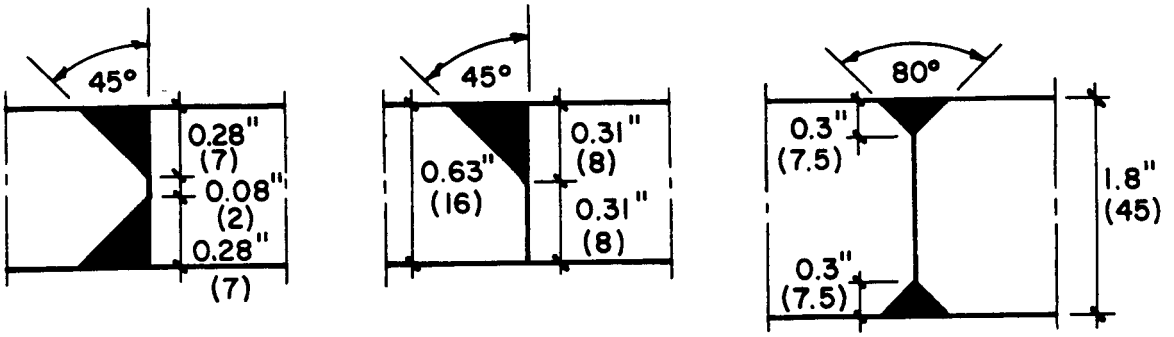

LONGITUDINAL GROOVE WELDS - FLAT PLATE SPECIMENS

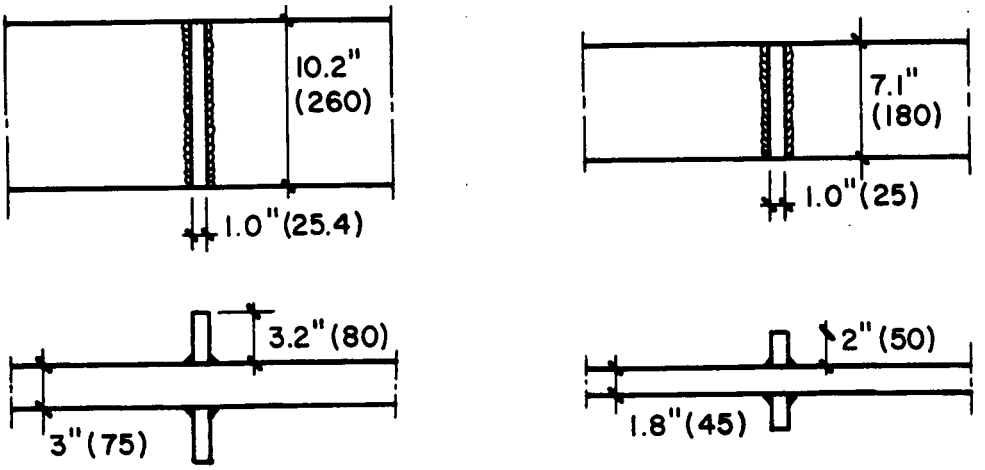

NON-LOAD CARRYING CRUCIFORM JOINT SPECIMENS

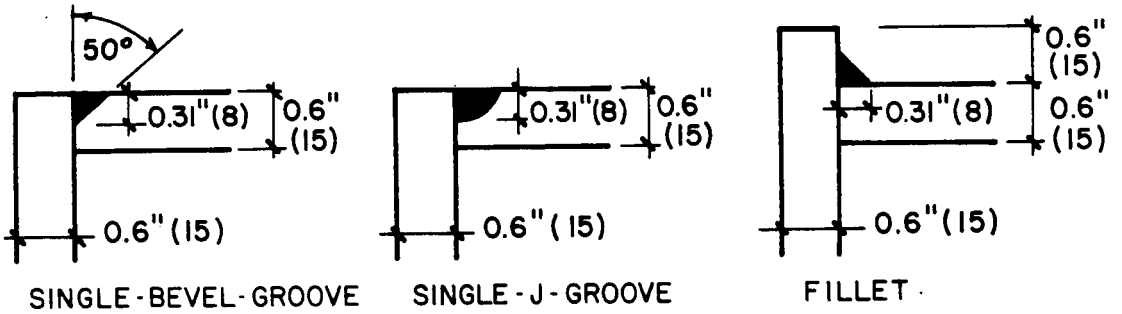

LONGITUDINAL WELD TYPES - BUILT-UP TEST MEMBERS

Figure: 27 Test Specimens for Japanese Test Programs

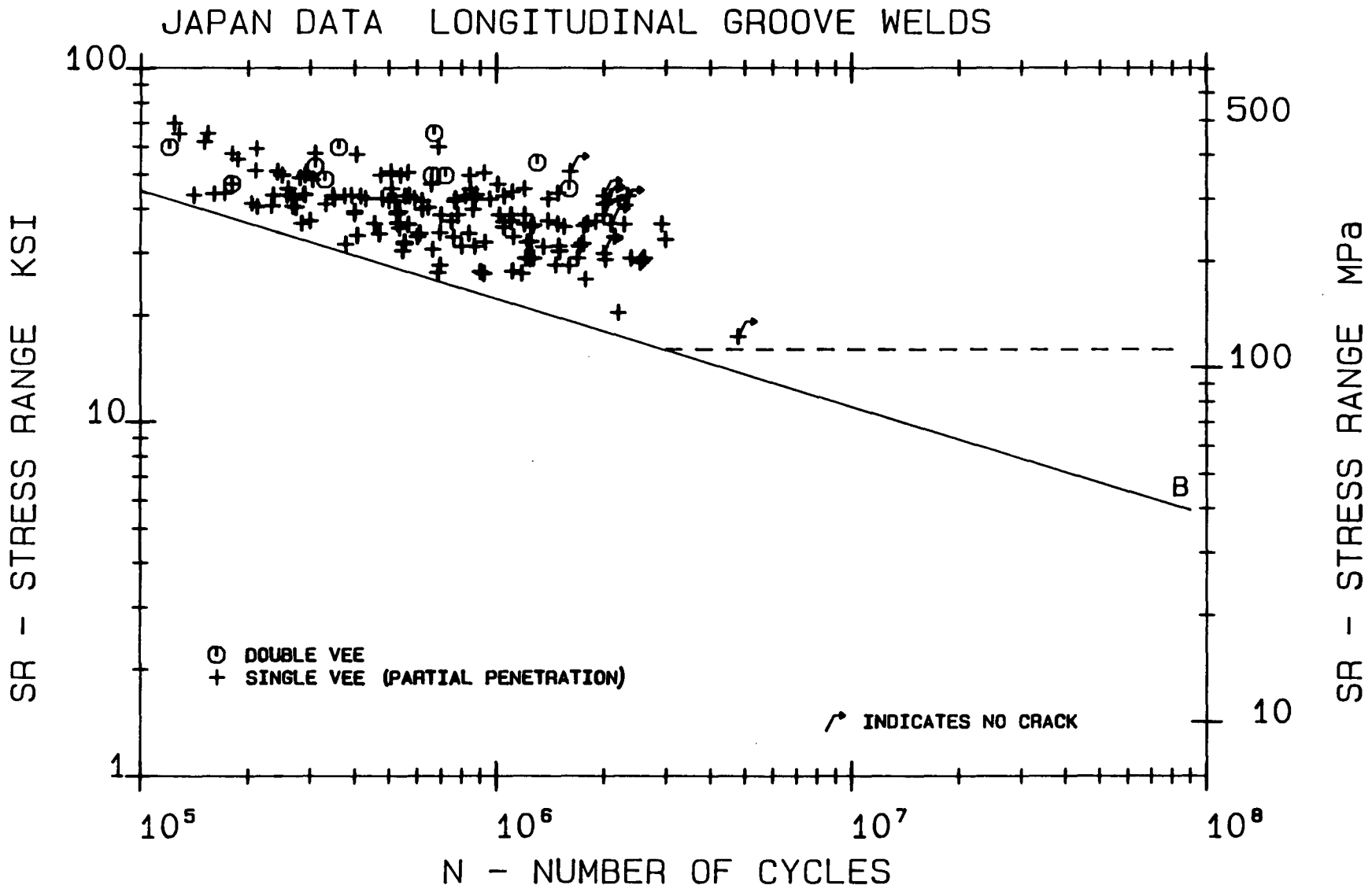

Figure: 28 Fatigue Resistance of Longitudinal Groove Welds, Japanese Data

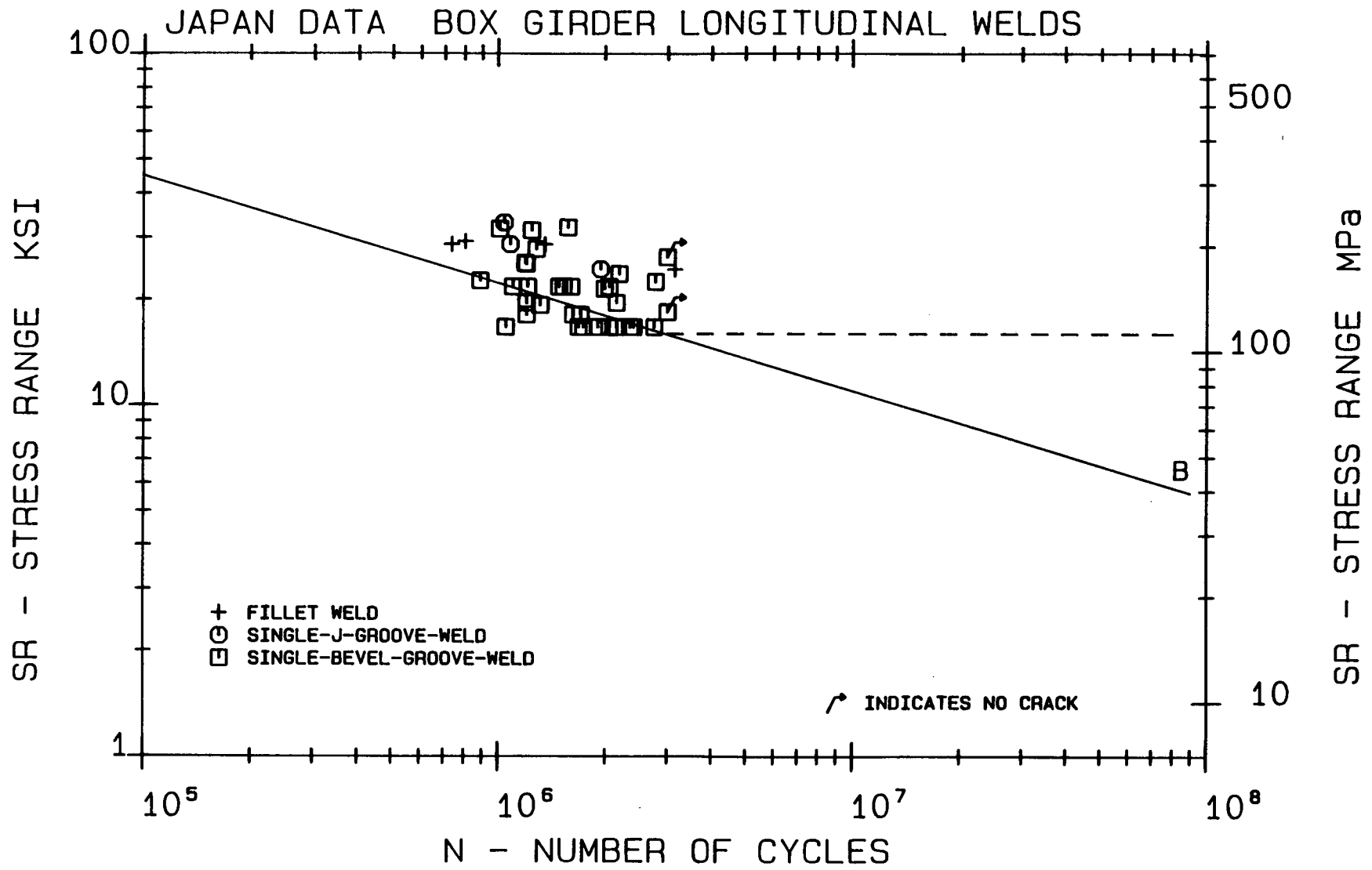

Figure: 29 Fatigue Resistance of Box Girder Longitudinal Welds, Japanese Data

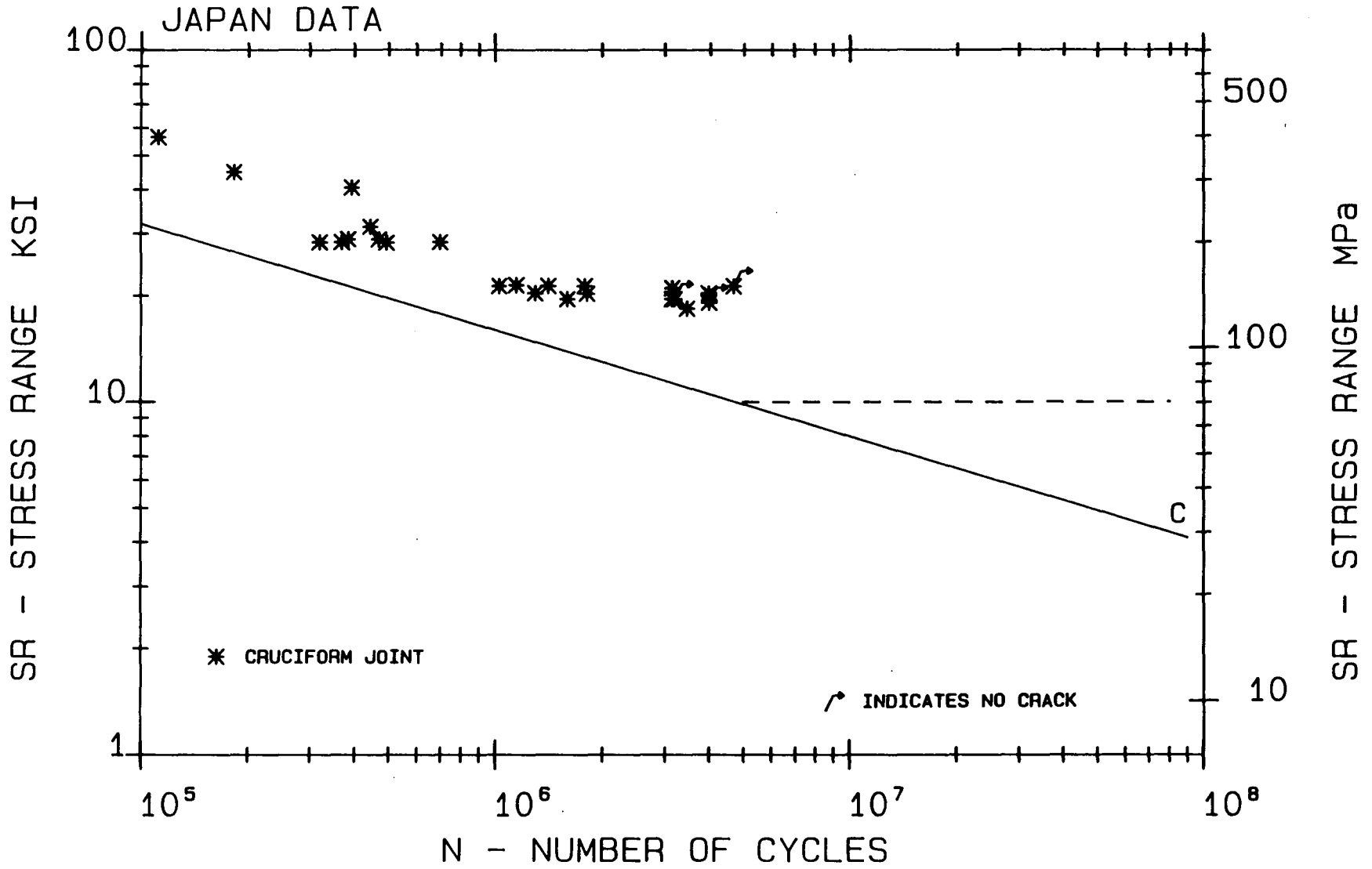

Figure: 30 Fatigue Resistance of Non-Load Carrying Cruciform Joints, Japanese Data

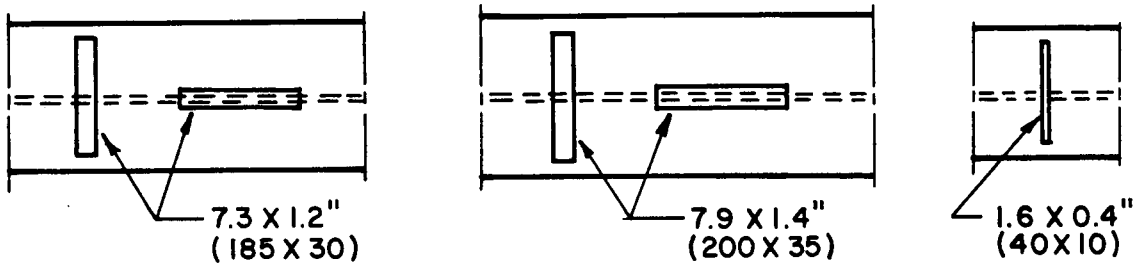

FLANGE ATTACHMENTS

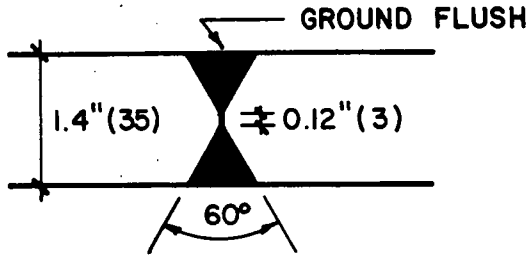

FLANGE BUTT WELD

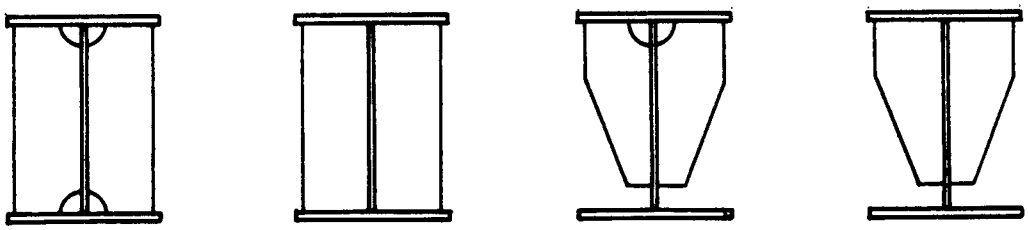

TRANSVERSE STIFFENER DETAIL TYPES

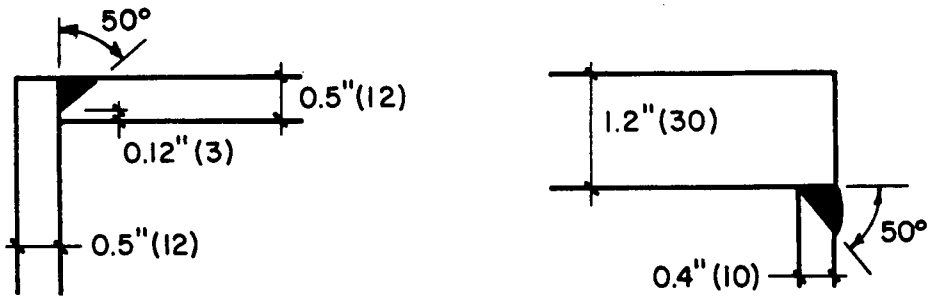

LONGITUDINAL WELD TYPES – BOX SECTIONS

Figure: 31 Test Specimens for ORE Test Programs

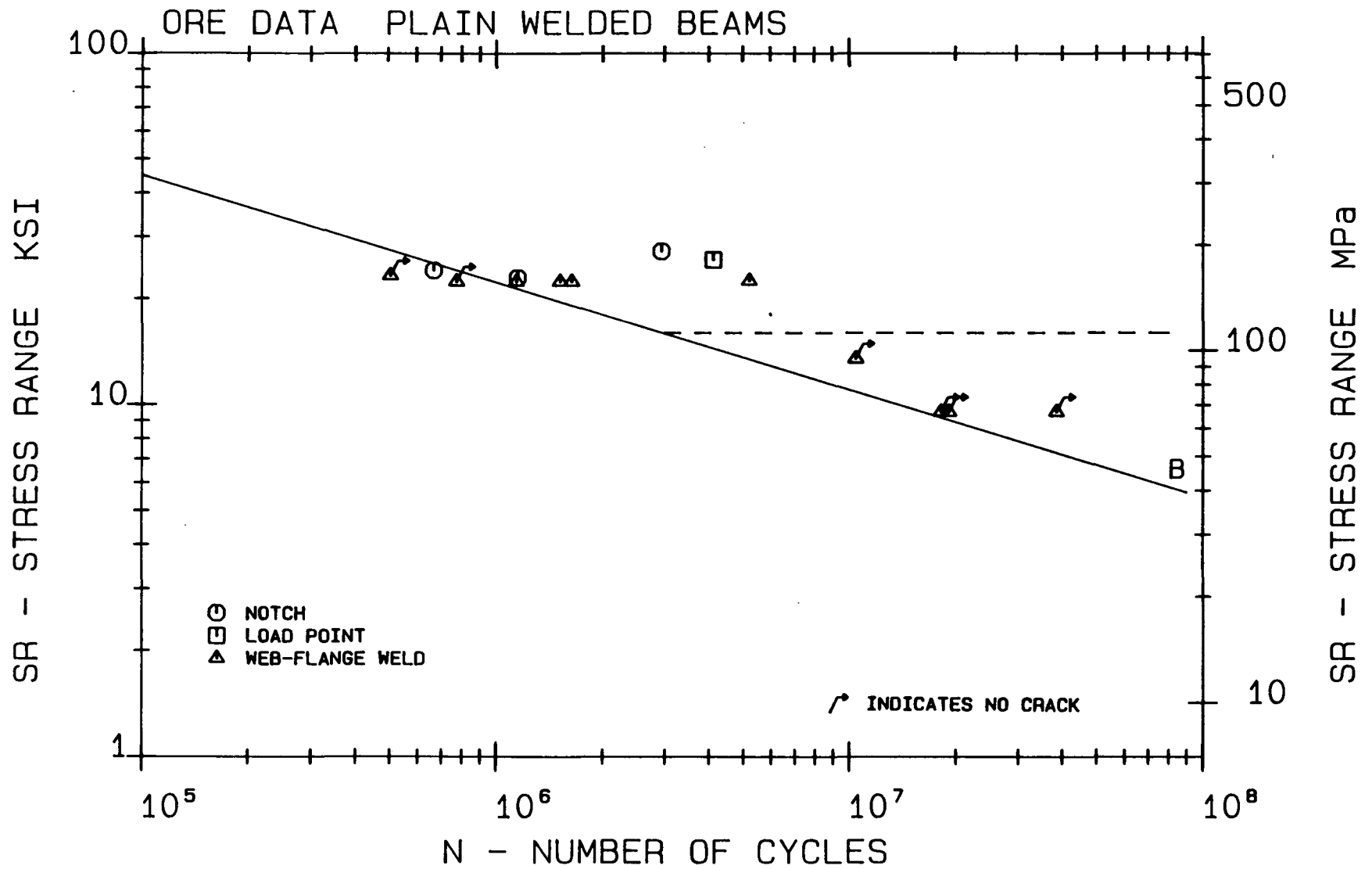

Figure: 32 Fatigue Resistance of Welded Beams, ORE Data

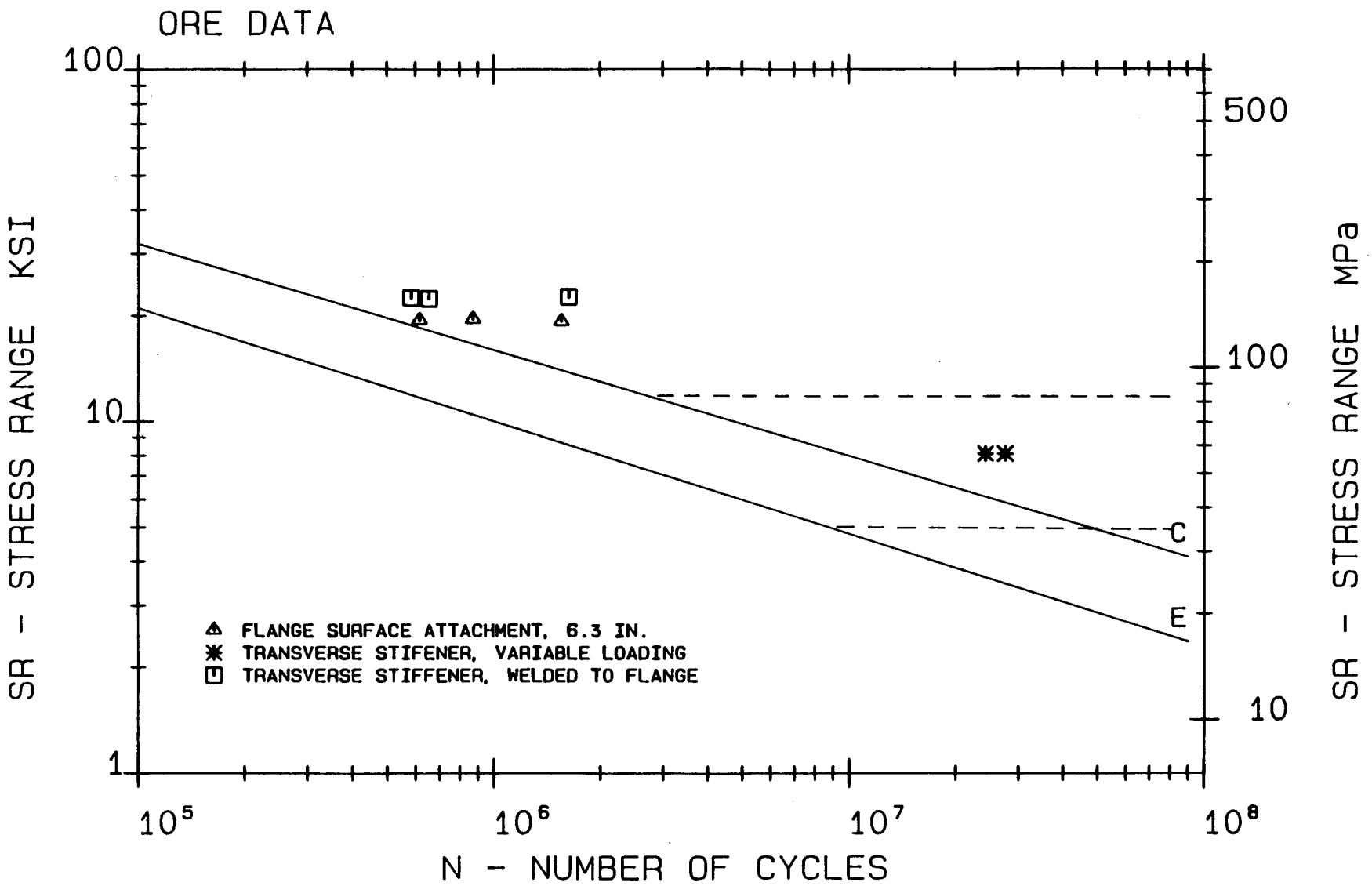

Figure: 33 Fatigue Resistance of Transverse Stiffeners and Flange Attachments, ORE Data

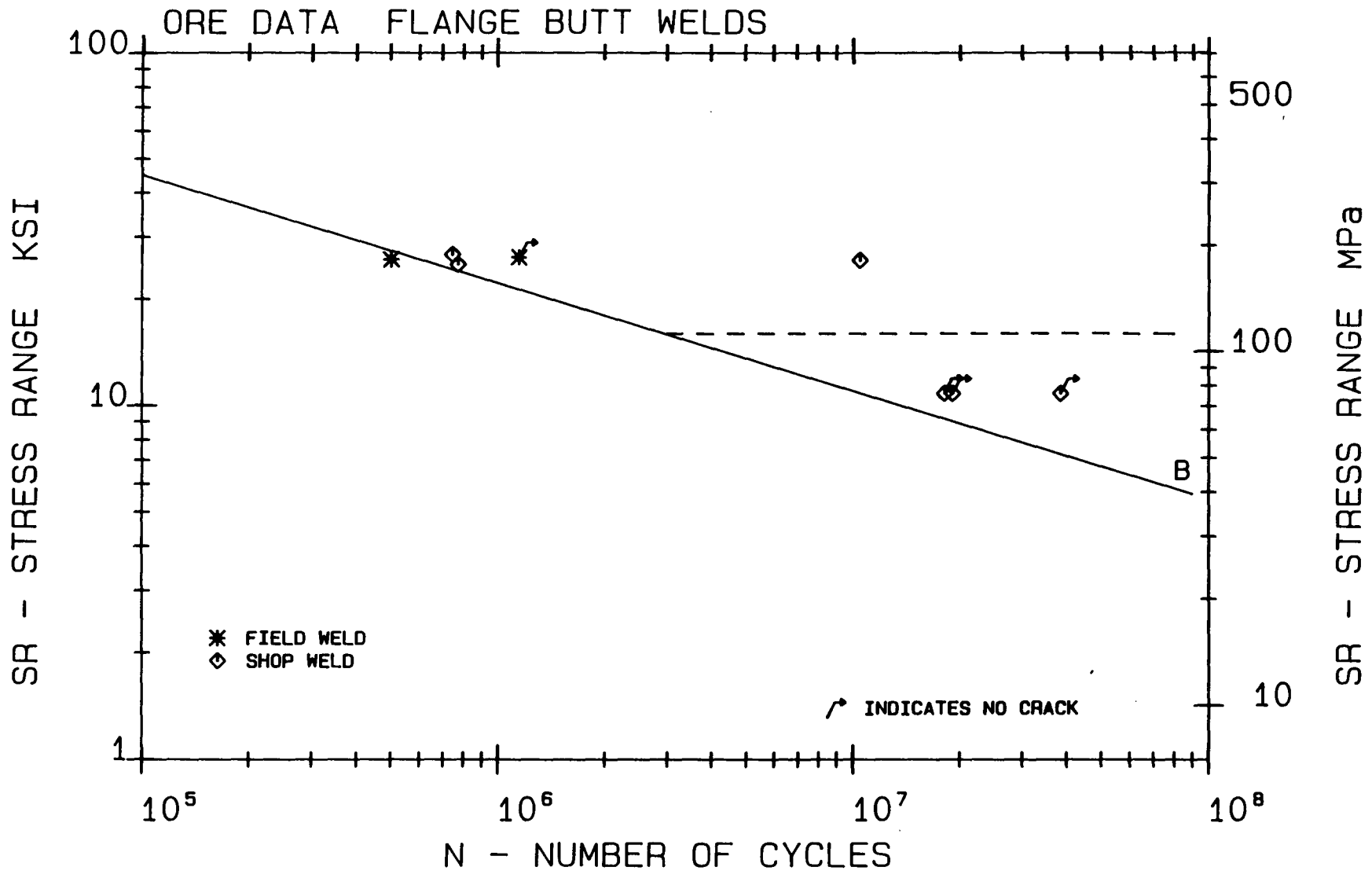

Figure: 34 Fatigue Resistance of Flange Butt Welds, ORE Data

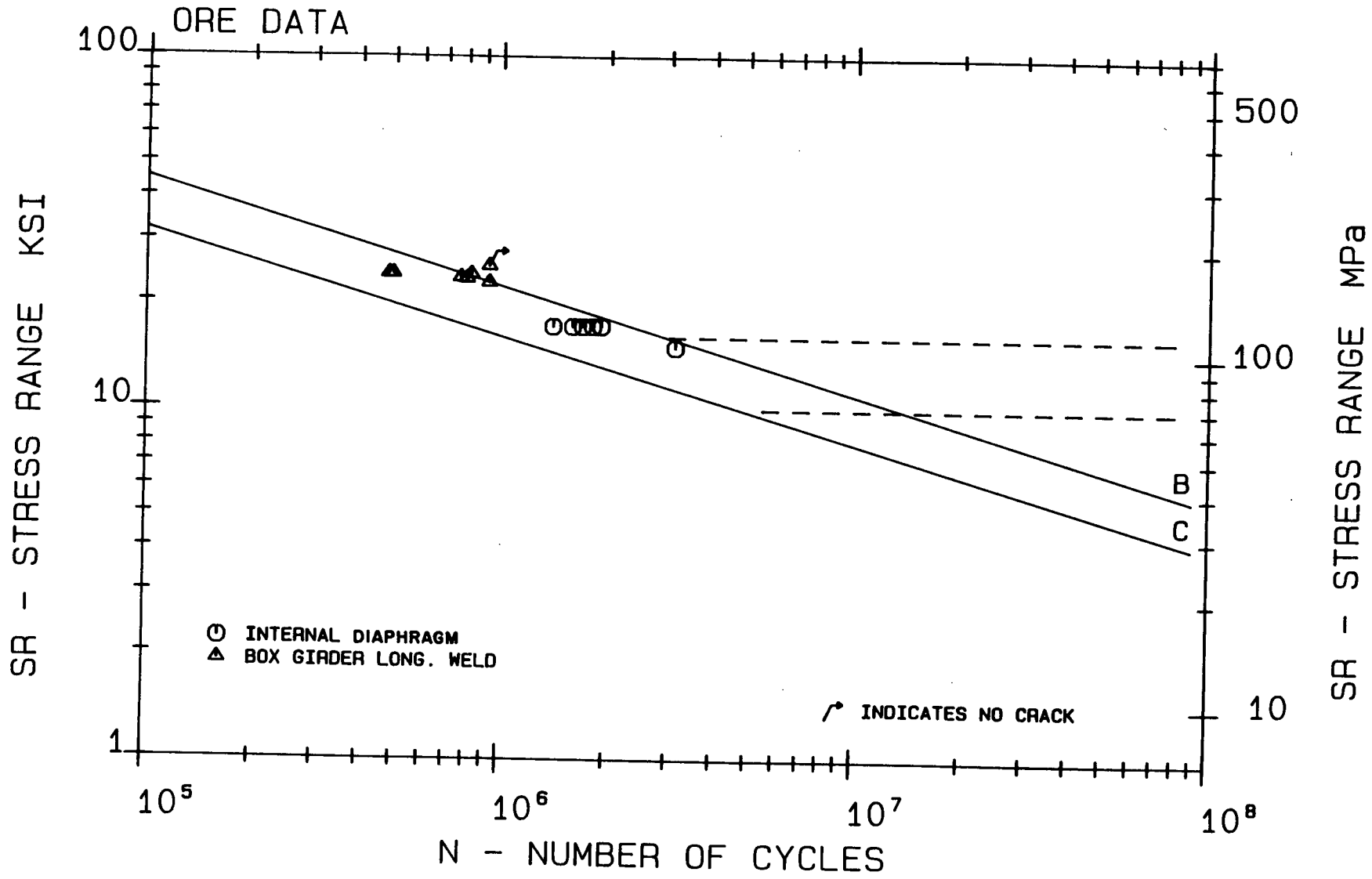

Figure: 35 Fatigue Resistance of Box Girder Longitudinal Welds and Internal Diaphragms, ORE Data

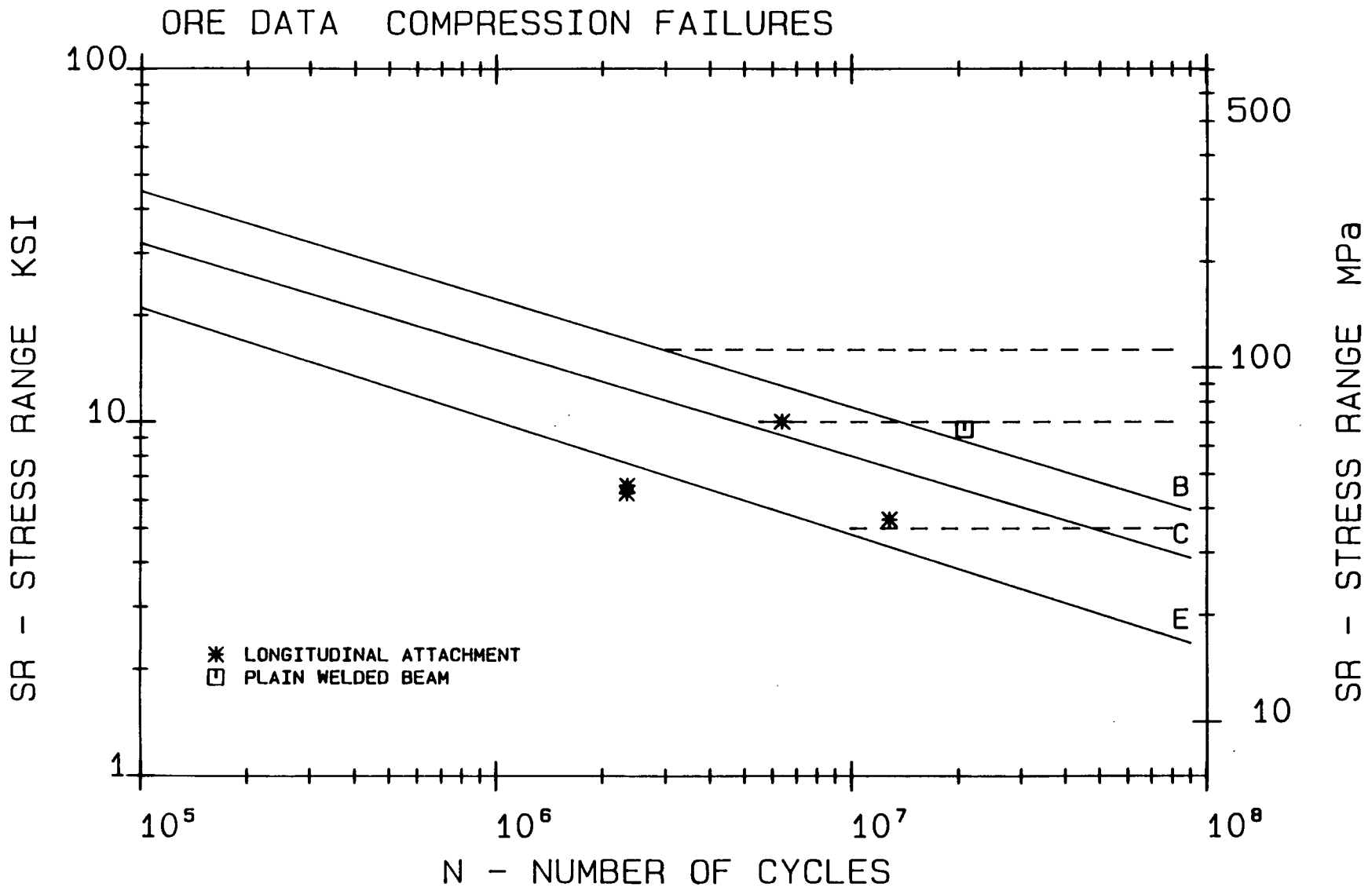

Figure: 36 Fatigue Resistance of Flange Attachment Compression Failures, ORE Data

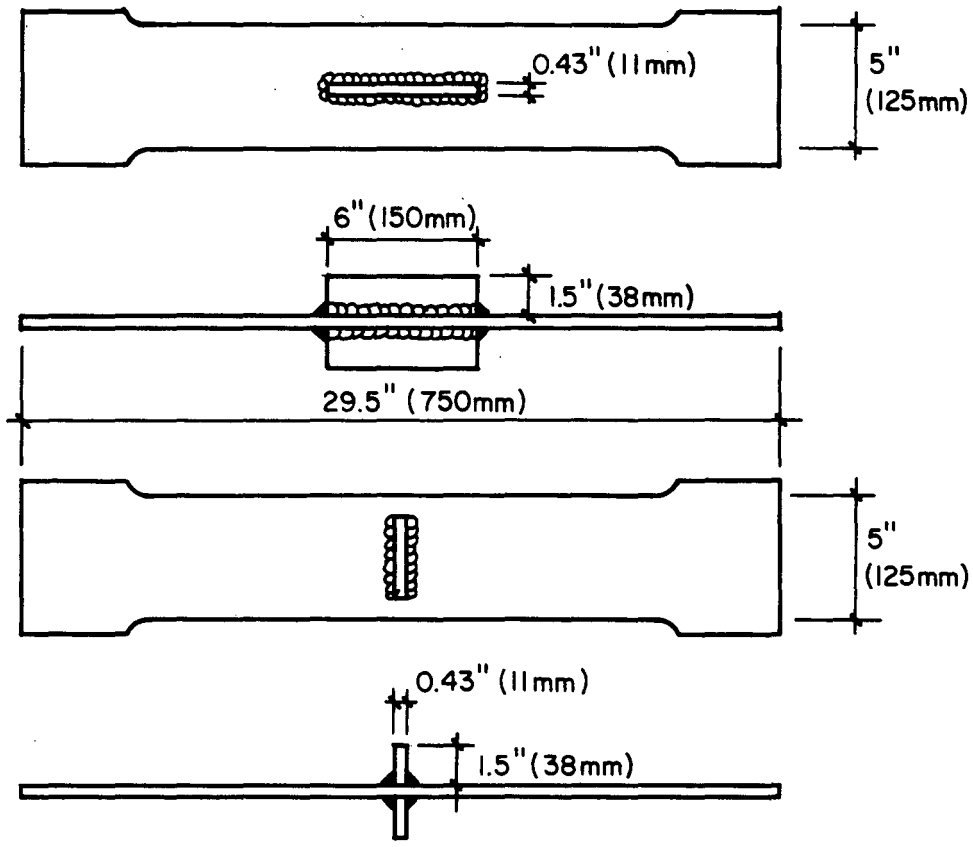

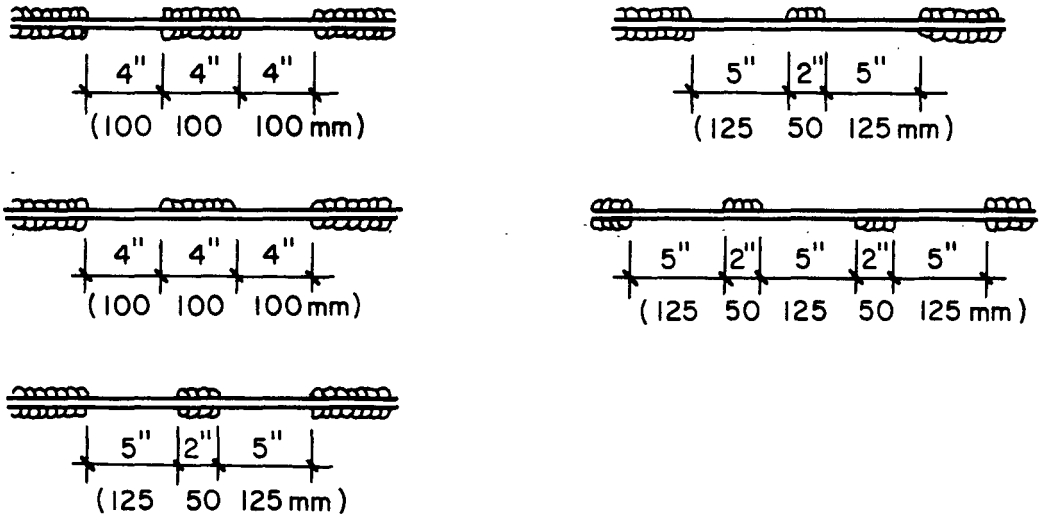

Figure: 37 Test Specimens for English Fatigue Tests

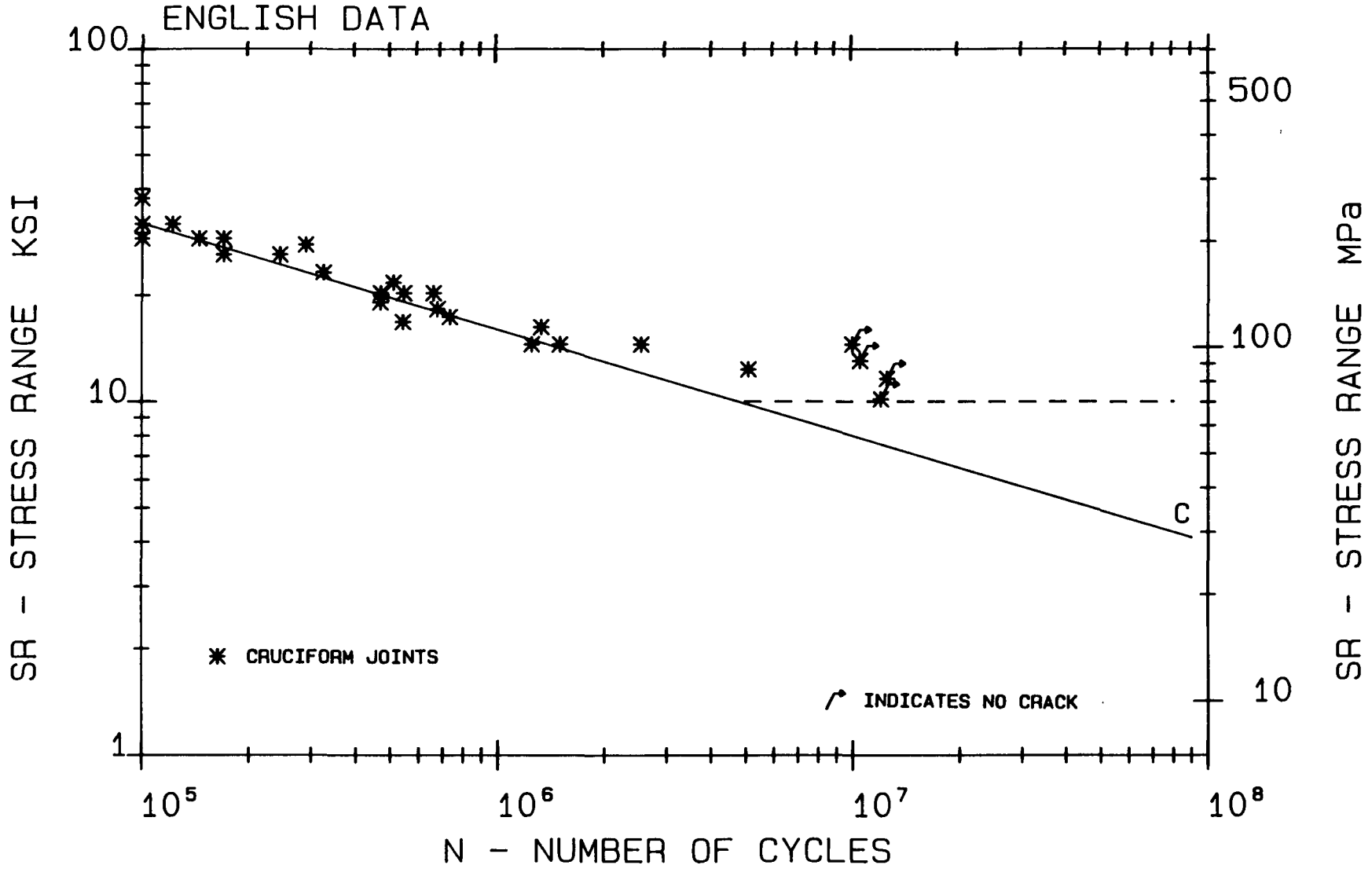

Figure: 38 Fatigue Resistance of Non-Load Carrying Cruciform Joints, English Data

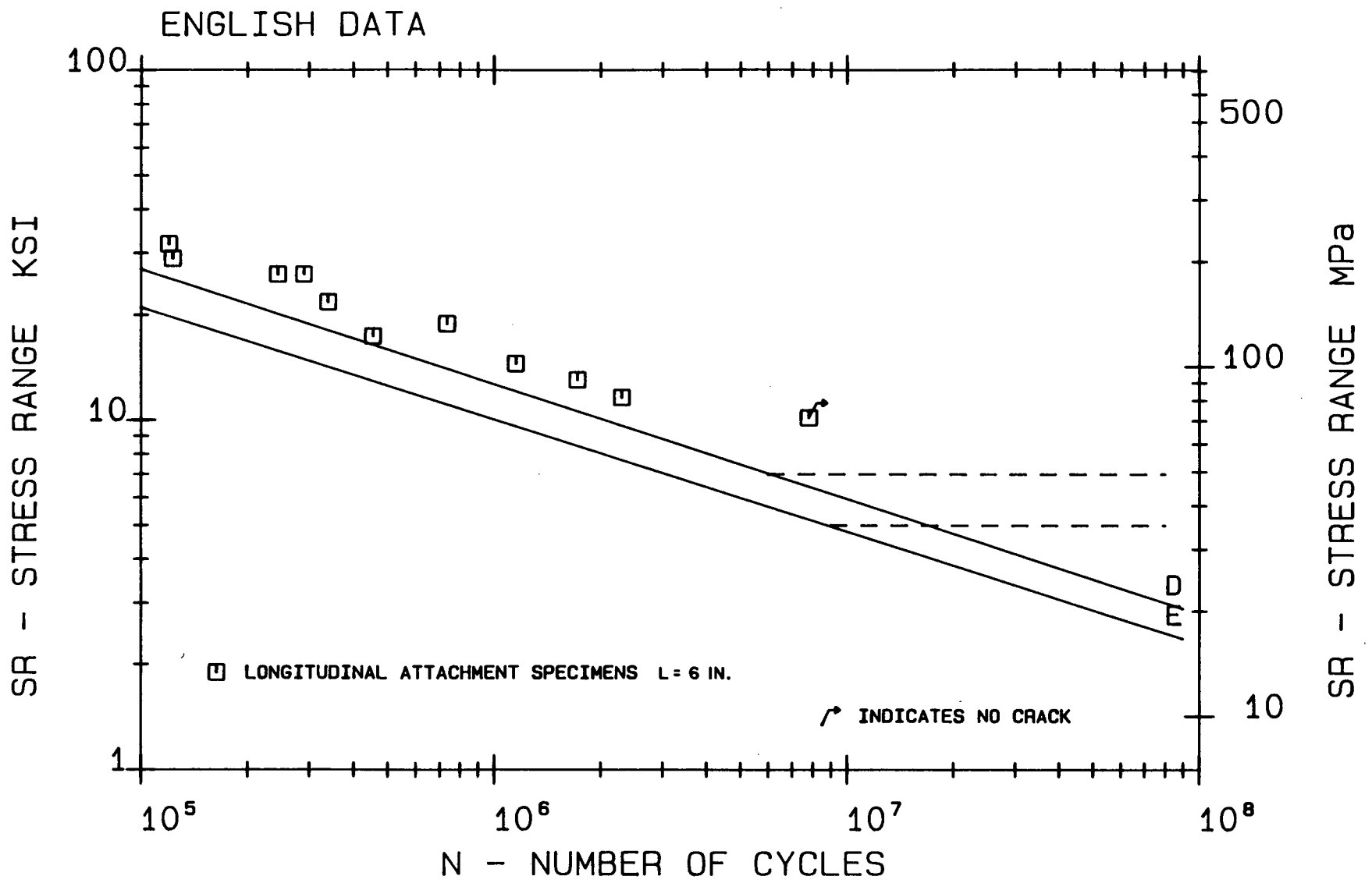

Figure: 39 Fatigue Resistance of Longitudinal Attachment Specimens, English Data

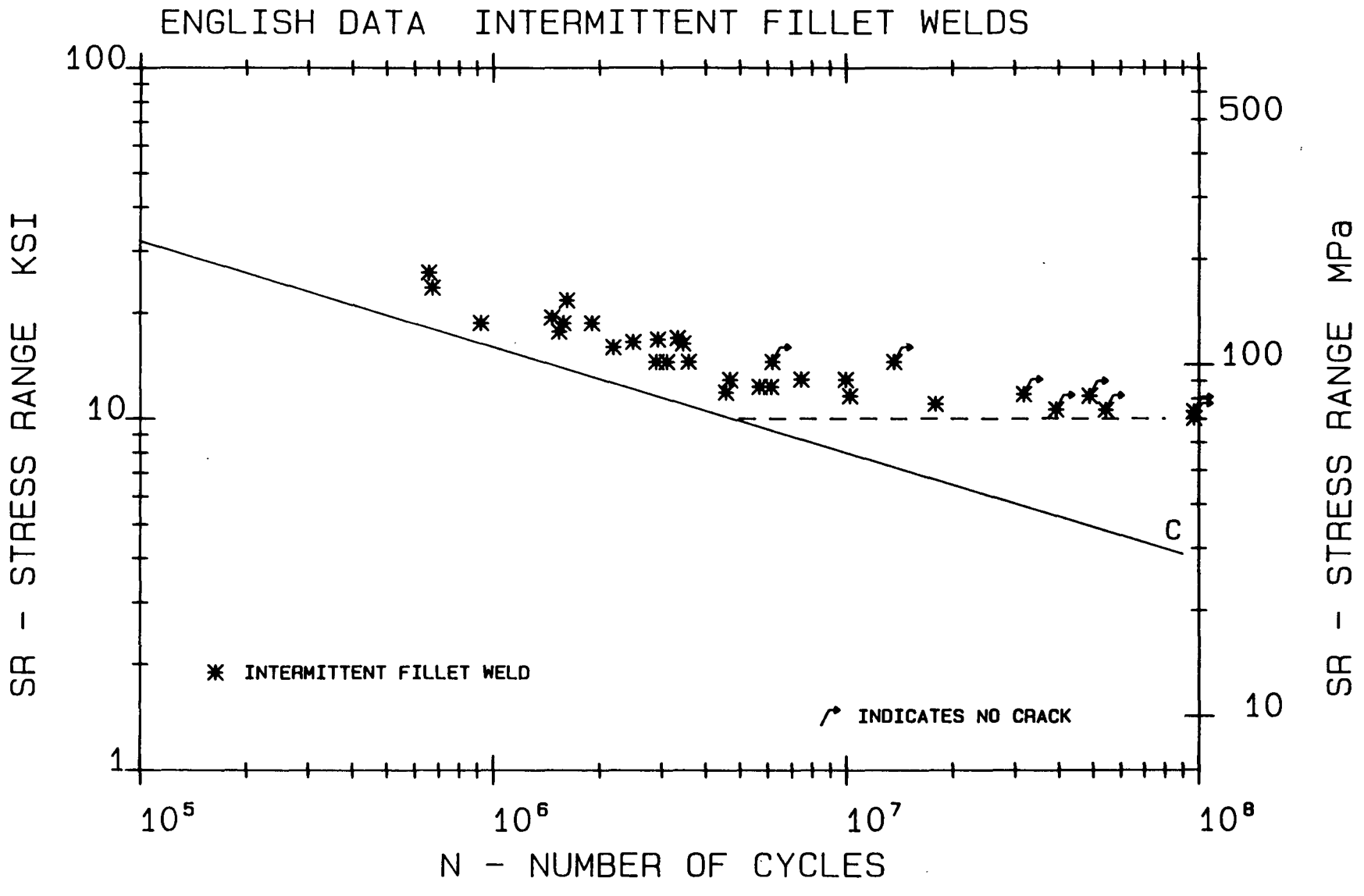

Figure: 40 Fatigue Resistance of Intermittent Longitudinal Fillet Welds, English Data

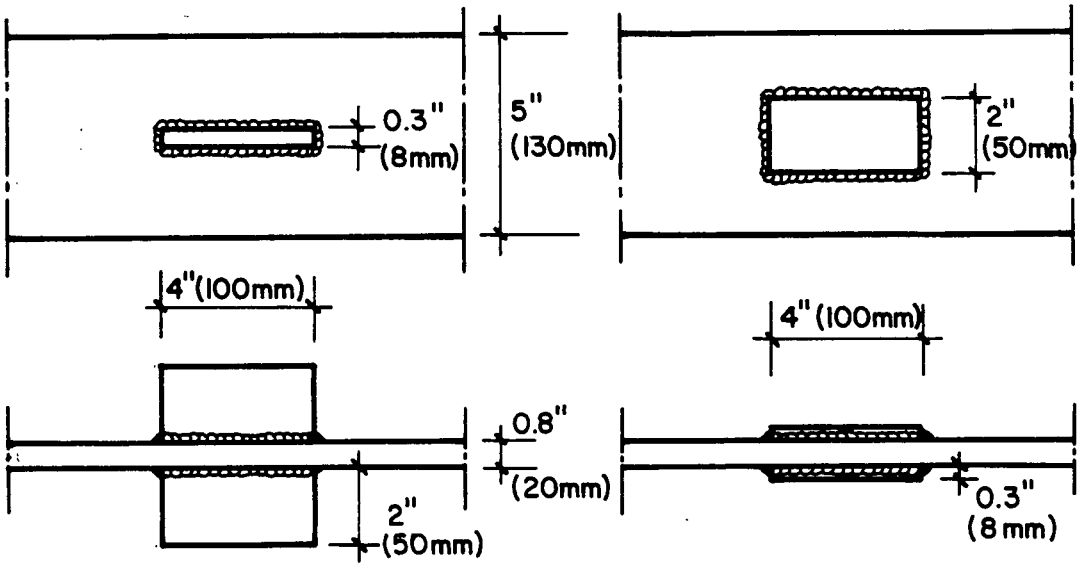

SIMULATED ATTACHMENT SPECIMENS

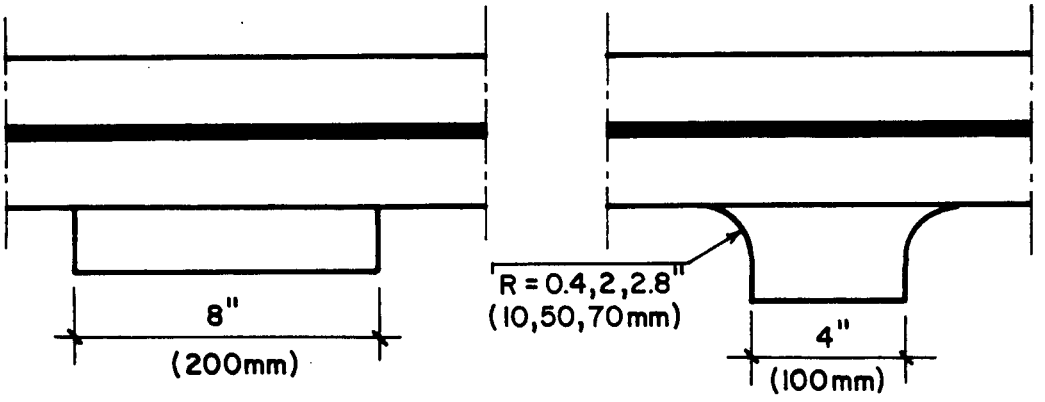

FLANGE TIP ATTACHMENTS

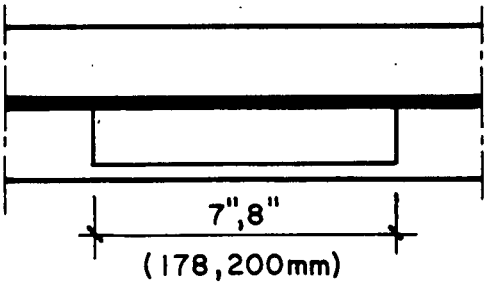

WEB ATTACHMENTS

Figure: 41 Test Specimens for ICOM Fatigue Test Programs

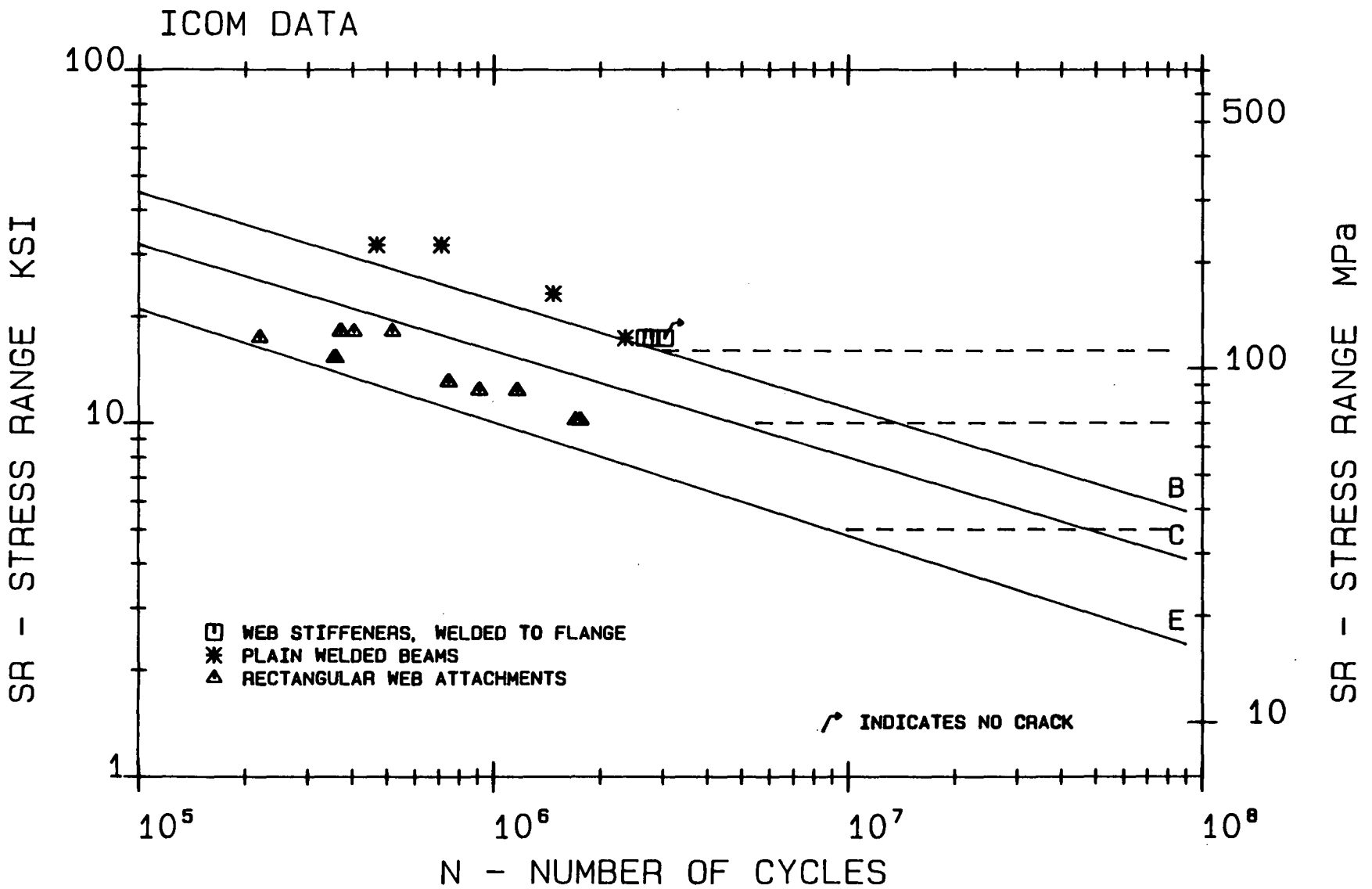

Figure: 42 Fatigue Resistance of Welded Beams, Web Stiffeners, and Web Attachments, ICOM Data

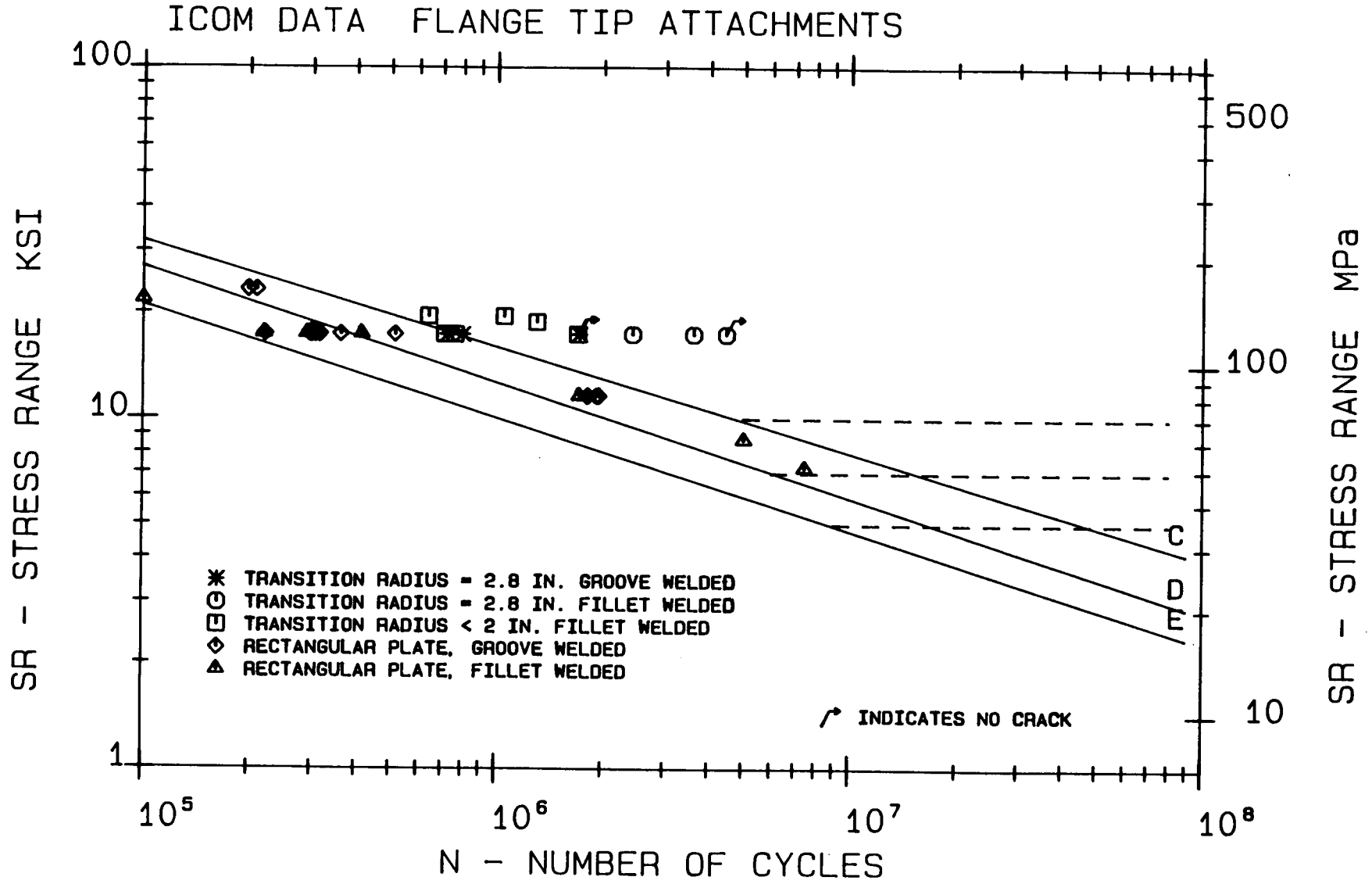

Figure: 43 Fatigue Resistance of Flange Tip Attachments, ICOM Data

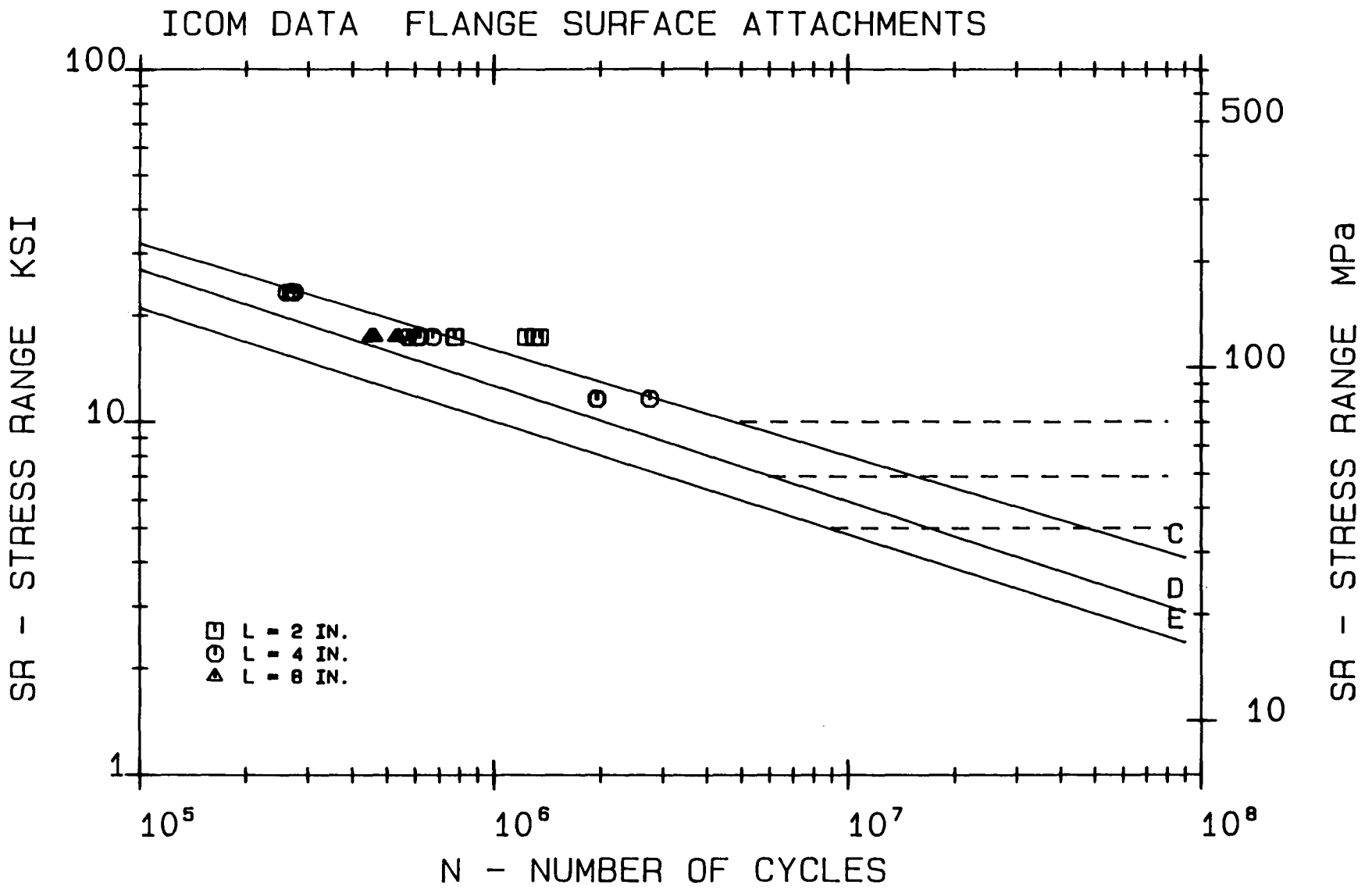

Figure: 44 Fatigue Resistance of Flange Surface Attachments, ICOM Data

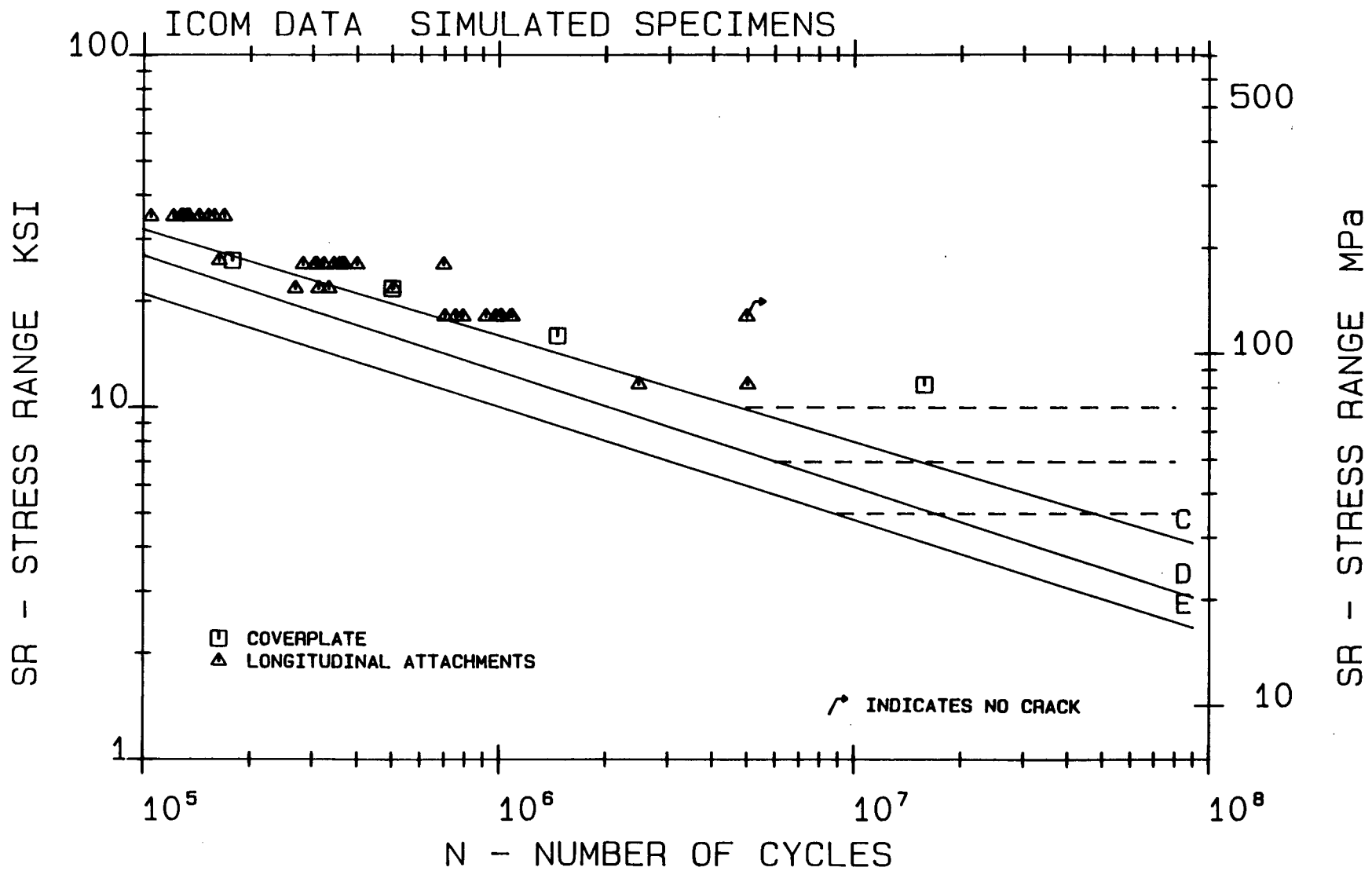

Figure: 45 Fatigue Resistance of Simulated Coverplate and Longitudinal Attachment Specimens, ICOM Data

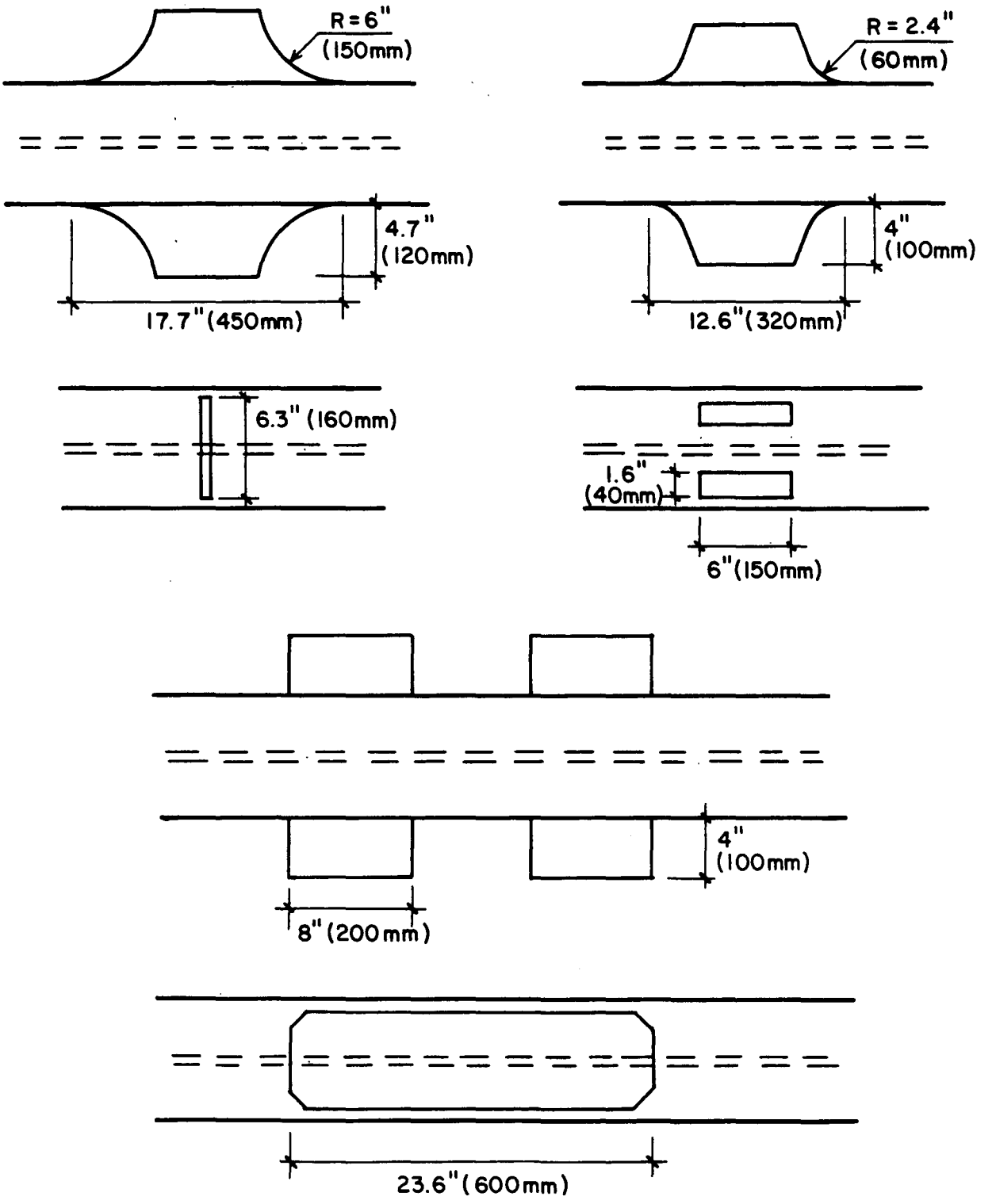

Figure: 46 Test Specimens for GDR Fatigue Test Programs

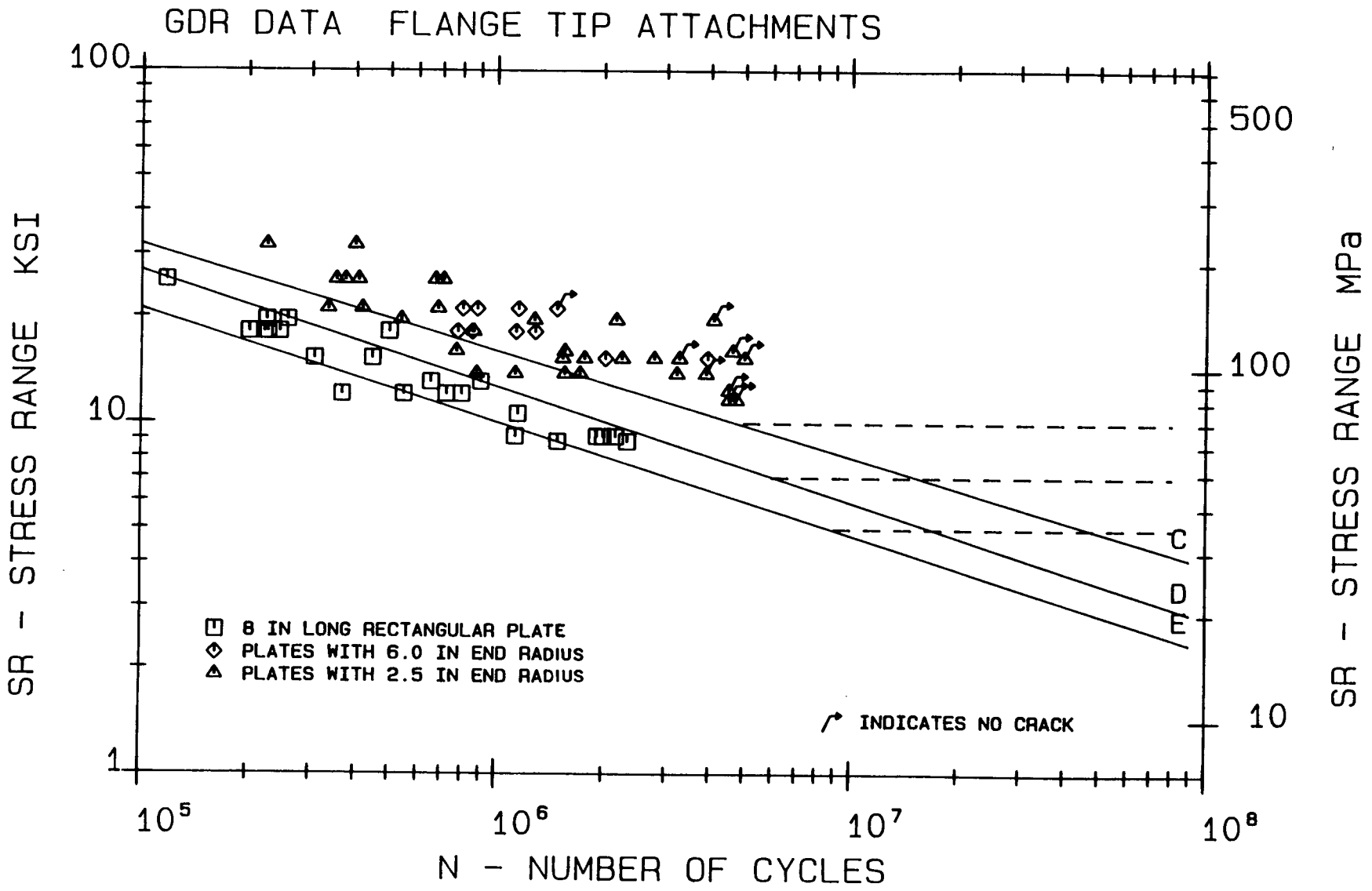

Figure: 47 Fatigue Resistance of Flange Tip Attachments, GDR Data

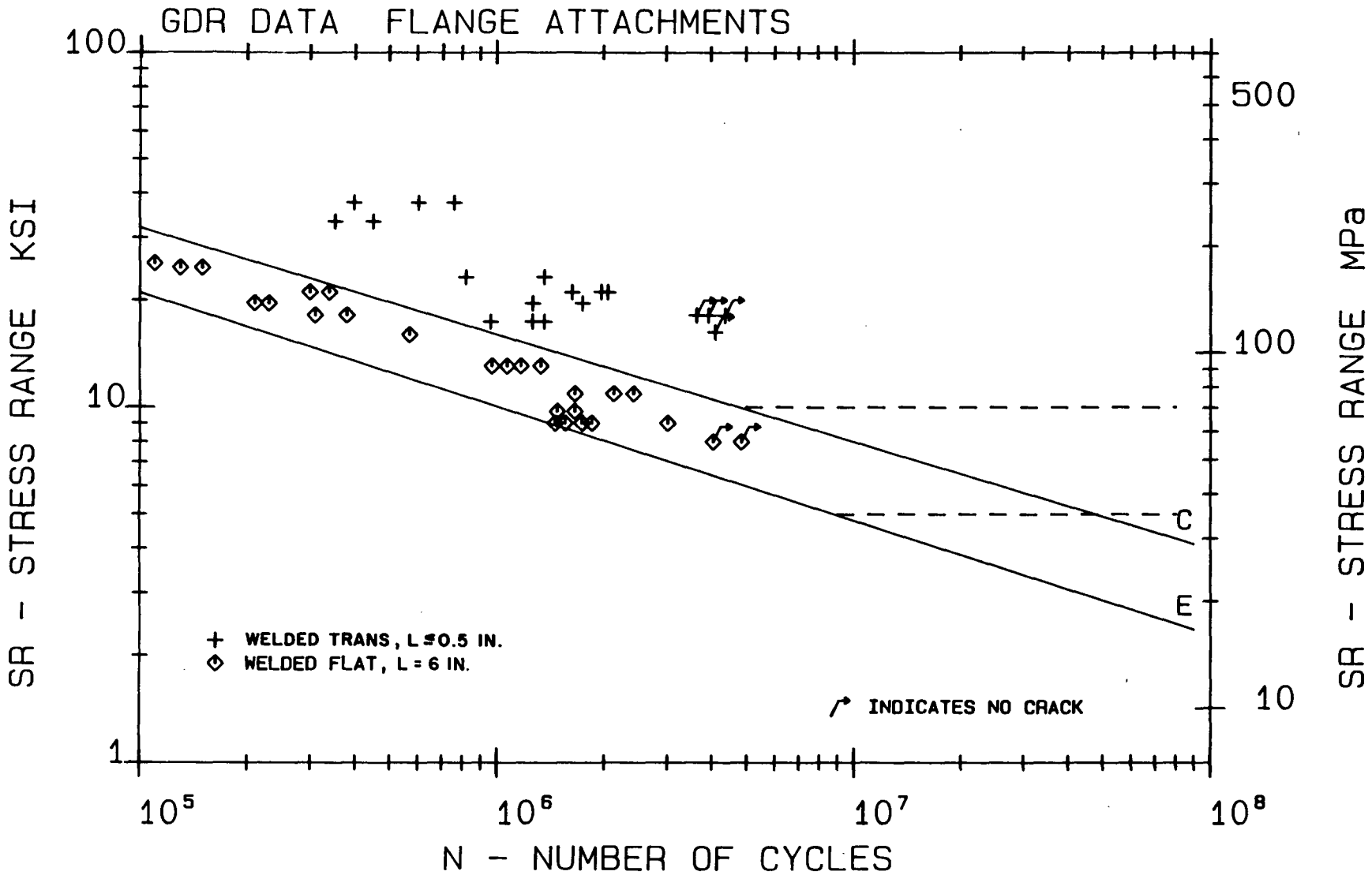

Figure: 48 Fatigue Resistance of Flange Attachments, GDR Data

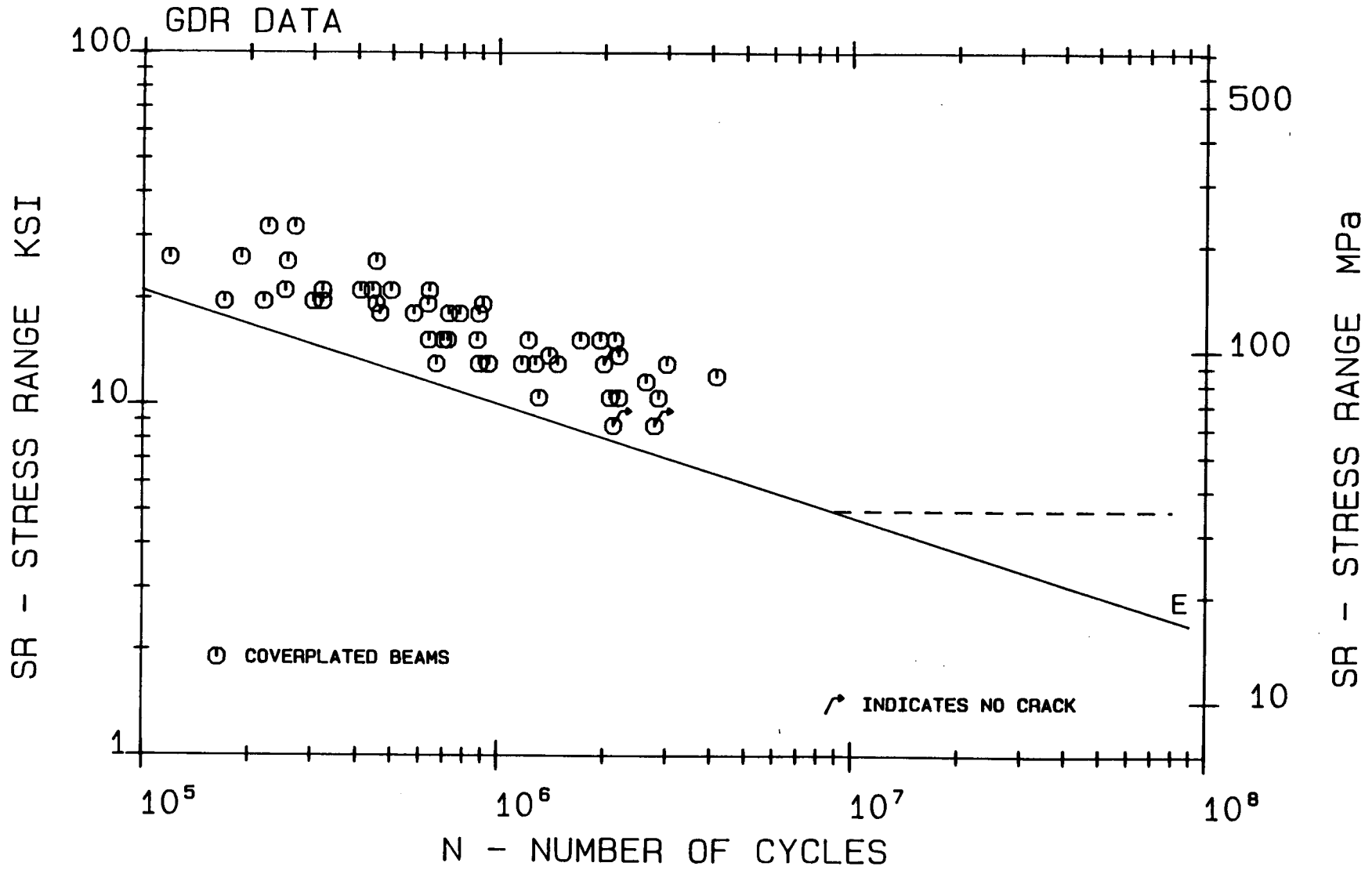

Figure: 49 Fatigue Resistance of Coverplated Beams, GDR Data

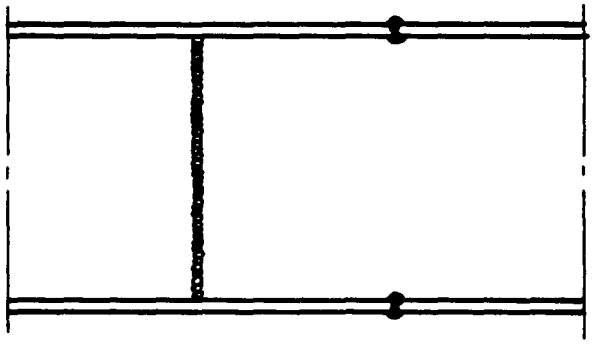

BEAM WITH STAGGERED SPLICE

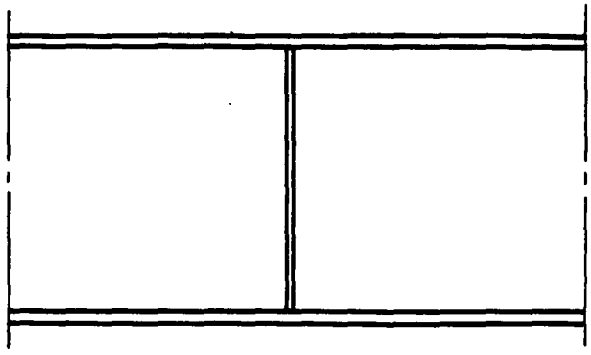

BEAM WITH STIFFENER

Figure: 50 Test Specimens for West German Fatigue Test Program

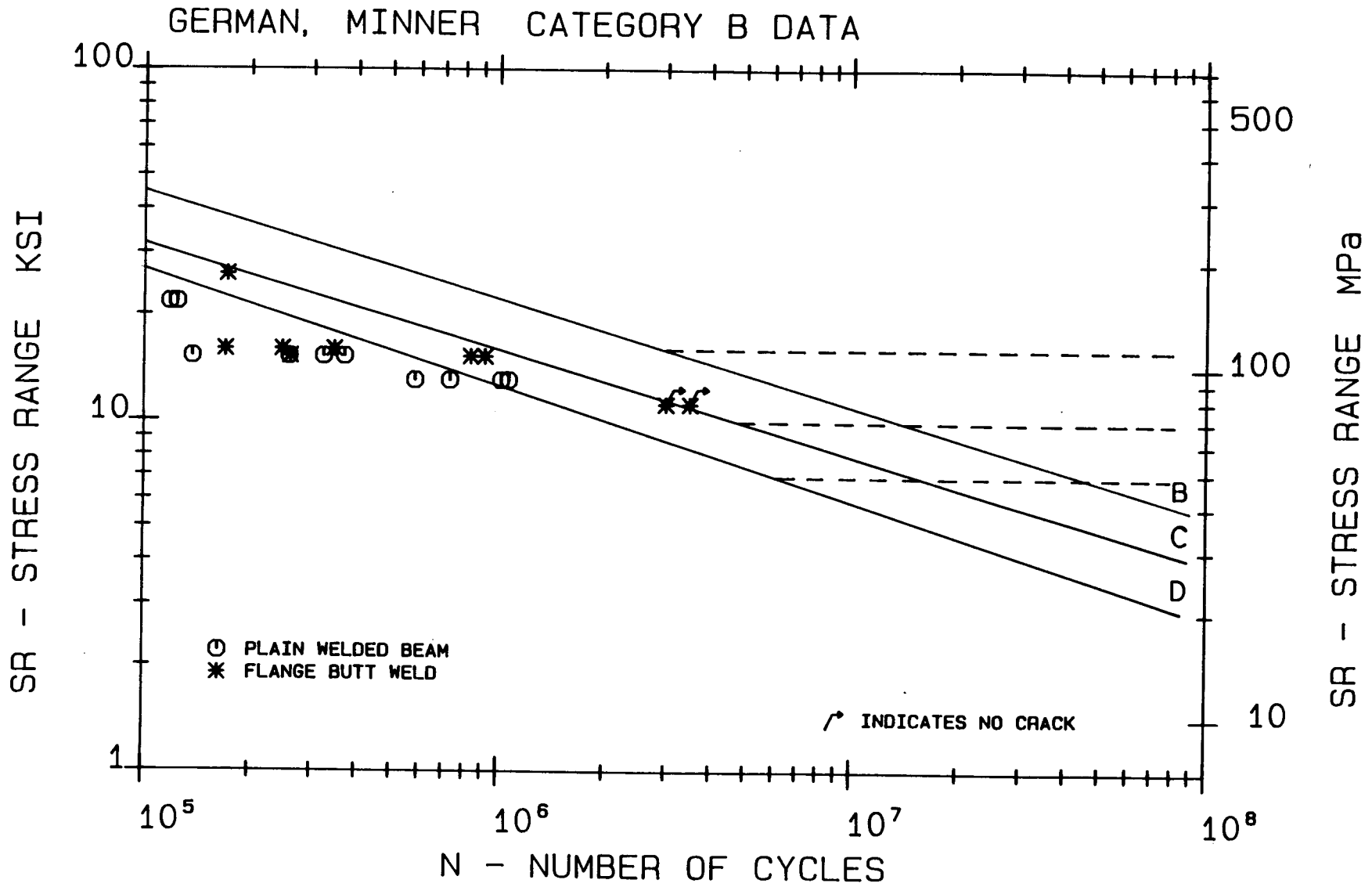

Figure: 51 Fatigue Resistance of Welded Beams and Flange Butt Welds, West German Data

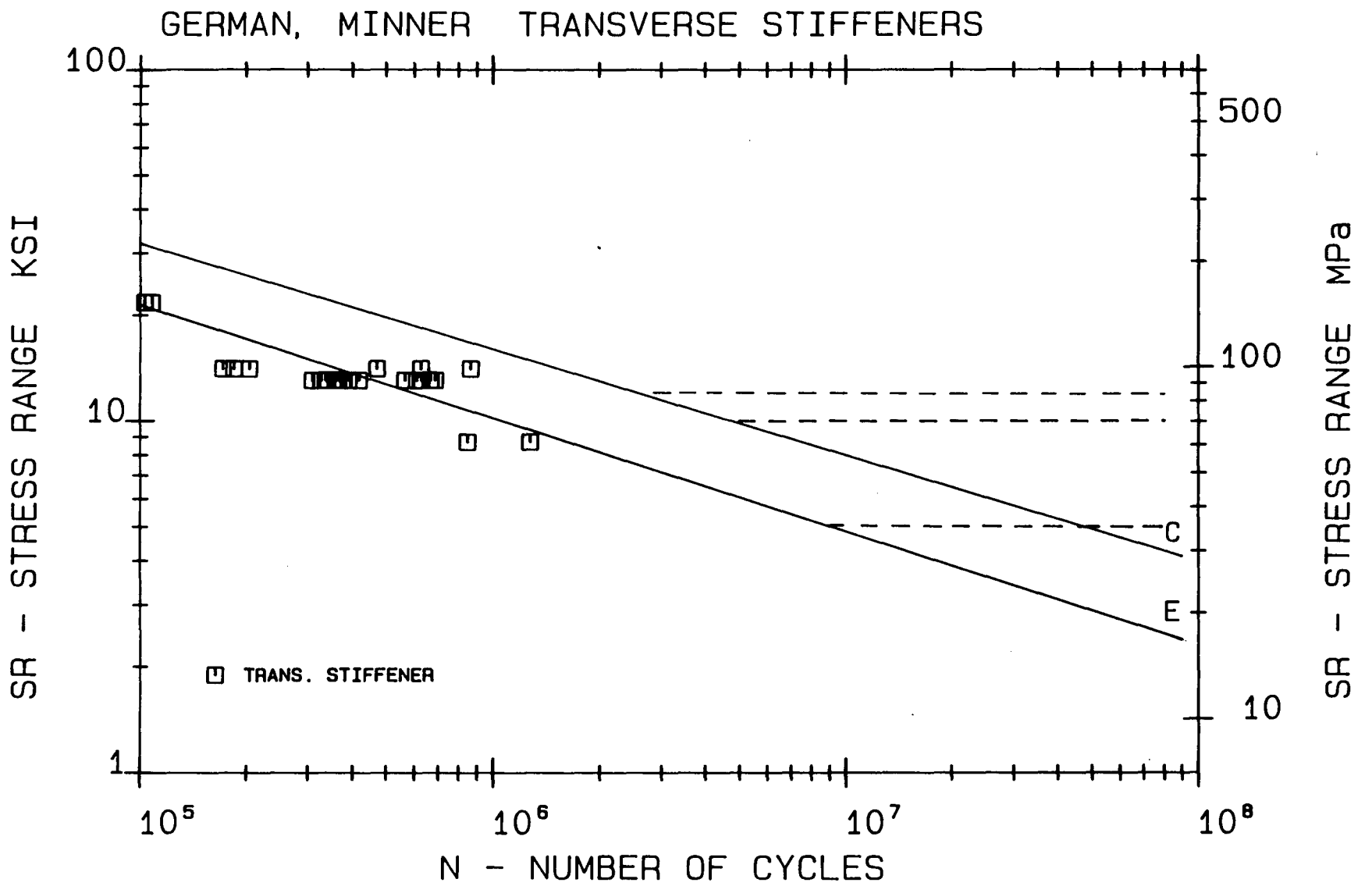

Figure: 52 Fatigue Resistance of Transverse Stiffeners, West German Data

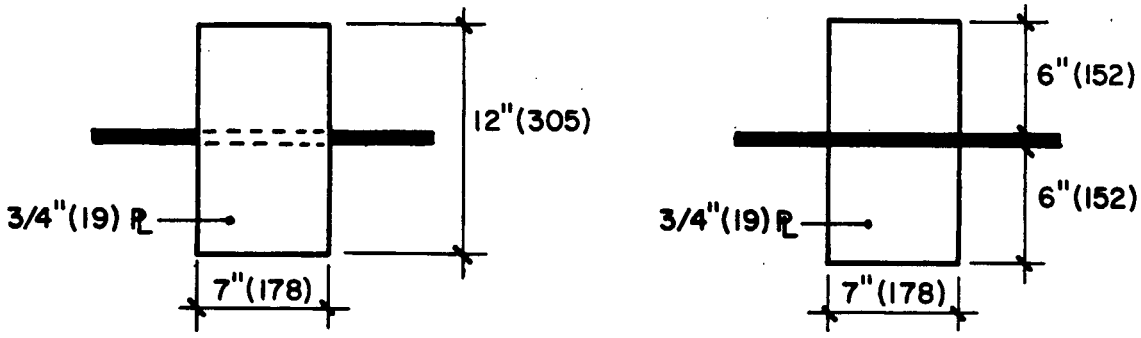

WEB ATTACHMENTS (1/4"(6) FILLET WELDS)

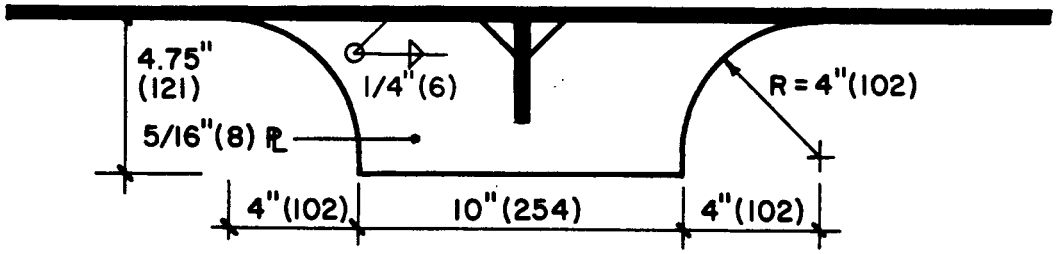

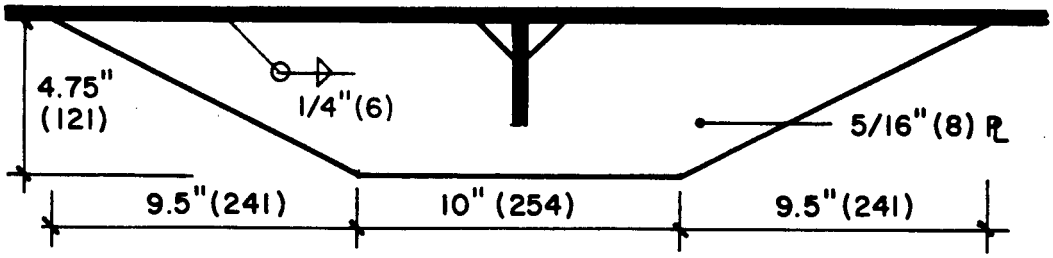

WEB GUSSET PLATES

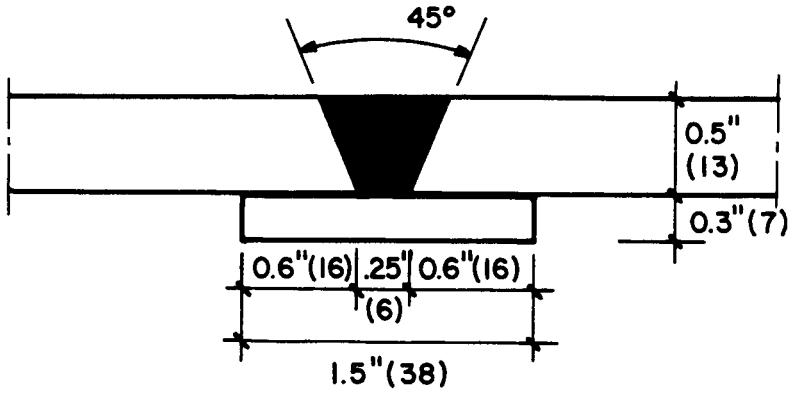

GROOVE WELD WITH BACKING BAR

Figure: 53 Test Specimens for Canadian Fatigue Test Programs

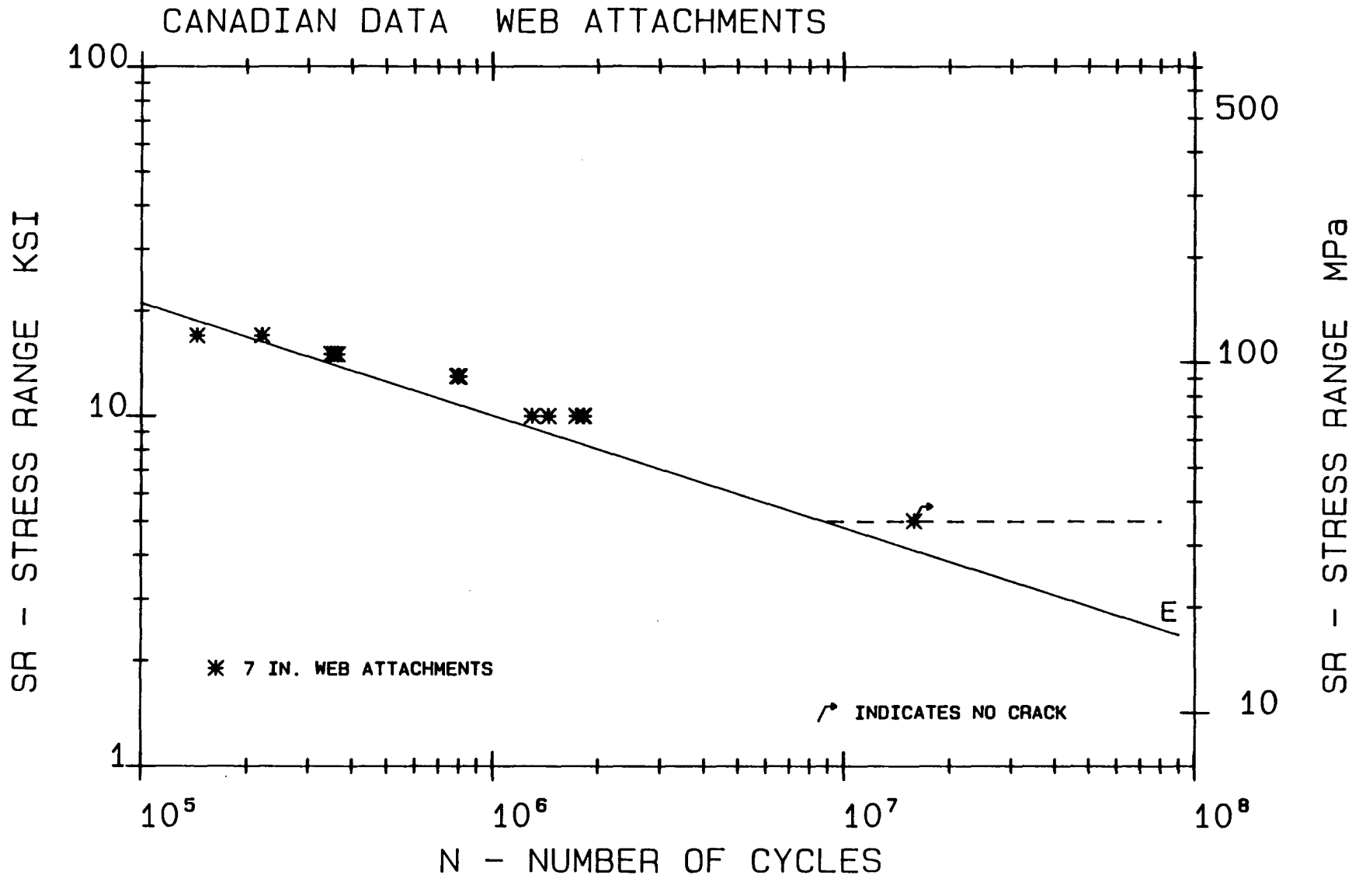

Figure: 54 Fatigue Resistance of Web Attachments, Canadian Data

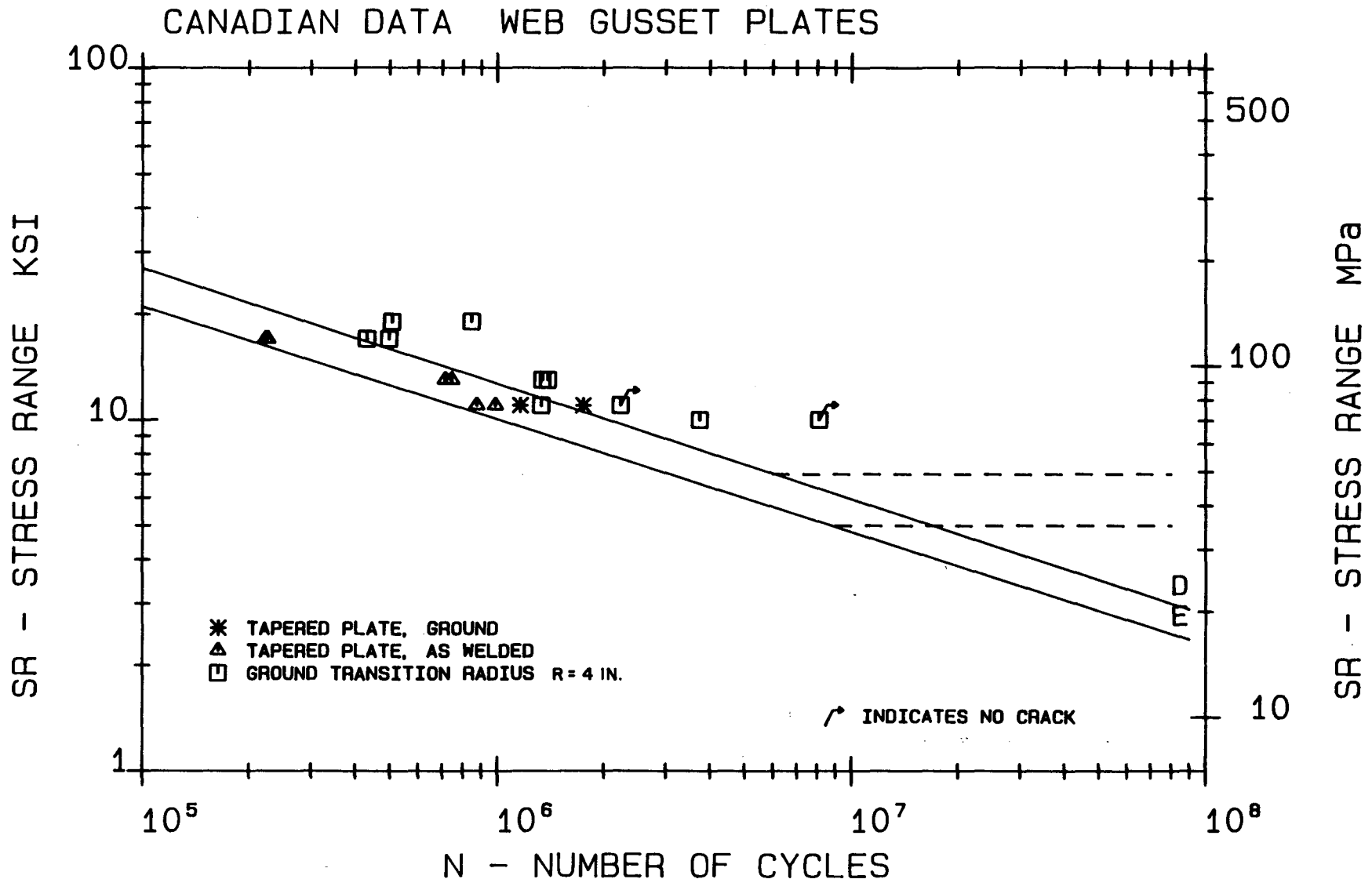

Figure: 55 Fatigue Resistance of Web Gusset Plates, Canadian Data

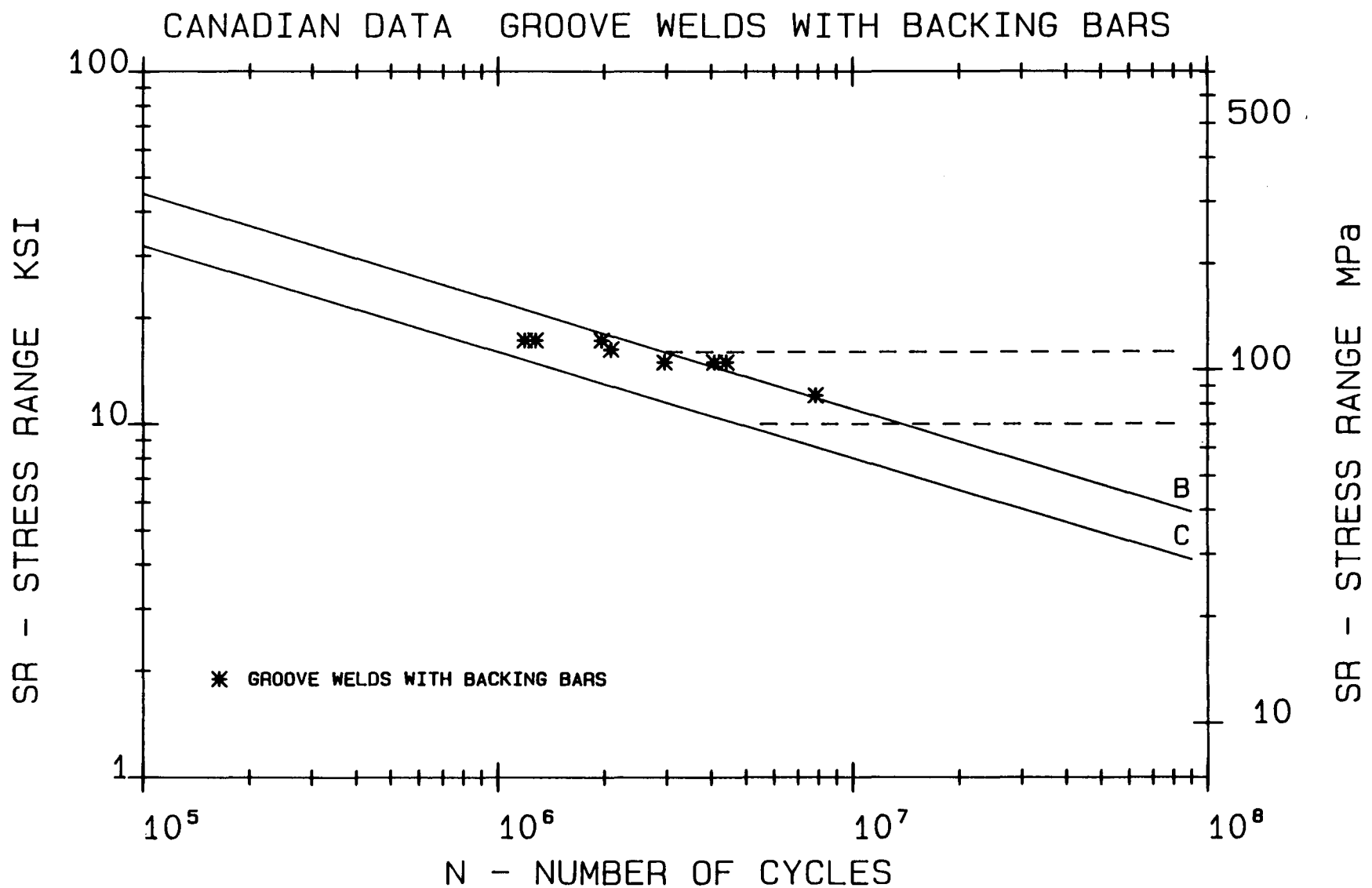

Figure: 56 Fatigue Resistance of Groove Welds with Backing Bars, Canadian Data

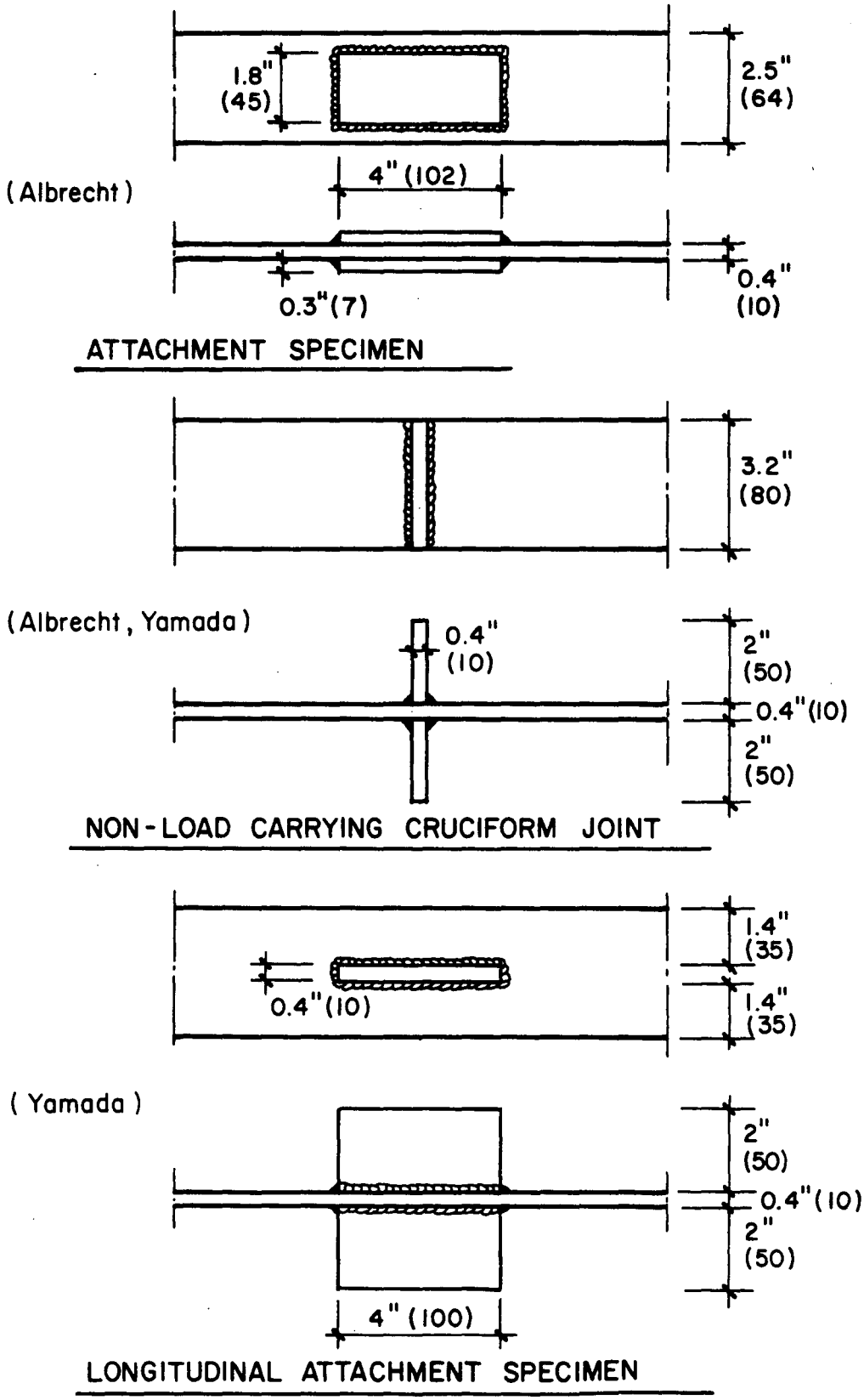

Figure: 57 Test Specimens for Weathering Steel Fatigue Test Programs

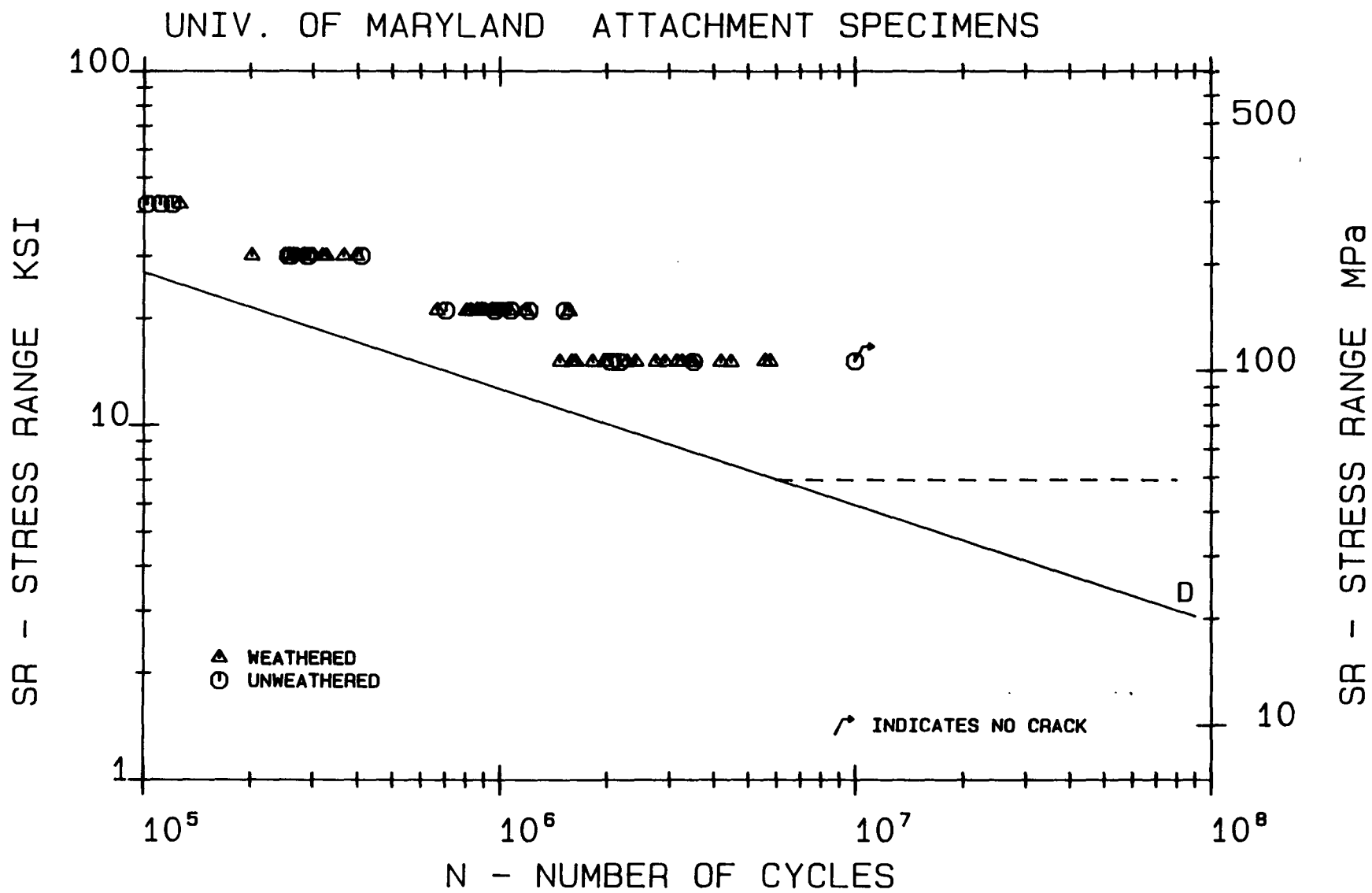

Figure: 58 Fatigue Resistance of Weathered Steel, Simulated Attachment Specimens, Albrecht

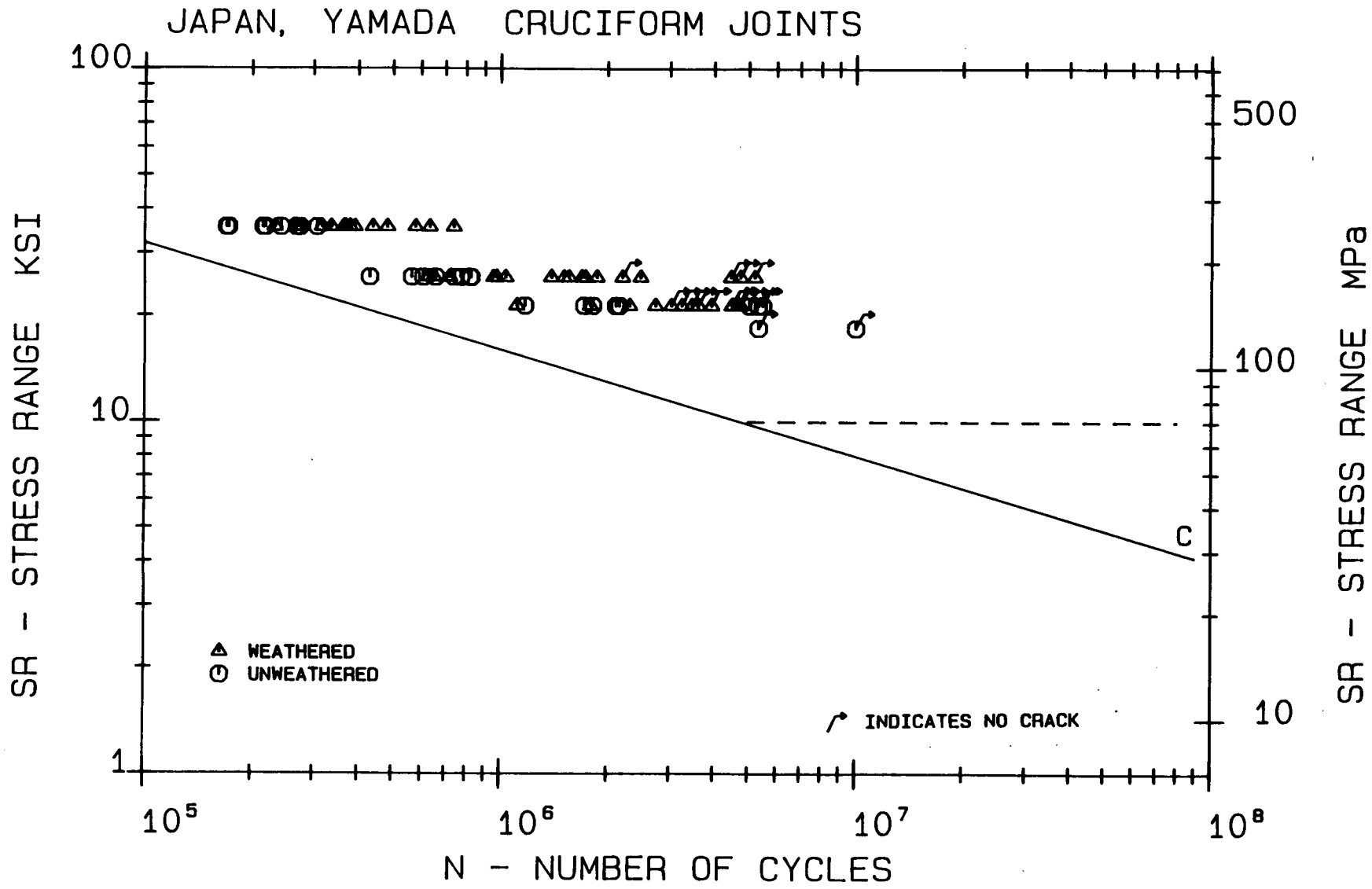

Figure: 59 Fatigue Resistance of Weathered Steel, Non-Load Carrying Cruciform Joints, Yamada

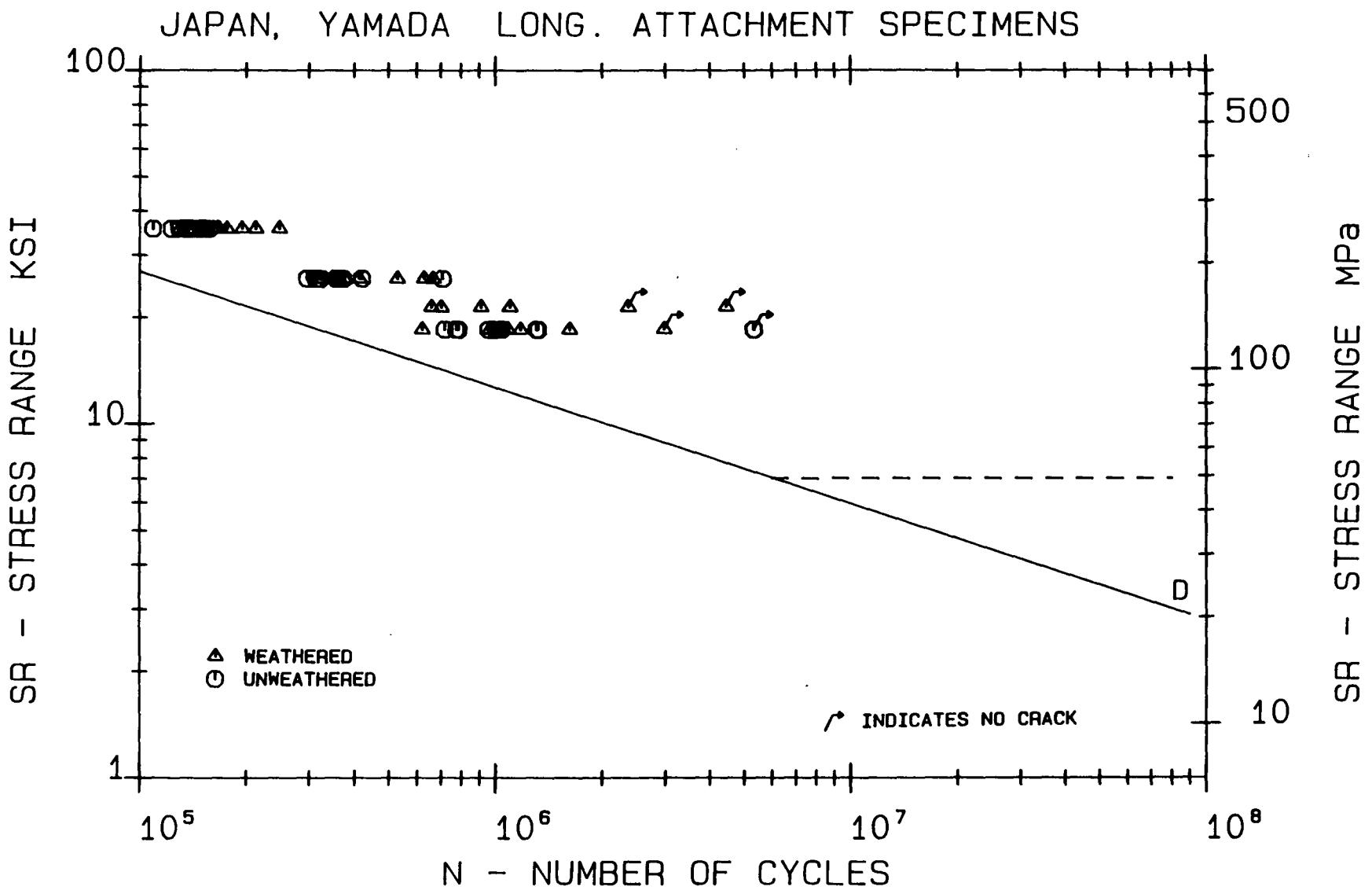

Figure: 60 Fatigue Resistance of Weathered Steel, Simulated Attachment Specimens, Yamada

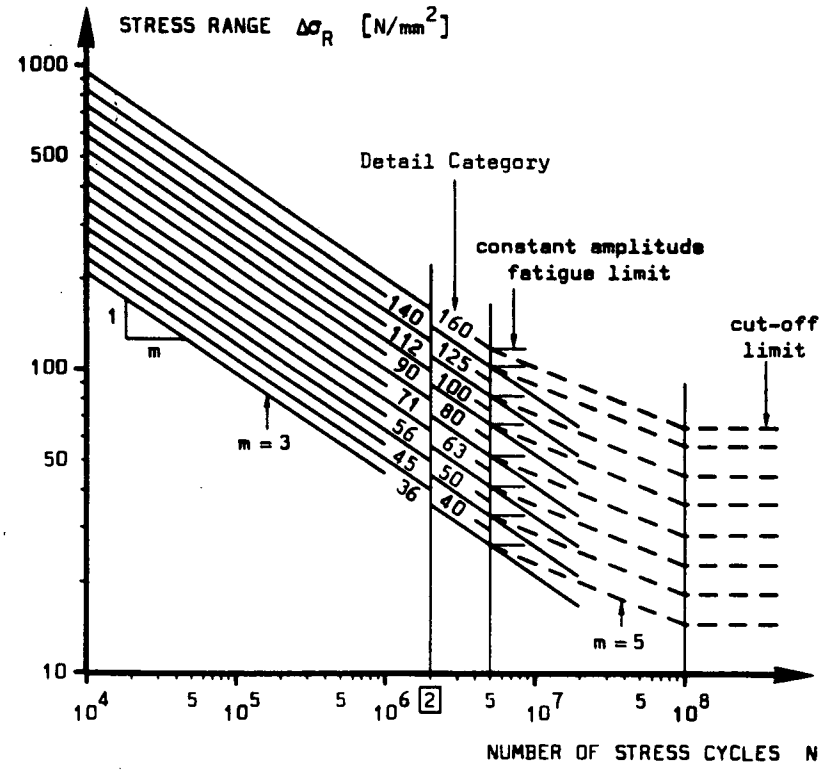

Figure: 61 Fatigue Design Curves Adopted by ECCS/ISO [Ref. 42]

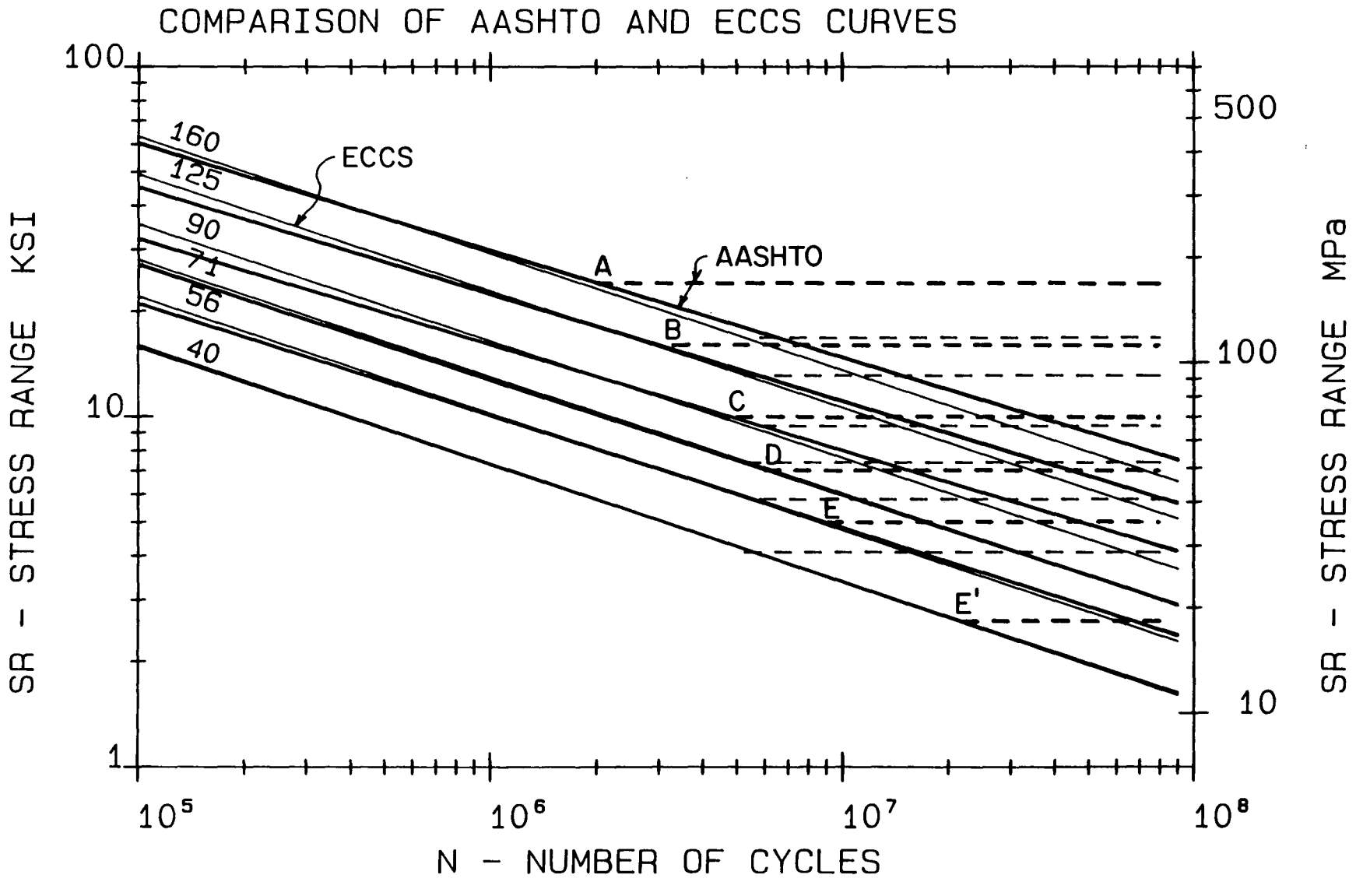

Figure: 62 Comparison of AASHTO and ECCS(ISO) Fatigue Design Curves

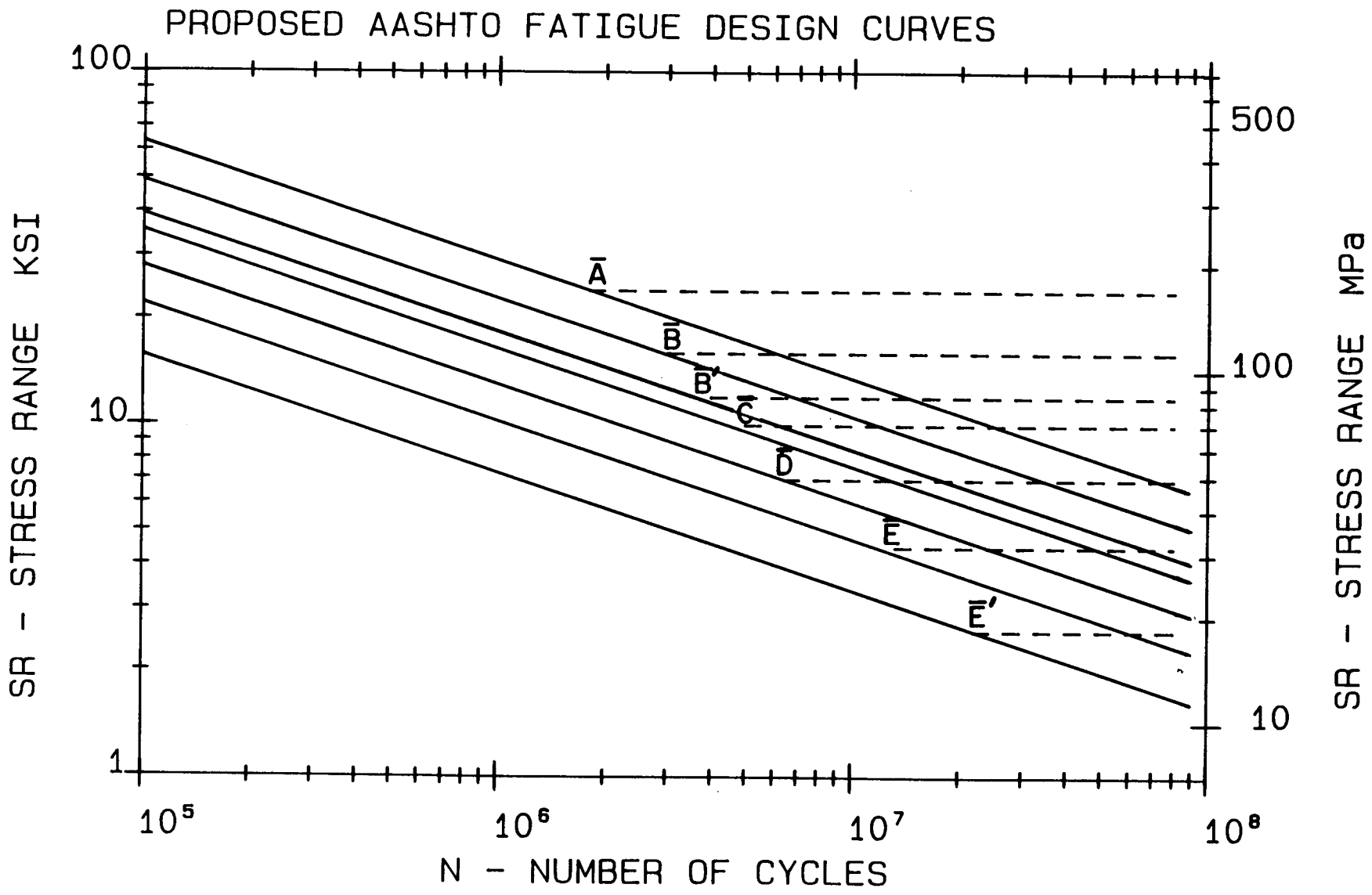

Figure: 63 Proposed AASHTO Fatigue Design Curves

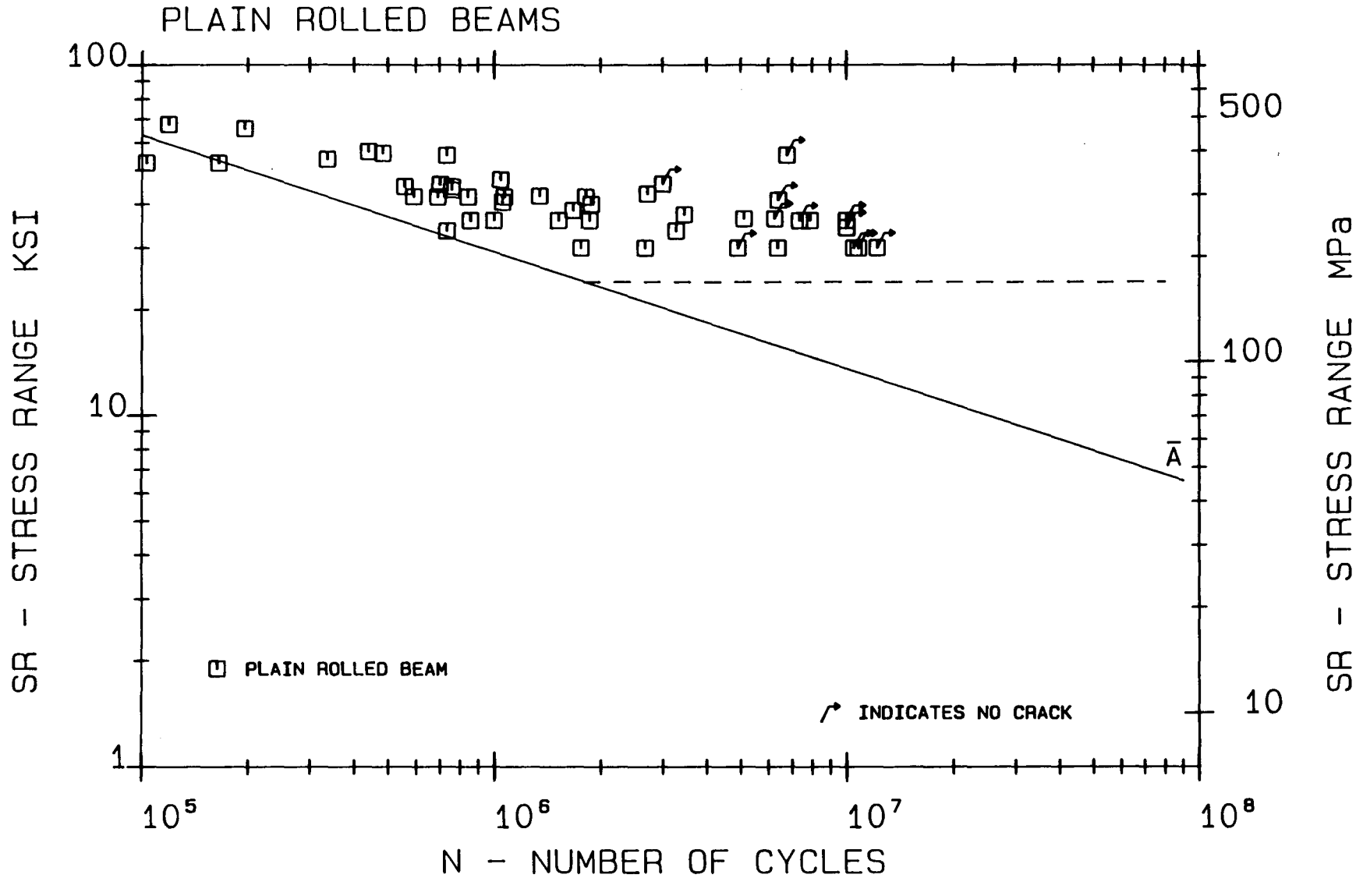

Figure: 64 Fatigue Resistance of Plain Rolled Beams with Proposed Category $\bar{A}$ Curve

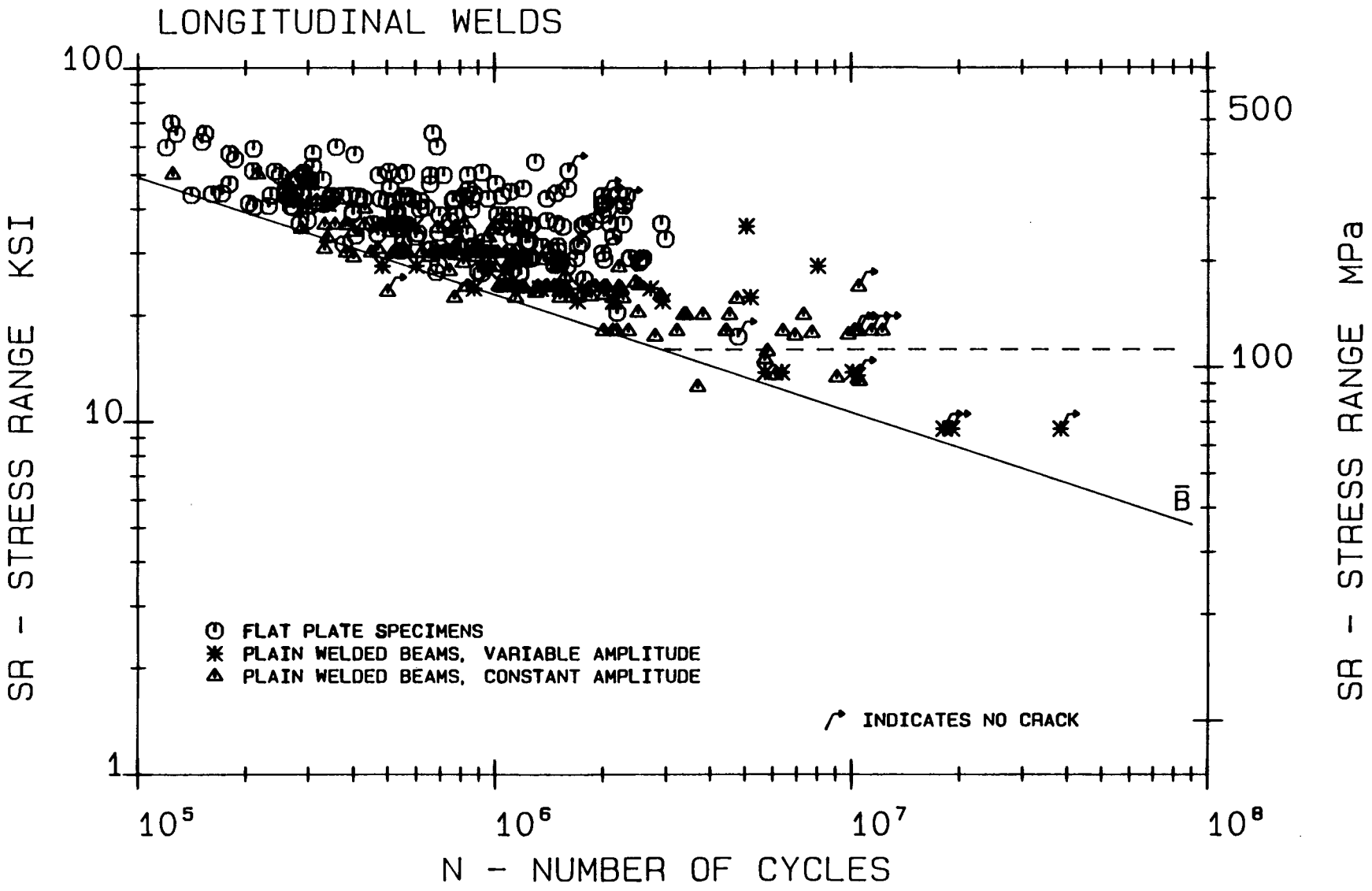

Figure: 65 Longitudinal Weld Test Data with Proposed Category $\overline{B}$ Resistance Curve

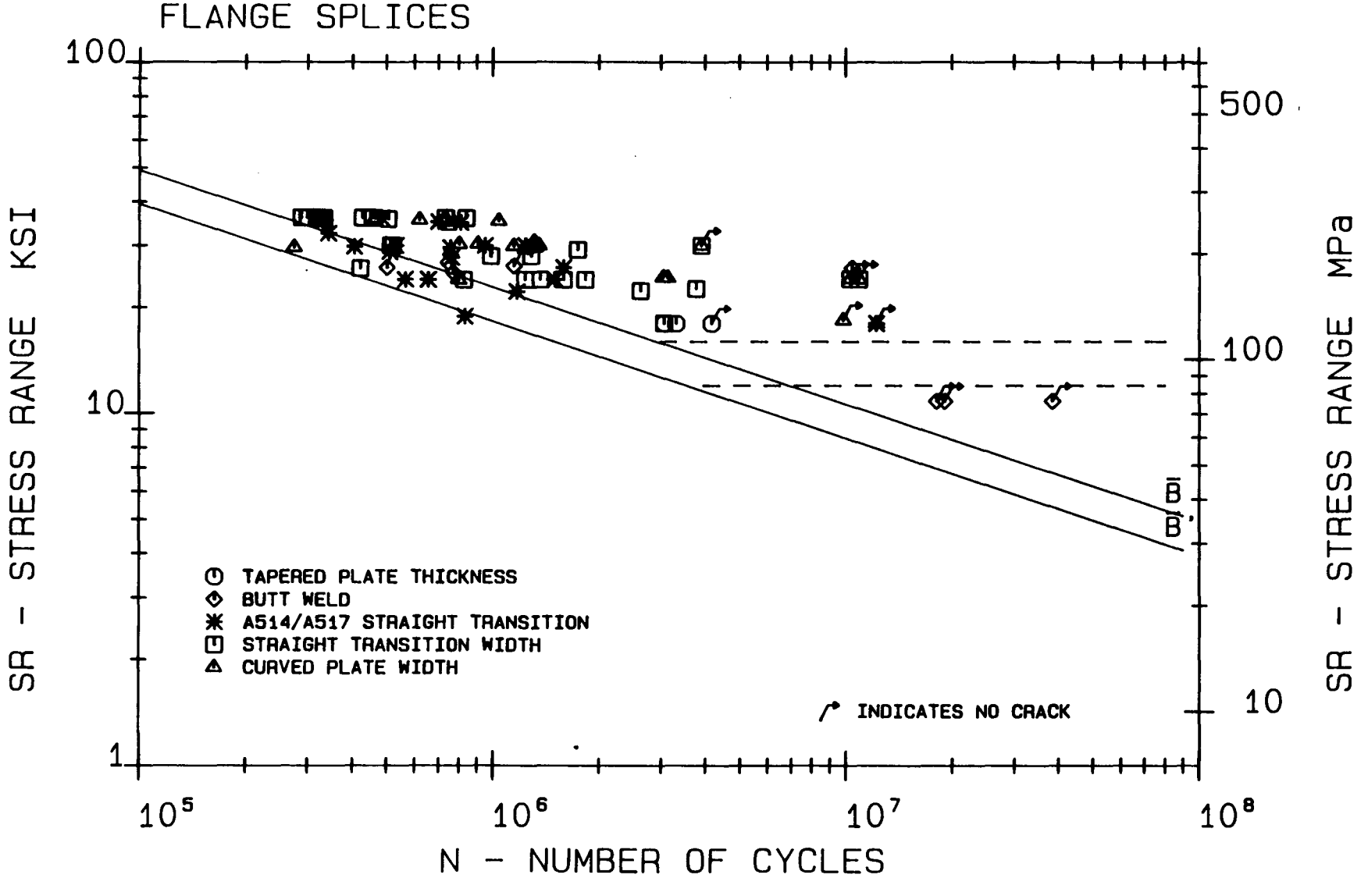

Figure: 66 Flange Splice Test Data with Proposed Category $\overline{B}$ and $\overline{B}'$ Resistance Curves

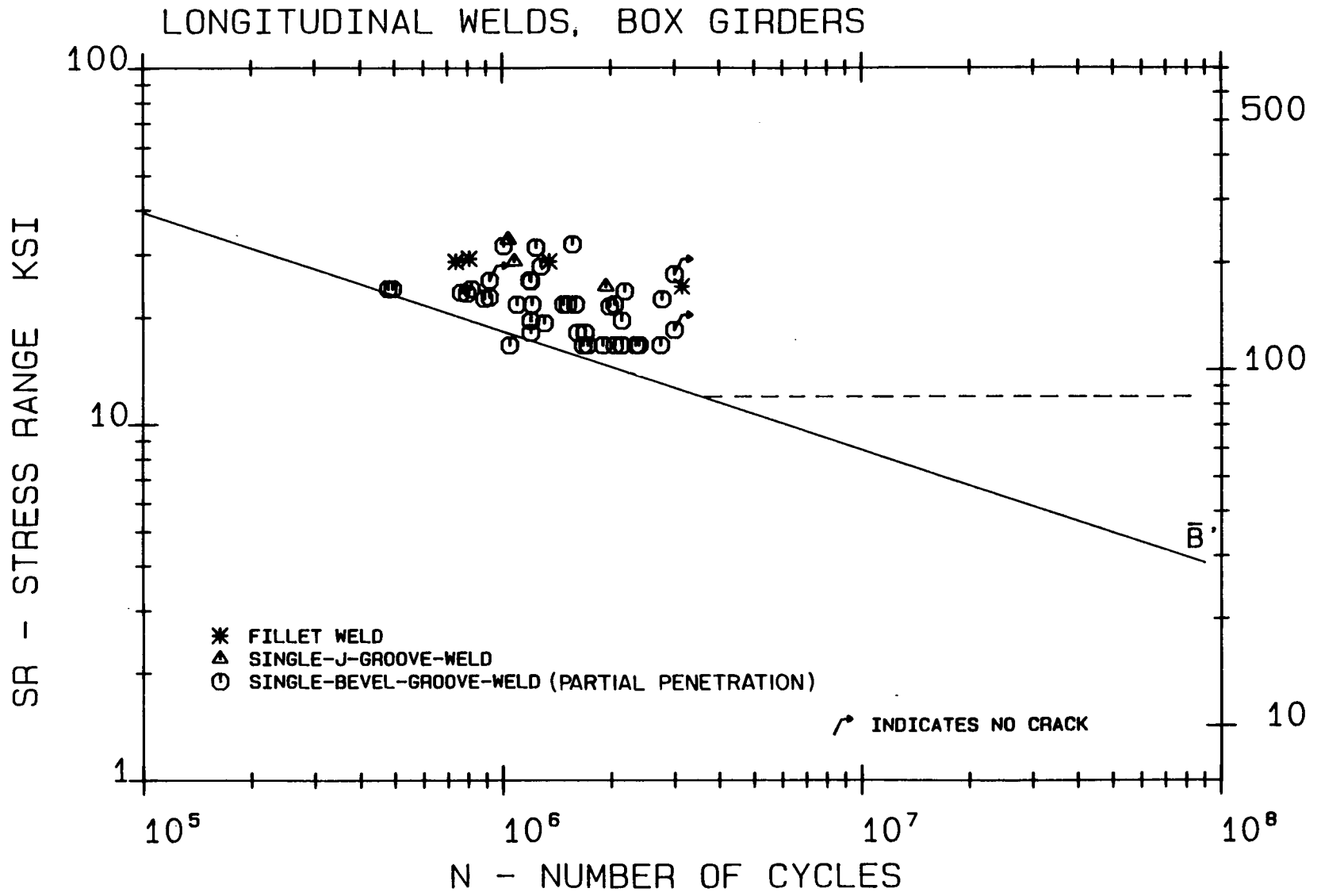

Figure: 67 Box Girder Longitudinal Weld Test Data with Proposed Category $\overline{B}'$ Resistance curve

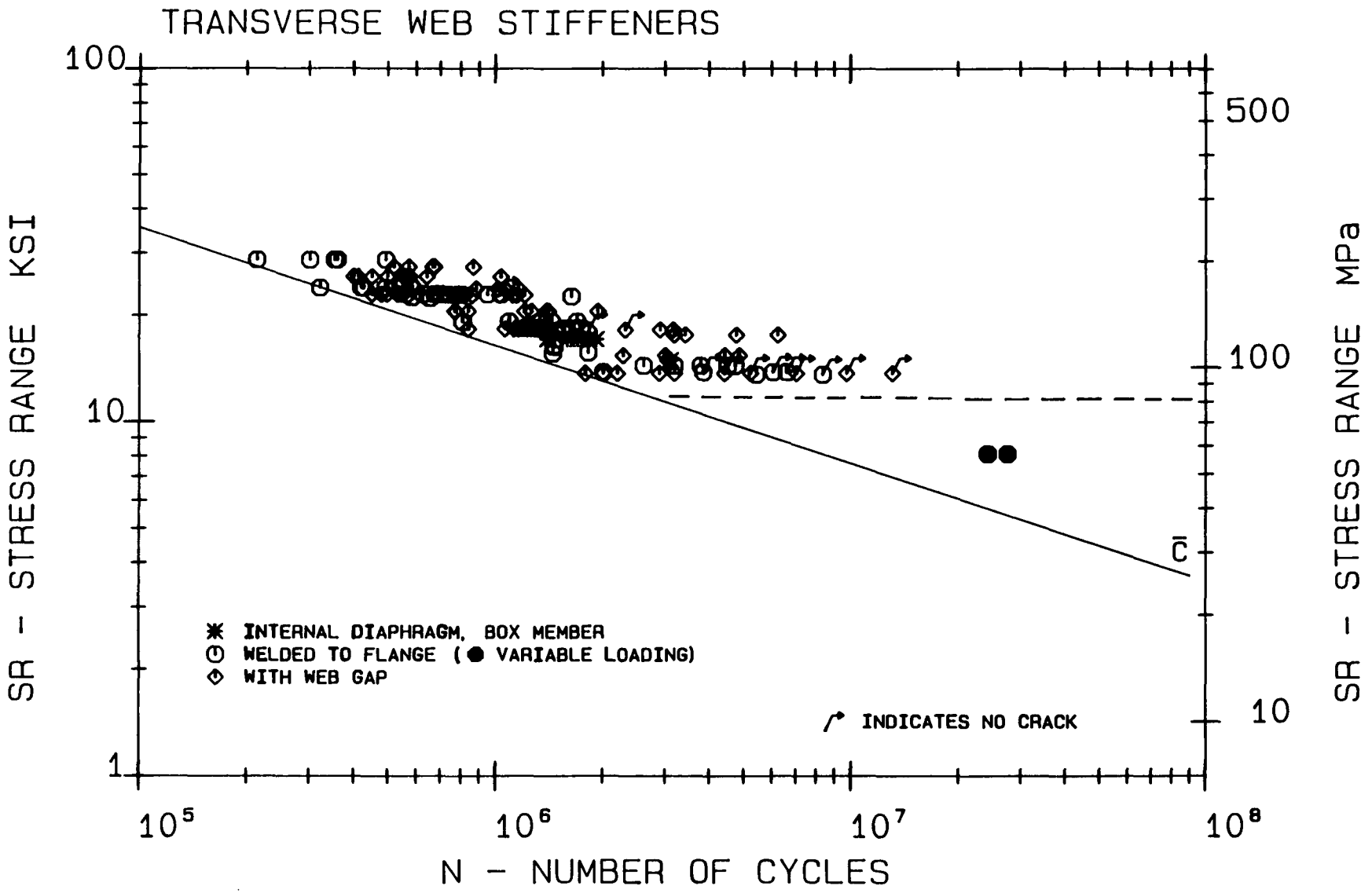

Figure: 68 Transverse Stiffener Test Data with Proposed Category $\overline{C}$ Resistance Curve

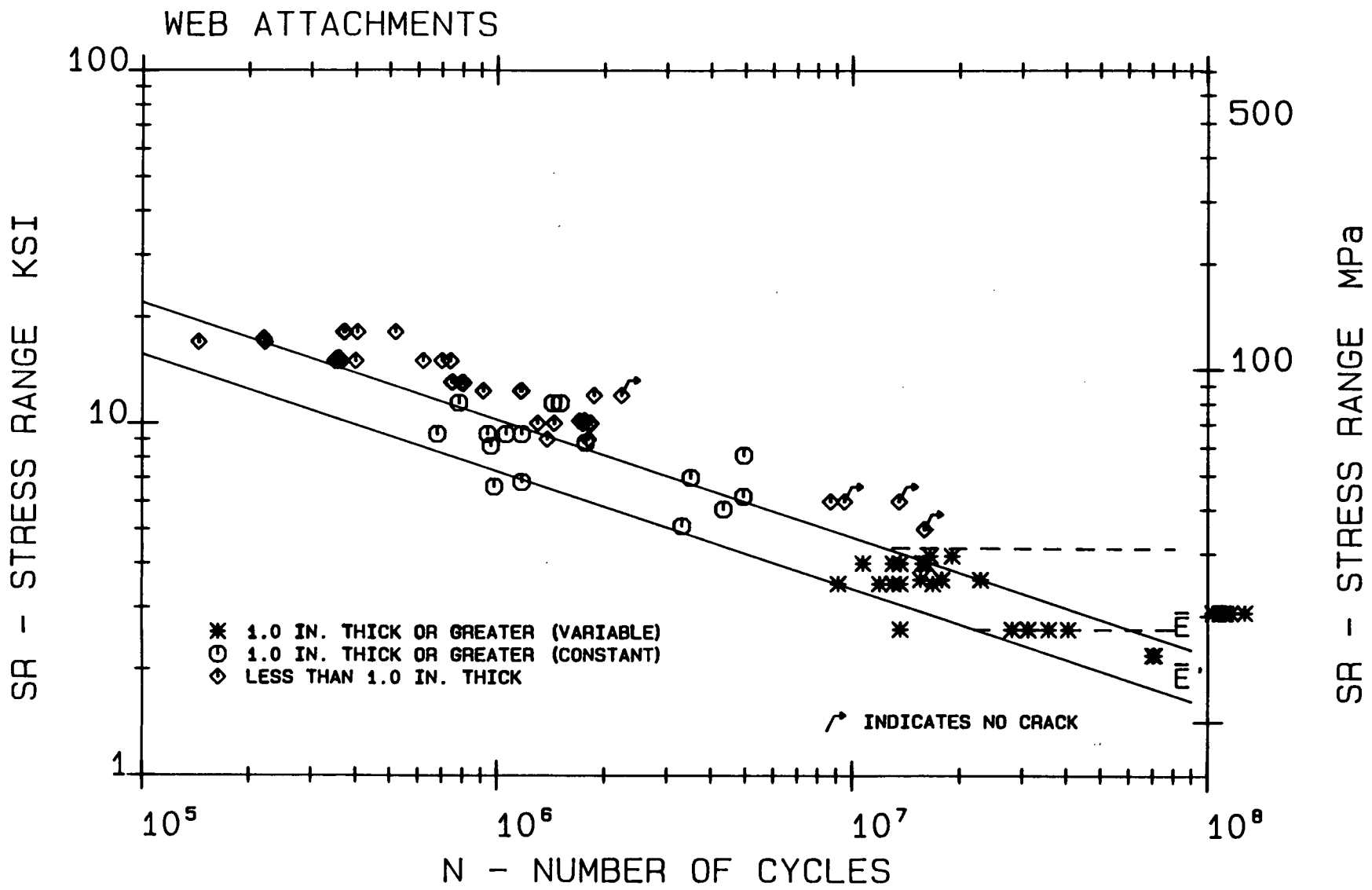

Figure: 69 Web Attachment Test Data with Proposed Category $\overline{E}$ and $\overline{E}'$ Resistance Curves

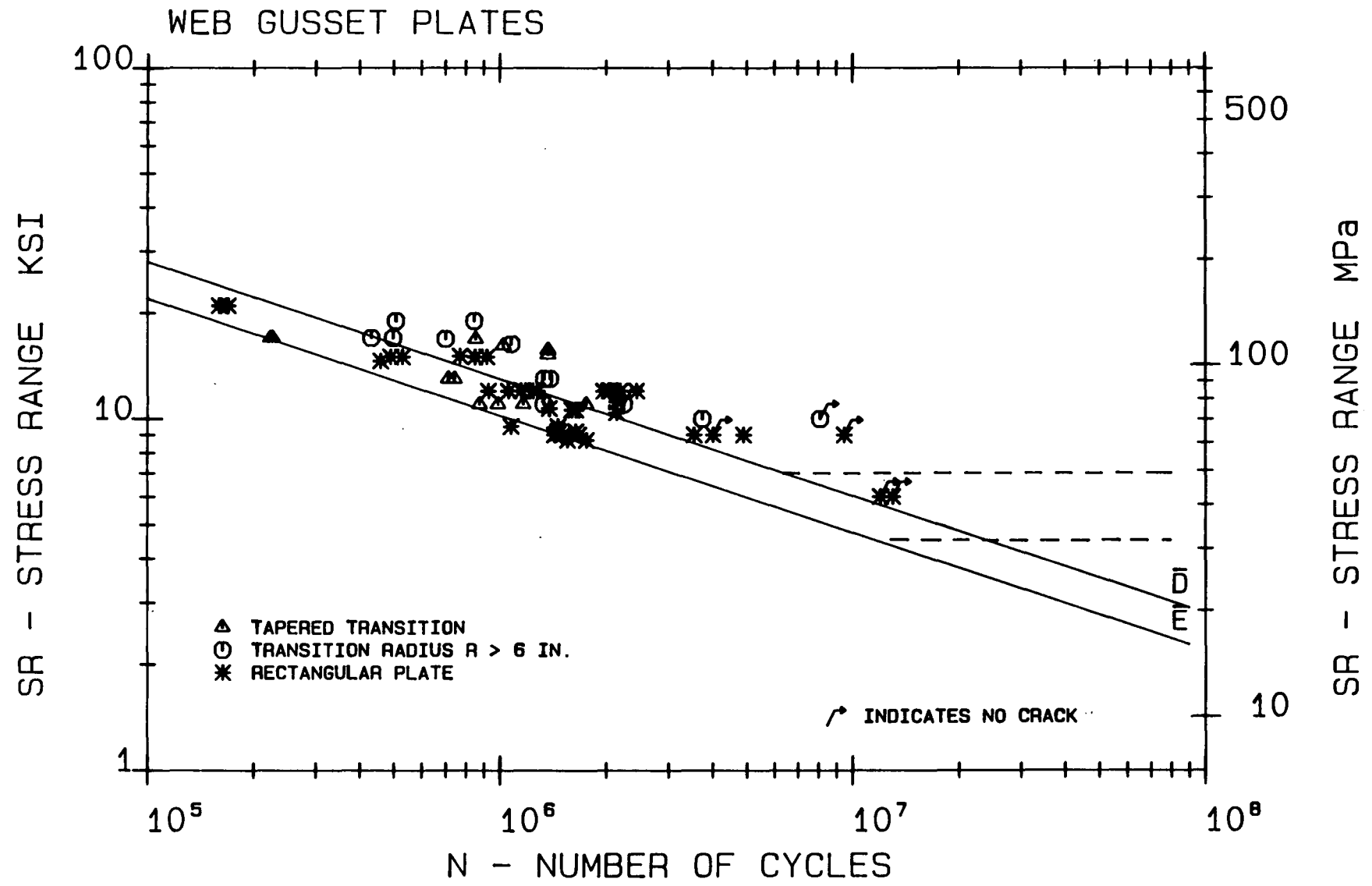

Figure: 70 Web Gusset Plate Test Data with Proposed Category $\overline{E}$ Resistance Curve

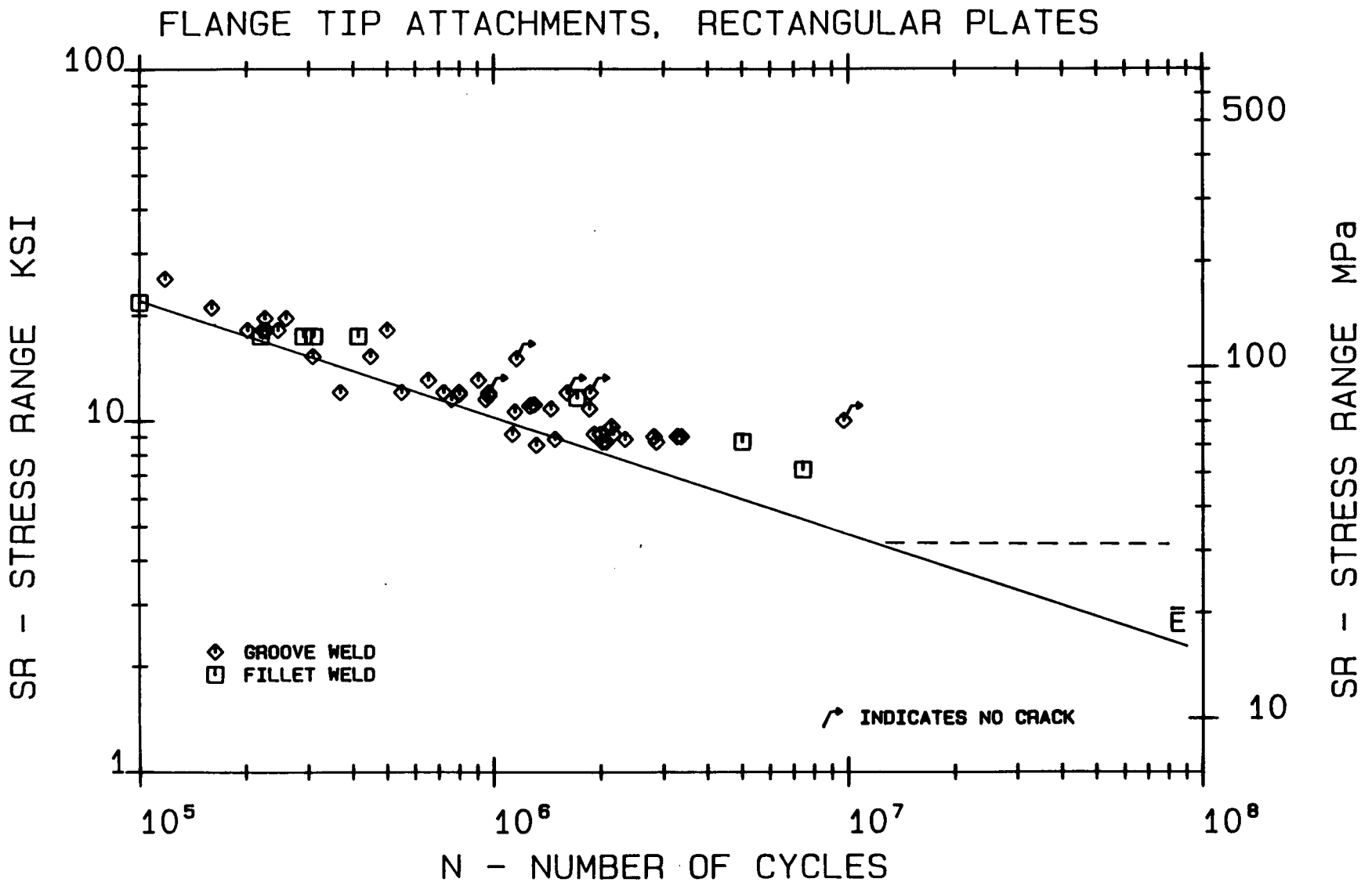

Figure: 71 Flange Tip Attachment Test Data with Proposed Category $\overline{E}$ Resistance Curve

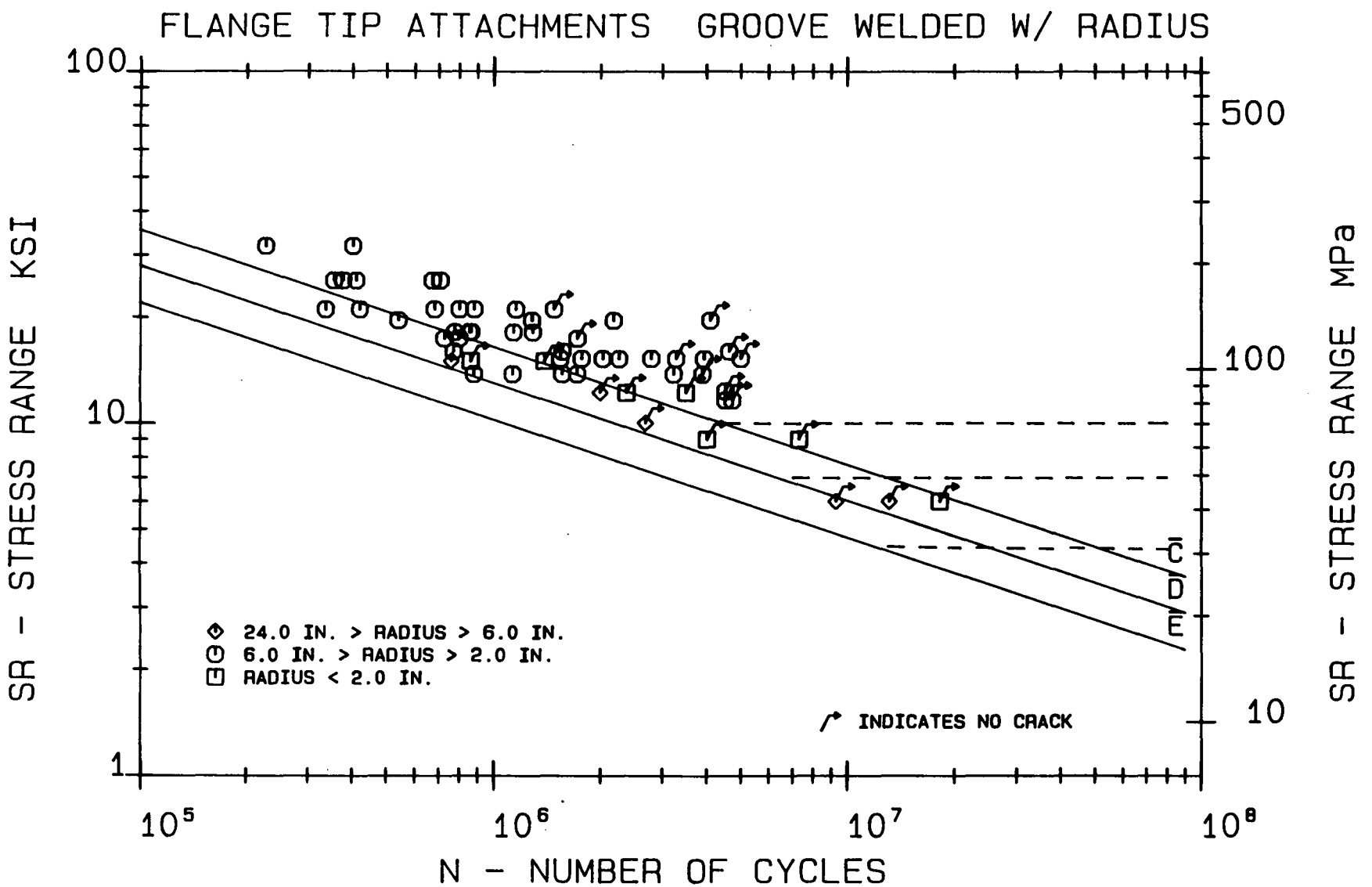

Figure: 72 Flange Tip Attachments with Groove Welded Transition Radius Test Data with Proposed Category $\overline{C}$, $\overline{D}$, and $\overline{E}$ Resistance Curves

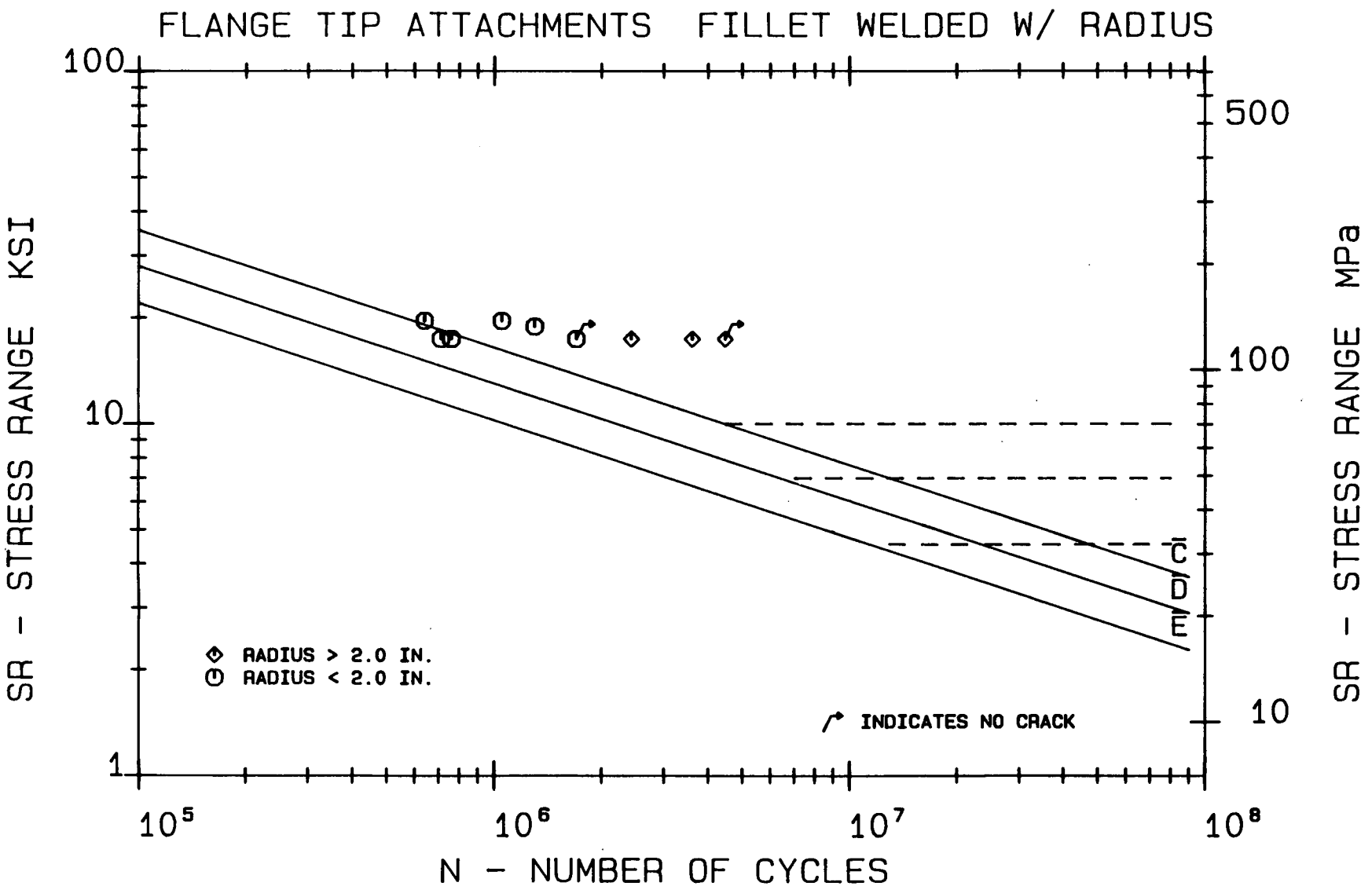

Figure: 73 Flange Tip Attachments With Fillet Welded Transition Radius Test Data with Proposed Category $\overline{C}$, $\overline{D}$,and $\overline{E}$ Resistance Curves

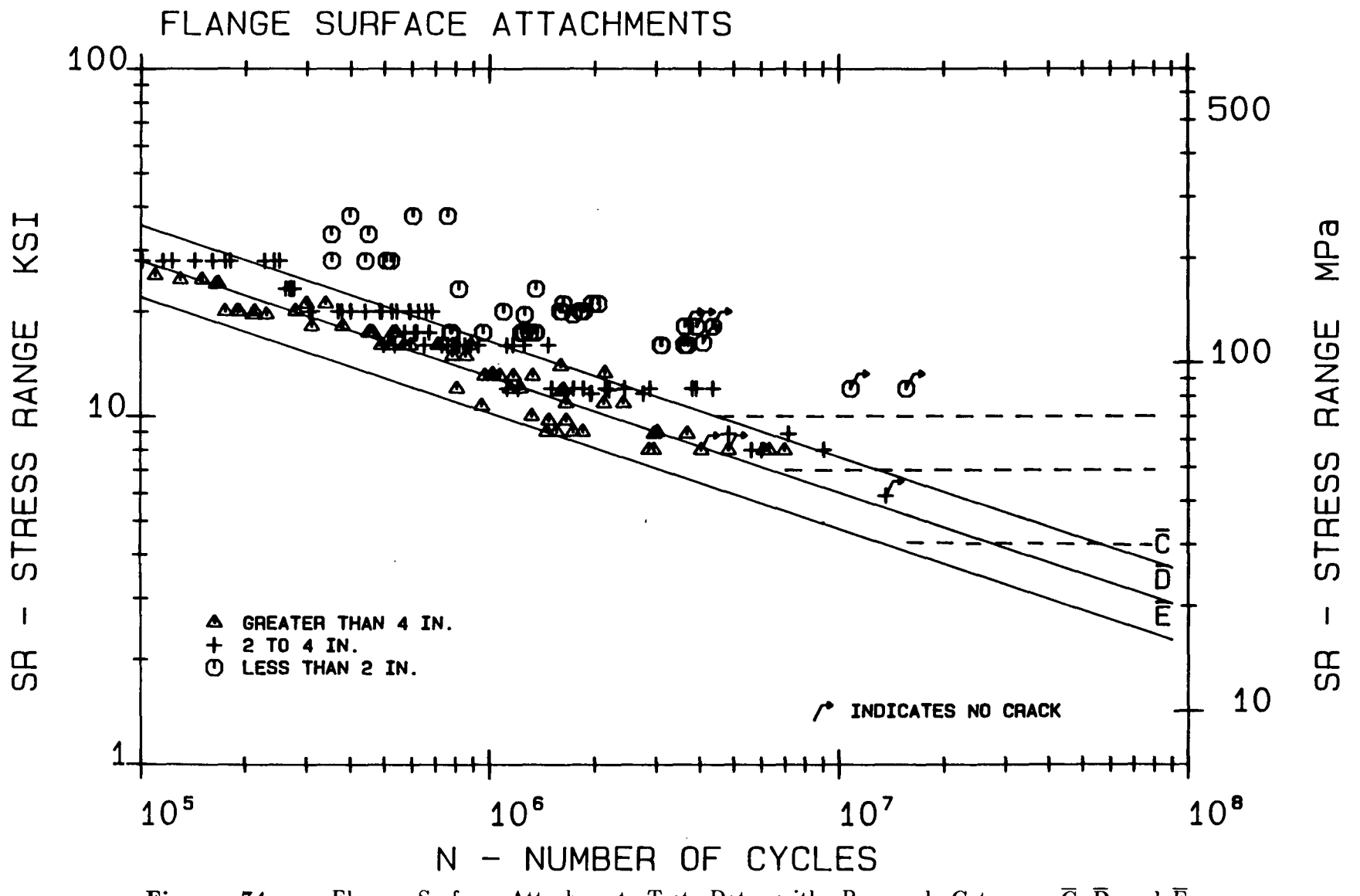

Figure: 74 Flange Surface Attachment Test Data with Proposed Category $\overline{C}$, $\overline{D}$, and $\overline{E}$ Resistance Curves

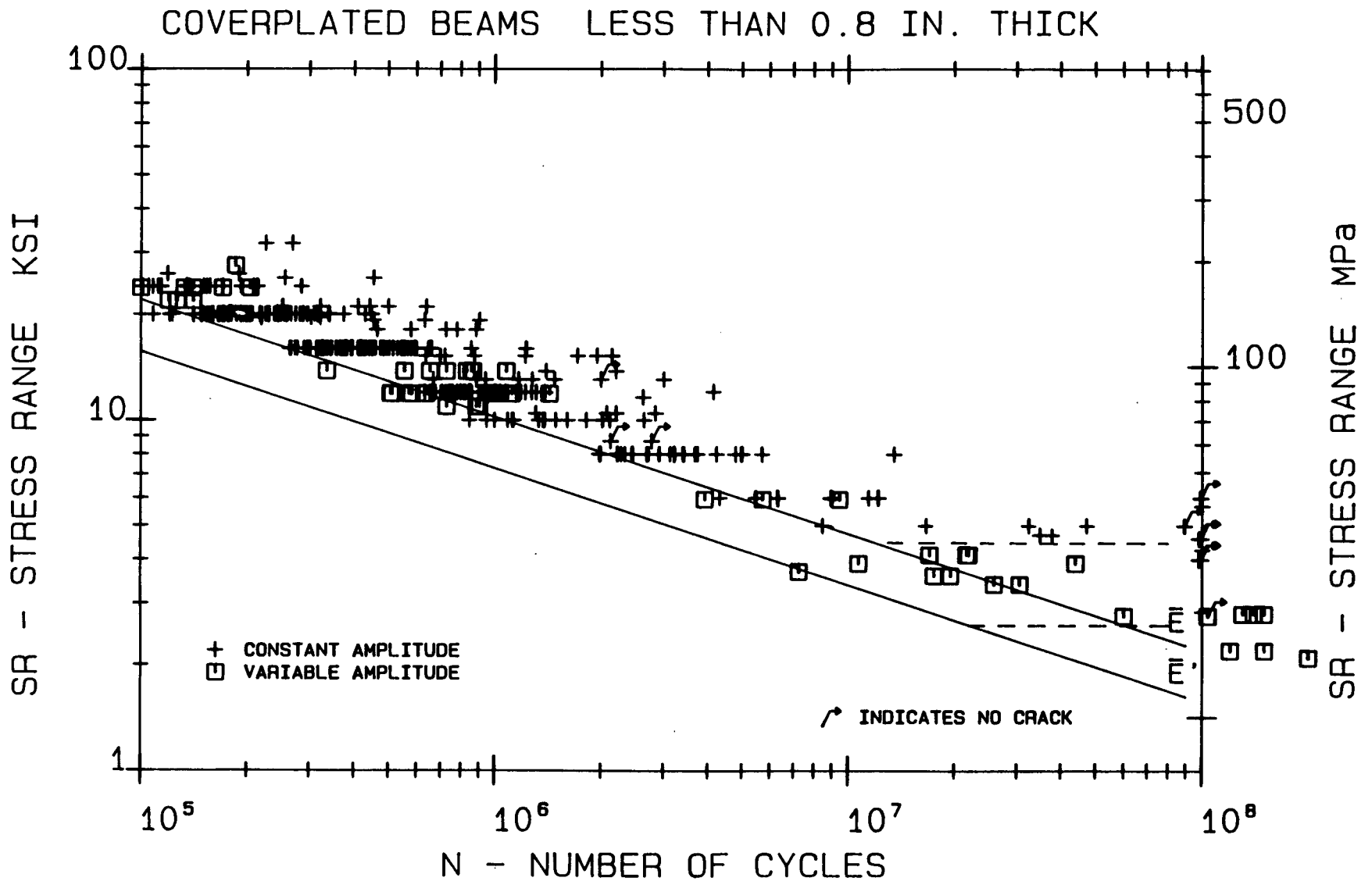

Figure: 75 Narrow Plate Coverplated Beam Test Data with Proposed Category $\bar{E}$ Resistance Curve

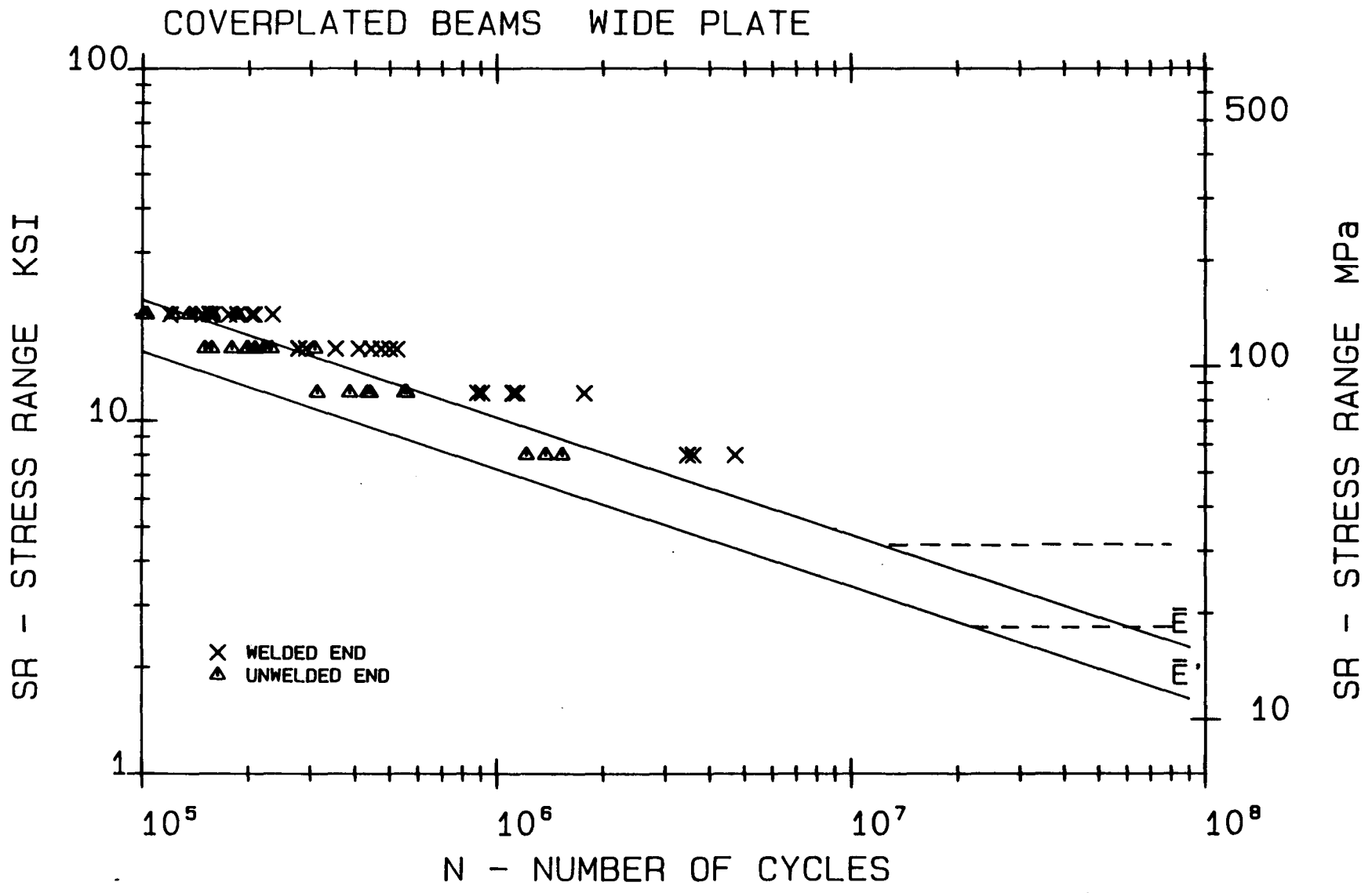

Figure: 76 Wide Plate Coverplated Beam Test Data with Proposed Category $\bar{E}$ and $\bar{E}'$ Resistance Curves

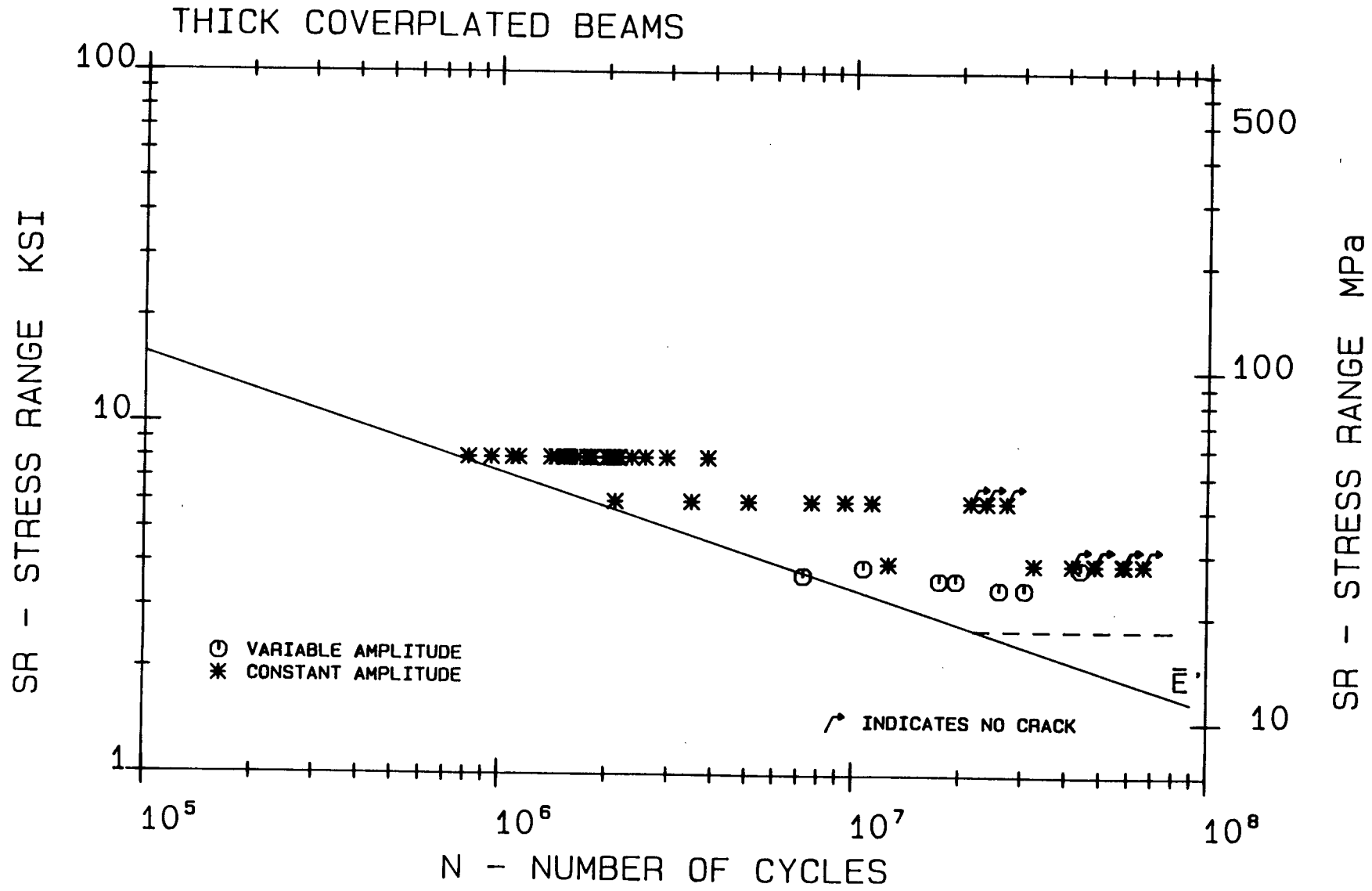

Figure: 77 Thick Flange Plate Coverplated Beams with Proposed Category $\overline{E}'$ Resistance Curves

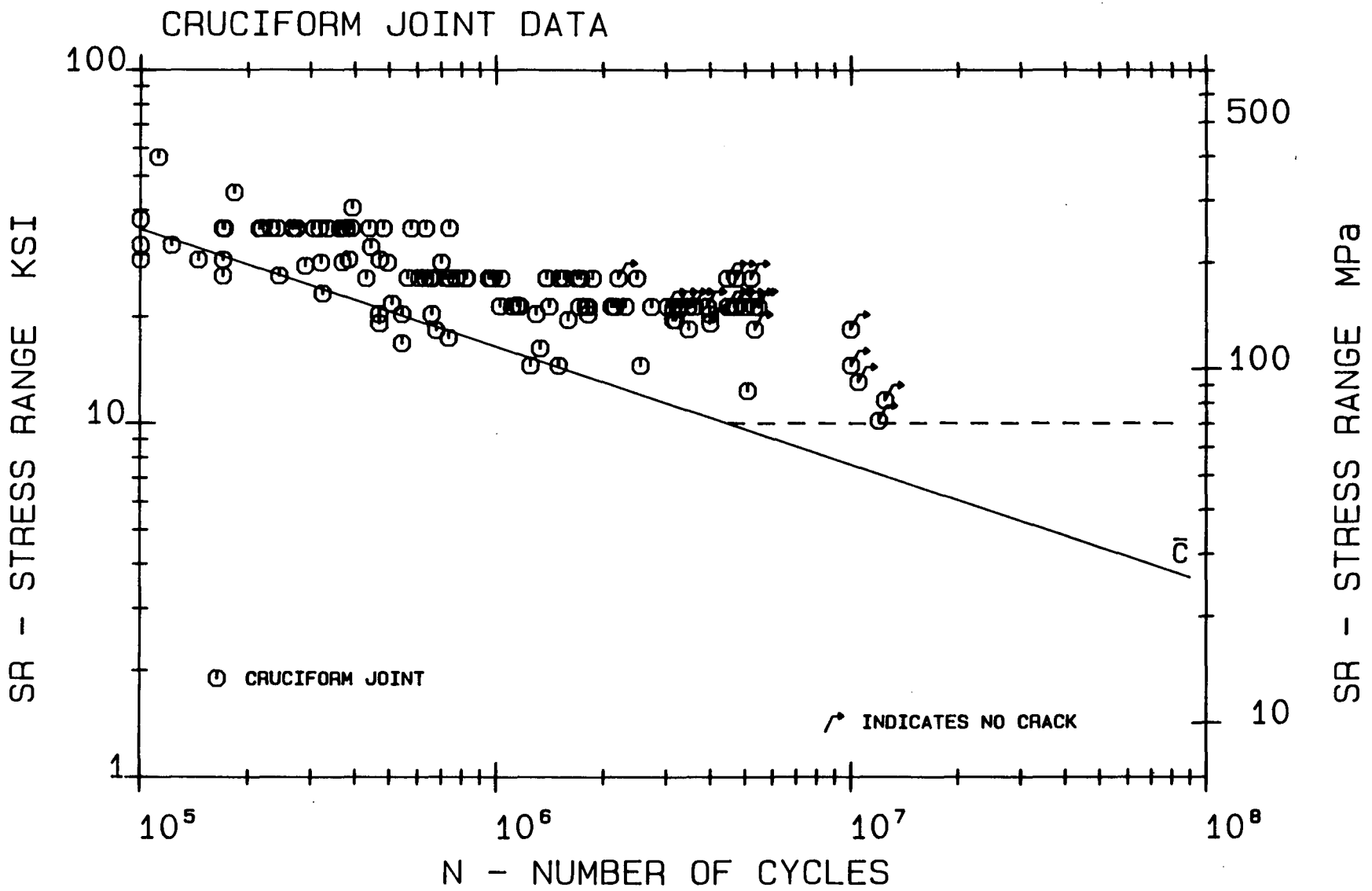

Figure: 78 Non-Load Carrying Cruciform Joint Test Date with Proposed Category $\overline{C}$ Resistance Curve

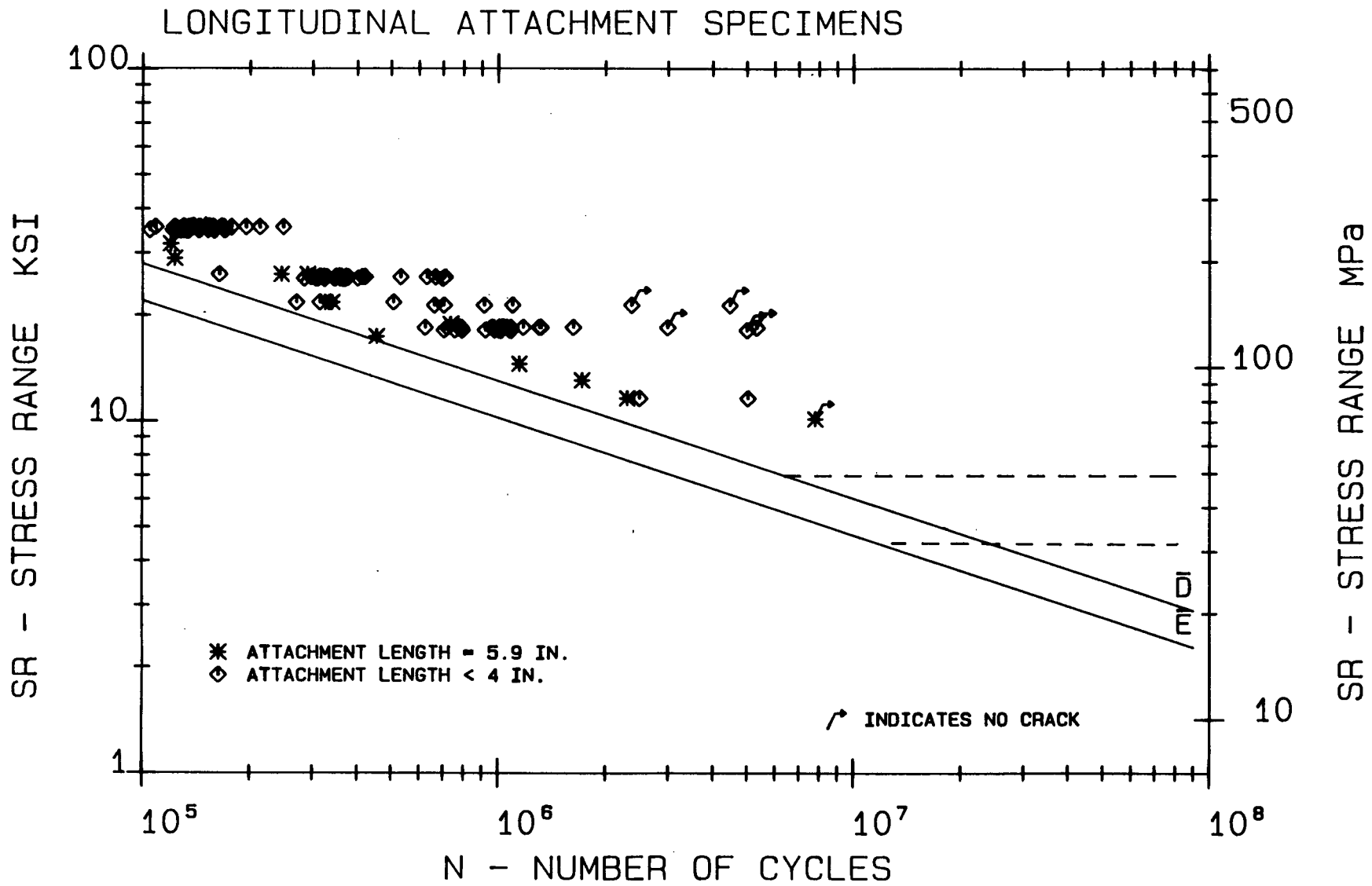

Figure: 79 Simulated Longitudinal Attachment Specimen Test Data with Proposed Category $\overline{D}$ Resistance Curve

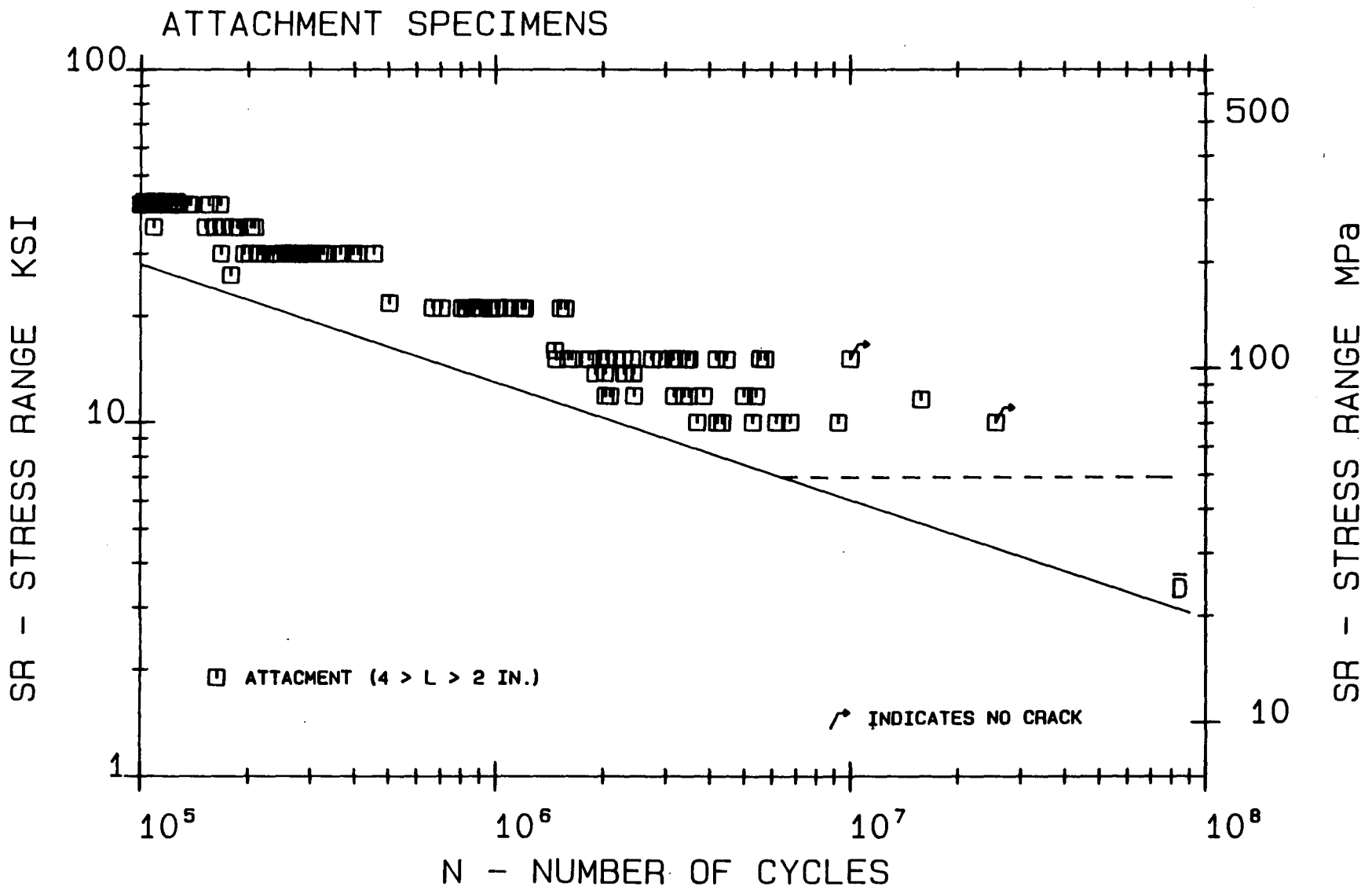

Figure: 80 Simulated Attachment Specimen Test Data with Proposed Category $\bar{D}$ Resistance Curve

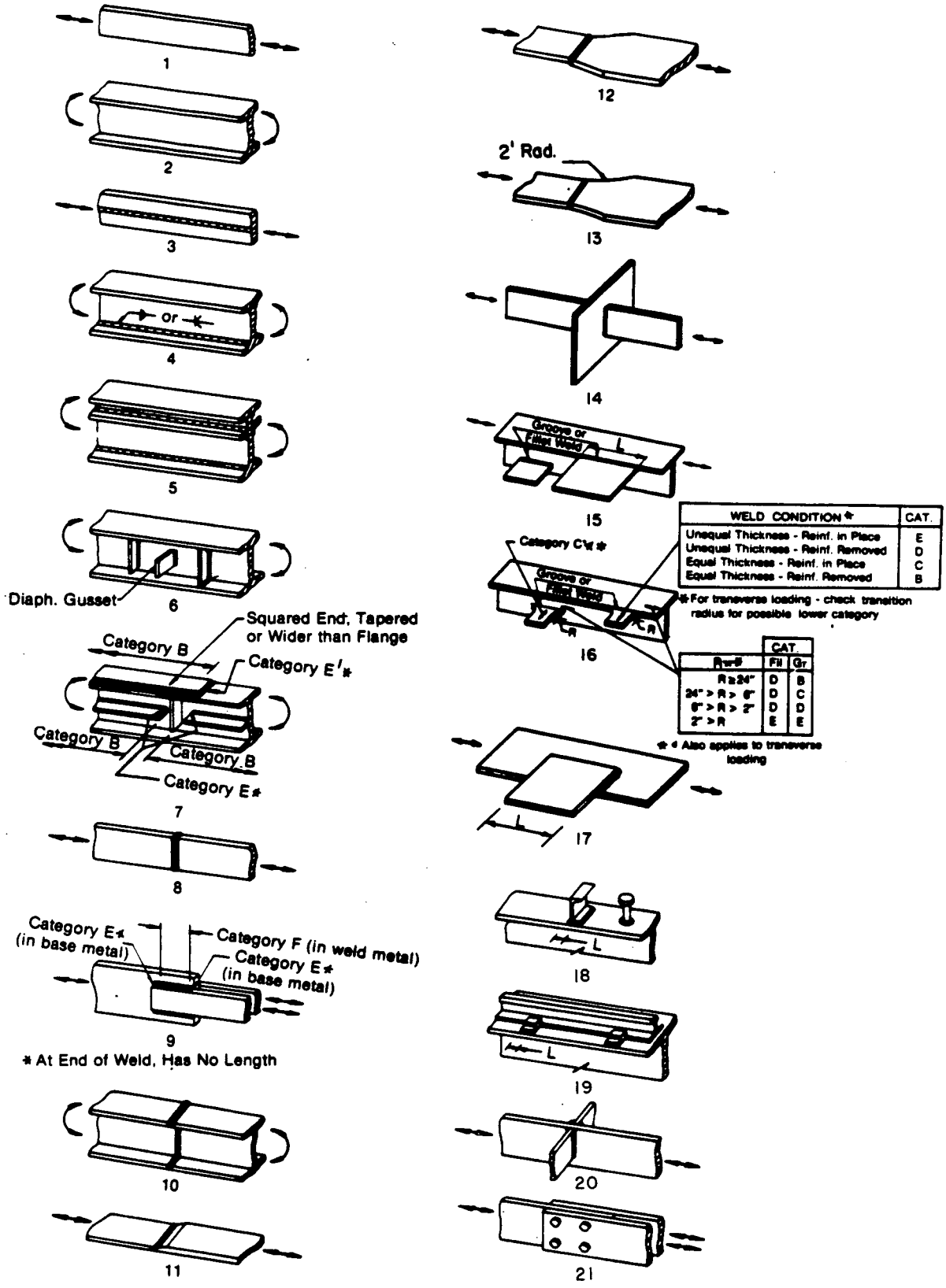

Figure: 81 Illustrative Examples of Detail Types (Figure 10.3.1C, AASHTO 1983)